The consequences of mutator-driven mutagenesis and analysis of lifespan extending compounds using outgrowth analysis and replicative lifespan in *Saccharomyces cerevisiae*

Mitchell Brendon Lee

A dissertation

submitted in partial fulfillment of the

requirements for the degree of

Doctor of Philosophy

University of Washington

2018

Reading Committee:

Matt Kaeberlein, Chair

Alan Herr

Daniel Promislow

Program Authorized to Offer Degree:

Pathology

University of Washington

Abstract

The consequences of mutator-driven mutagenesis and analysis of lifespan extending compounds using outgrowth analysis and replicative lifespan in *Saccharomyces cerevisiae*

Mitchell Brendon Lee

Chair of the Supervisory Committee:
Professor Matt Kaeberlein
Pathology

The hope of dramatically extending our lifespan has captivated humanity for millennia. Over the last two decades, the biology of aging has matured as a field of study and led to greater engagement and investment in aging as a biological problem that can be understood at the molecular level and treated. Translational Geroscience is an interdisciplinary field descended from basic gerontology that seeks to identify, validate, and clinically apply interventions to maximize healthy, disease-free lifespan. To identify and validate interventions, a translational geroscience research pipeline is proposed that begins with identifying and characterizing interventions in wild type model systems (either invertebrate or vertebrate), validating these interventions using models of genetic diversity and disease models, and finally, testing validated interventions in companion animals and humans (Chapter one). A model of mutator-driven mutagenesis, a potent mechanism to induce genetic diversity in cancer and other microbial populations, using budding yeast is then described. Defects in DNA polymerase δ or ε proofreading alone or combined with defects in mismatch repair are used to model mutator phenotypes and mutator-driven mutation burden in haploid and diploid

yeast. This model is used to understand the effects of active mutagenesis and accrued mutation burden on cellular aging (Chapter two). Next, a new system to identify chemical inhibitors of mechanistic Target Of Rapamycin (mTOR) is described. This yeast outgrowth based system measures sensitivity of WT and mutant strains sensitized to mTOR inhibition. A set of nutraceutical compounds were screened using this assay. Of these compounds, caffeine was confirmed to be an mTOR inhibitor (Chapter three). Lastly, this set of nutraceuticals were screened for changes in yeast replicative lifespan (RLS). Two treatments, berberine and green tea extract, reduced RLS. Only one treatment, *Pterocarpus marsupium* extract (PME), extended cellular lifespan. Within this extract are two molecules with reported healthspan and lifespan properties: pterostilbene and (-)-epicatechin. We tested concentrations of these compounds comparable to those found in PME but did not recapitulate extended lifespan (Chapter four).

TABLE OF CONTENTS

LIST OF FIGURES

LIST OF TABLES

ACKNOWLEDGEMENTS

I have numerous people to thank for their help during the completion of my PhD. Without my mom and dad, I would not have had the self-confidence and determination to succeed. This comes from parents that love and support their children unconditionally. Thank you to my brother, Matthew Loeffelholz. My successes are yours. Thank you to Dr. Aaron Mahoney and Amelia Mahoney for emotional support and conversations on the nature of science, as well as formatting dissertation formatting help. Thanks to my advisers, Matt Kaeberlein and Alan Herr. I knew you would both help me become a better scientist during my PhD studies. I did not expect that you both would also help me become a better person. My research committee kept me on track and helped me develop my research during my PhD studies. For that I thank Matt Kaeberlein, Alan Herr, Daniel Promislow, Maitreya Dunham, Junko Oshima, and my clinical mentor, Fuki Hisama. Thanks to my numerous other mentors, particularly Jean Campbell, Daniel Promislow, and Scott Kennedy. I have been tremendously fortunate to work alongside and mentor some of the smartest and hardest working students I've had the good fortune to know. Thank you all for your support and dedication to our research. Thanks to all members of the Kaeberlein lab for scientific development and moral support. The MBD/M3D support staff and leadership has been a tremendous help, namely Bill Mahoney, Megan Barker, Steve Berard, and Milu Worku. Lastly, thanks to my funding sources that supported this research: UW GO-MAP Bank of America Fellowship, NIH CMB Training Grant T32GM7270-39, and the Howard Hughes Medical Institute Gilliam Fellowship for Advanced Study.

DEDICATION

This

dissertation research

is dedicated to

the memory of

Esteban Ray Salinas.

Chapter 1. Translational Geroscience: From invertebrate models to companion animal and human interventions

Mitchell B. Lee and Matt Kaeberlein

Department of Pathology, University of Washington, Seattle, WA USA

1.2 Abstract

Translational Geroscience is an interdisciplinary field descended from basic gerontology that seeks to identify, validate, and clinically apply interventions to maximize healthy, disease-free lifespan. In this review, we describe a research pipeline for the identification and validation of healthspan extending interventions. Beginning in invertebrate model systems, interventions are discovered and then characterized using other invertebrate model systems (evolutionary translation), models of genetic diversity, and disease models. Vertebrate model systems, particularly mice, can then be utilized to validate interventions in mammalian systems. Collaborative, multi-site efforts, like the Interventions Testing Program (ITP), provide a key resource to assess intervention robustness in genetically diverse mice. Mouse disease models provide a tool to understand the broader utility of healthspan interventions. Beyond mouse models, we advocate for studies in companion pets. The Dog Aging Project is an exciting example of translating research in dogs, both to develop a model system and to extend their healthy lifespan as a goal in itself. Finally, we discuss proposed and ongoing intervention studies in humans, unmet needs for validating interventions in humans, and speculate on how differences in survival among human populations may influence intervention efficacy.

1.3 Introduction

What is Translational Geroscience?

The hope of dramatically extending our lifespan has captivated humanity for millennia. Over the last two decades, the biology of aging has matured as a field of study and led to greater engagement and investment in aging as a biological problem that can be understood at the molecular level (VIJG AND SUH 2005; LOPEZ-OTIN *et al.* 2013; PITT AND KAEBERLEIN 2015). In addition to the functional decline and loss of vigor associated with age, a generalized increase in disease susceptibility is now regarded as a consequence of biological aging (KAEBERLEIN 2013a; SIERRA 2016). Numerous chronic diseases manifest during aging. In fact, of the ten leading causes of mortality in high income countries (as of 2016, the last year with available data), eight have advanced age as their greatest predisposing factor (WHO 2018). Developing interventions that target the molecular mechanisms of aging (or "hallmarks of aging", as they're commonly referred) should not only add vigorous years to our lives, but also reduce overall human disease burden. Translational Geroscience is an emerging, interdisciplinary field descended from basic gerontology that seeks to identify, validate, and clinically apply interventions to maximize healthy, disease-free lifespan (KENNEDY *et al.* 2014; SEALS AND MELOV 2014; KAEBERLEIN *et al.* 2016).

Why drug aging?

In some ways, the secrets of healthy aging are not enigmatic. Proper diet with care to include necessary micronutrients, exercise, adequate sleep, and effective management of stress are

all well-known and intuitive ways to add to our healthy years. An important question to address in light of this is why we should focus on developing interventions if lifestyle management alone is sufficient to extend healthy lifespan? One answer is that many people do not have the resources (either in terms of money, time, or both) to proactively invest in maintaining their health. For some, making sure there is enough to eat is a priority over eating healthy. Instead of exercise after a long day of work, many instead prioritize family time and relaxation. This situation is common, even in economically-thriving countries. Those people, whose limited resources keep them focused on day-to-day survival, are as equally deserving of living long, disease-free, lives as those with resources to invest in their long-term health. All of this is not to say that lifestyle choices should not be pursued, or even prioritized, as healthy aging strategies, only that pharmacological interventions that increase healthy lifespan are an option to address an important inequity that exists in human health.

Another reason to consider pharmacological intervention to maintain our health as we age comes from early successes in preclinical geroscience to identify compounds that can impressively extend lifespan and healthspan in model systems. Several compounds are now known to extend lifespan across broad evolutionary distances (PHILLIPS AND LEEUWENBURGH 2004; WAN *et al.* 2013; HE *et al.* 2014; BARZILAI *et al.* 2016; KENNEDY AND LAMMING 2016). For example, rapamycin, among the most promising current interventions, can extend lifespan in yeast, worms, flies, and multiple mouse models (POWERS *et al.* 2006; HARRISON *et al.* 2009; BJEDOV *et al.* 2010; ROBIDA-STUBBS *et al.* 2012; MILLER *et al.* 2014; WANG *et al.* 2016). While the magnitude of effect varies between organisms and genetic backgrounds, experiments in genetically heterogeneous mice show average lifespan extension between 10-25% (MILLER *et al.* 2014). Applied to human populations, a 15% increase in average life expectancy at birth in the US would

change from 78.8 (as of 2015, the last year with available data) to 90.6 years (MURPHY *et al.* 2017). This would be a dramatic improvement in human survival. In addition to improving lifespan in wild type model systems, rapamycin also promotes extended lifespan in multiple mouse disease models (JOHNSON *et al.* 2013c; SIEGMUND *et al.* 2017), including heart disease (RAMOS *et al.* 2012) and cancer models (HUBER *et al.* 2007; ANISIMOV *et al.* 2011; LIVI *et al.* 2013; POPOVICH *et al.* 2014). This bolsters the hypothesis that there are broad clinical applications for rapamycin and other mTOR inhibitors. In a first of its kind test, short-term rapamycin administration improved measures of cardiac function in pet dogs (URFER *et al.* 2017b). While no lifespan data are available for humans, the rapamycin derivative everolimus (RAD001) improved immune function upon flu vaccine challenge in elderly patients given a short-term treatment (MANNICK *et al.* 2014). These studies indicate that increased healthspan is promoted along with lifespan via rapamycin treatment and hint at the power small molecule interventions to improve health.

In addition to rapamycin, multiple other compounds show promise as healthspan and lifespan extending interventions. Metformin, typically used to treat type II diabetes, extends lifespan in worms and mice (CABREIRO *et al.* 2013; MARTIN-MONTALVO *et al.* 2013). In humans, numerous meta analyses suggest an association between metformin use and lowered cancer incidence (EVANS *et al.* 2005; NOTO *et al.* 2012; ZHANG *et al.* 2013; PRESTON *et al.* 2014; ZHANG *et al.* 2014; PROVINCIALI *et al.* 2015; LI *et al.* 2016; NIE *et al.* 2016; SEEBACHER *et al.* 2016). Further tests in non-diabetic individuals, like the proposed Targeting Aging with Metformin (TAME) study, will better establish metformin's potential to broadly reduce cancer and other age-related disease incidence in humans (BARZILAI *et al.* 2016). Nicotinamide riboside (NR) and nicotinamide mononucleotide (NMN) are NAD(+) precursors that improve several features of aging, including muscle and cognitive function and vascular aging, and treatment with NR

beginning at midlife is reported to increase lifespan in mice (RYU *et al.* 2016; ZHANG *et al.* 2016; DAS *et al.* 2018). Senolytics, compounds that specifically target senescent cells for destruction, are important therapies that could increase lifespan and reduce age-related disease burden, particularly cancer and diseases driven by chronic inflammation (BAKER *et al.* 2011; TCHKONIA *et al.* 2013; BAKER *et al.* 2016). Other compounds commonly used by humans, including caffeine, aspirin, and ibuprofen have successfully extended lifespan in model systems (STRONG *et al.* 2008; WANKE *et al.* 2008; SUTPHIN *et al.* 2012; WAN *et al.* 2013; HE *et al.* 2014). This raises the question: what other commonly consumed and FDA-regulated compounds alter physiology in such a way as to promote longevity?

How do we identify and validate healthspan promoting compounds?

What other molecules extend healthspan and lifespan? What combinations of molecules can be designed such that they target multiple pathways associated with aging and increased disease risk? Most importantly, how does individual genetic variation influence success of these interventions? We are only beginning to explore this "intervention space" and understand what is possible with regards to healthspan and lifespan intervention. In addition to broader options with regard to mTOR inhibition, compounds that target other pathways known to regulate aging, or stated more precisely, other nodes in the "aging network", are critical to develop and validate. Breakthroughs in healthspan interventions can lead the way to a precision medicine like approach to maximize individual healthspan by utilizing combinatorial treatment strategies coupled with individualized dosing based on genotype. In what follows, we describe a translational geroscientific workflow to identify and validate lifespan-extending interventions. We envision

this as a translational pyramid with identification of compounds in invertebrate systems, like yeast, forming the base of our translational research pipeline and leading to experiments in other invertebrate systems, in models of genetic diversity, into wild type and genetically diverse vertebrate systems, then finally, in companion pets and humans (**Figure 1**).

1.4 Invertebrate systems

For basic biology, single-celled yeast and invertebrate systems (referred to hereafter simply as "invertebrates") boast unrivaled benefits. These organisms are inexpensive to culture in large populations and have a variety of phenotypes and disease models that can be analyzed using multiple techniques. There are also well-developed genetic tools, models of genetic diversity, and cost-effective genome sequencing methods that are broadly utilized. Taken together, invertebrate systems are optimal for discovery-driven research. For biology of aging in particular, most invertebrates are short-lived, which allows experiments to be conducted in a reasonable time frame. Using multiple invertebrate models to identify and validate interventions provides assessment of evolutionary translatability that is important to consider when developing mammalian interventions (BITTO *et al.* 2015). Beyond these general characteristics, each of the three major invertebrate genetic model systems (yeast, worms, and flies) have unique strengths and weaknesses.

1.5 Wild type (WT) lab models

Wild type (WT) originally described the collective traits of organisms isolated from the wild, namely flies (MORGAN 1910). Today, the term is more commonly used to denote the genetic background of laboratory organisms used in a given experimental system. There is growing appreciation that these organisms really no longer represent the ancestral state, but are instead adapted to conditions in the lab (MORTIMER AND JOHNSTON 1986; STERKEN *et al.* 2015). Laboratory conditions often alter developmental and reproductive life history traits and not always the same way, depending on the model system (SGRO AND PARTRIDGE 2000; KAYA *et al.* 2015b; STERKEN *et al.* 2015). These adaptations may be particularly important in studies of longevity, where factors like environmental nutrient status and reproductive timing strongly influence aging. It remains an open and important question whether genetic and environmental interventions that increase longevity in lab-evolved backgrounds have similar effects in genotypes that are not domesticated to the lab (discussed further below).

Within each model organism, the WT strain used in one study may differ substantially from the WT strain used in a different study, even among studies from the same laboratory. Such strain background differences have the potential to confound interpretation if not carefully considered and addressed by the researchers performing the studies. For example, the relationship between Sir2 and caloric restriction (CR) in budding yeast was complicated by the fact that Sir2 overexpression was shown to increase lifespan in one yeast WT strain (W303-1A)(KAEBERLEIN *et al.* 1999), while CR extended lifespan in a second yeast WT strain (PSY316) (LIN *et al.* 2000; LIN *et al.* 2002). Although a model was initially proposed that Sir2 and CR act within the same genetic pathway, it was not appreciated for several years that neither intervention extended lifespan in the other strain background (KAEBERLEIN *et al.* 2004a; KAEBERLEIN *et al.* 2005a). In a third WT strain

background (BY4742), however, both interventions significantly extend lifespan allowing for more formal analysis of their genetic relationship (KAEBERLEIN *et al.* 2004a).

Historically, there have been numerous yeast and fly genetic backgrounds commonly used across different labs. In recent years, the yeast aging field has mostly adopted the strain background used for the yeast ORF deletion collection (WINZELER *et al.* 1999; GIAEVER *et al.* 2002): BY4743 for diploids and the corresponding haploid derivatives BY4741 (MAT**a**) and BY4742 (MATα). In *C. elegans*, the vast majority of research is performed in a single genetic background, Bristol N2.

Yeast

The budding yeast *Saccharomyces cerevisiae*, just as in genetics and molecular biology in general, is an important workhorse in geroscience (LONGO *et al.* 2012). Some of the most well-established longevity regulating pathways were first identified in yeast, including sirtuins and mTOR signaling (KAEBERLEIN *et al.* 1999; FABRIZIO *et al.* 2001; KAEBERLEIN *et al.* 2005c; POWERS *et al.* 2006). Two major aging paradigms exist in yeast: chronological and replicative (MIRISOLA *et al.* 2014). In the chronological model, populations of yeast are grown to quiescence in liquid culture and changes in viability are assessed over time by outgrowth challenge in rich media, either on plates or in liquid media outgrowth (FABRIZIO AND LONGO 2007; MURAKAMI AND KAEBERLEIN 2009; HU *et al.* 2013). At the cellular level, yeast chronological aging can be thought of as a model of post-mitotic cell aging (MACLEAN *et al.* 2001). These cells, like neurons in humans, are non-dividing and must maintain cellular function while bearing whatever burden is imposed upon them by the environment and their continued cellular metabolism. This is

particularly important during yeast chronological aging, where media acidification resulting from carbon metabolism is a strong driver of lost cellular viability (BURTNER *et al.* 2009).

Yeast replicative aging, instead of monitoring population viability over time, measures the replicative potential of individual yeast cells (MORTIMER AND JOHNSTON 1959; WASKO AND KAEBERLEIN 2014). To do this, individual "mother" cells are arrayed on plates using a compound microscope equipped with a optical fiber dissection needle (STEFFEN *et al.* 2009). Cycles of incubation, microdissection of daughter cells, and quantification are then performed until all mother cells cease dividing. This model of aging is akin to stem cell aging, where numbers of divisions that cells undergo before replicative senescence importantly influences tissue-level health and function. Newer methods of quantifying replicative lifespan and age-related changes in cell biology using microfluidics hold promise to increase throughput by decreasing assay time (from three weeks using microdissection to three days using microfluidics) and allowing for longitudinal studies of cellular aging at the single cell level (LEE *et al.* 2012b; CHEN *et al.* 2017).

Worms

The nematode *Caenorhabditis elegans* is one of the simplest animal model systems with tissue-level differentiation, which includes a nervous system, muscle, intestine, and a pharynx whose pumping is likened to a heart. The first breakthrough in molecular genetics of aging that established the role of insulin-like signaling as a key longevity pathway was made using worms, underscoring the importance of this model system (FRIEDMAN AND JOHNSON 1988; KENYON *et al.* 1993; KIMURA *et al.* 1997; TISSENBAUM 2015). As opposed to yeast, measuring worm lifespan is conceptually more straightforward (KLASS 1977). Synchronized populations of animals are plated

on media containing a bacterial lawn (typically *E.coli*) as a food source and monitored until all animals cease moving (SUTPHIN AND KAEBERLEIN 2009). The lifespan of a typical wild type animal is around three weeks. Lifespan in worms, however, is highly sensitive to changes in environment, including temperature and food source (HAN *et al.* 2017; MILLER *et al.* 2017). As with yeast replicative lifespan, new technologies are utilizing platforms like microfluidics and so-called "lifespan machines", incubation and culturing systems combined with image capturing to facilitate automated lifespan analysis (STROUSTRUP *et al.* 2013; XIAN *et al.* 2013). Utilizing these standardized technologies to perform lifespan analysis reduces technical hurdles to performing assays while increasing output, allowing for higher-throughput survival analysis.

Flies

The fruit fly *Drosophila melanogaster* is the most physiologically complex of the three major invertebrate aging models (HE AND JASPER 2014). Along with greater complexity comes more opportunities to study tissue level aging, sex-specific lifespan differences, and more complex healthspan measures, like age-related behavioral changes and impaired learning (GROTEWIEL *et al.* 2005; TOIVONEN AND PARTRIDGE 2009; JONES AND GROTEWIEL 2011; CANNON *et al.* 2017). This allowed for some of the first targeted studies on the evolution of lifespan characteristics, where researchers evolved short or long lived fly populations by controlling reproductive age of parents (ROSE 1984; MUELLER 1987). Early validation, and better understanding, of the role that insulin signaling plays in regulating aging was performed using flies (CLANCY *et al.* 2001; TATAR *et al.* 2001; TU *et al.* 2002). Other processes likely to play a role in mammalian health and aging, like sleep and circadian rhythms, are also effectively studied using fruit flies (BUSHEY *et al.* 2010).

An interesting difference from other invertebrate models is that fruit flies do not have a dominant wild type background in which the majority of research is performed. Multiple genetic backgrounds are utilized, including Oregon R, Canton S, w^{118}, and yw. Importantly, these backgrounds have different survival characteristics (GRANDISON *et al.* 2009; ILIADI *et al.* 2009). The typical fruit fly lifespan is 2-3 months but, just as with nematodes, this is highly dependent on culture conditions (HOLLINGSWORTH 1969; CHAPMAN AND PARTRIDGE 1996). Again, like nematodes, cohorts of age-matched animals are separately cultured (LINFORD *et al.* 2013; PIPER AND PARTRIDGE 2016). Instead of on plates, fruit flies are typically reared in vials containing a yeast-based food source and transferred to new vials periodically.

Once an intervention is identified using a WT invertebrate system, the next step is to validate its translatability, identify natural genetic variants that influence intervention efficacy, and evaluate how the intervention impacts age-associated and other disease models. There are three common ways these goals are achieved using other invertebrate models and genetic collections.

1.6 Evolutionary translation between invertebrate model systems

Utilizing short-lived invertebrate models is ideal for rapidly identifying lifespan-extending molecules and extracts. Once an intervention is identified, how do we proceed? We can divide lifespan and healthspan interventions by whether they impact private or public mechanisms of aging (PARTRIDGE AND GEMS 2002). Private interventions target cellular processes that uniquely contribute to aging in certain model systems. For instance, yeast accumulate a type of genome instability with replicative age marked by proliferation of repeating ribosomal DNA (rDNA) in the form of extrachromosomal circular rDNA (SINCLAIR AND GUARENTE 1997). Inhibiting

accumulation of rDNA circles leads to extended lifespan in yeast (DEFOSSEZ *et al.* 1999). While the role of rDNA instability in some disease states is becoming better appreciated (HALLGREN *et al.* 2014), rDNA circle accumulation is likely a private mechanism of yeast aging that is not shared, at least by mammals.

Public interventions are those that impact cellular mechanisms that contribute to aging in many different organisms. These shared mechanisms comprise the "Hallmarks of Aging" and include genomic instability, telomere attrition, epigenetic alterations, loss of proteostasis, deregulated nutrient sensing, mitochondrial dysfunction, cellular senescence, stem cell exhaustion, and altered intercellular communication (LOPEZ-OTIN *et al.* 2013). Interventions that target fundamental cellular processes that fail as organisms age, or those that elicit evolutionarily conserved cellular stress responses are likely to be public. These interventions have the greatest potential to extend lifespan in multiple organisms, including mammals. One way to validate whether an intervention impacts public or private mechanisms of aging is to test for conserved longevity and/or healthspan effects in multiple model systems. Utilizing invertebrate systems to validate interventions harnesses the research power of each system while also testing whether the intervention effect is conserved across hundreds of millions of years of evolutionary divergence (**Figure 2**) (DOS REIS *et al.* 2015; LETUNIC AND BORK 2016). This strategy is effectively used to validate newly identified and commonly used compounds (CABREIRO *et al.* 2013; WAN *et al.* 2013; HE *et al.* 2014). Evolutionary conservation of this sort provides an important foundation for choosing interventions to move forward in translational geroscience and compliments traditional genetic and mechanistic approaches.

1.7 Genetically-diverse collections

Besides testing interventions across invertebrate model organisms, other diverse invertebrate collections and genetic libraries are useful for evaluating lifespan extending interventions. Some of these collections and libraries represent engineered genetic variation, while others capture natural genetic diversity. There are genetically diverse panels and libraries for all three major invertebrate systems that can be utilized to develop a more sophisticated understanding of lifespan and healthspan interventions.

Yeast

The best utilized collection of engineered genetic mutants is the yeast single gene deletion collection (WINZELER *et al.* 1999; GIAEVER AND NISLOW 2014). This library of nearly 6000 mutants is constructed by systematic replacement of every non-essential yeast gene with a selectable marker. Using this collection, comprehensive genome wide analyses of genes that modulate both replicative and chronological lifespan have been performed (POWERS *et al.* 2006; FABRIZIO *et al.* 2010; BURTNER *et al.* 2011; MCCORMICK *et al.* 2015). These studies have revealed numerous pathways that regulate cellular aging. In a screen of deletion mutants, the particular benefits of CR in suppressing diminished lifespan in mitochondrial mutant was identified (SCHLEIT *et al.* 2013). Insights here led to using the mTOR inhibitor rapamycin as a novel treatment for mitochondrial disease in mice (discussed in detail below). For intervention studies, this collection is particularly valuable as a means of performing epistasis analysis that allows a better understanding of which cellular pathways the intervention interacts. Testing interventions in

deletion mutants is also a useful means of identifying new interventions that target known longevity pathways (LEE *et al.* 2017a).

For natural genetic diversity, the *Saccharomyces* Genome Resequencing Project (SGRP) collects a global assortment of two different *Saccharomyces* species (*S. cerevisiae* and *S. paradoxus*) representing wild and domesticated yeast from multiple ecotypes (LITI *et al.* 2009). Initial characterization of strains from this collection reveal substantial natural variation in replicative lifespan (KAYA *et al.* 2015b). Given the large evolutionary distance between yeast isolates (YUE *et al.* 2017), this collection represents another resource for evolutionary translation approaches. Perhaps more interesting for translational geroscience, this collection captures a substantial amount of natural genetic variation that can be probed in the context of intervention evaluation. Across these strains, there are over 235,000 SNPs (LITI *et al.* 2009). Understand drug efficacy across a range of genotypes provides insights into safety of the drug when given to genetically diverse populations and how well individual genotypes respond. Understanding these factors are critical for precision medicine approaches to translational geroscience.

Worms

Worms, like yeast, boast a large genetic library that allows for whole genome analysis at the single gene level. In contrast to yeast, however, this library is not composed of genetic mutants, but is instead made up of *E. coli* housing unique vectors, each of which targets a worm gene for post-transcriptional knockdown using feeding-based RNA interference (RNAi) (FIRE *et al.* 1998; KAMATH *et al.* 2001; KAMATH AND AHRINGER 2003; KAMATH *et al.* 2003; RUAL *et al.* 2004). Several genome wide screens have identified lifespan extending mutants using RNAi in WT and

other mutant backgrounds (DILLIN *et al.* 2002; LEE *et al.* 2003; HAMILTON *et al.* 2005; HANSEN *et al.* 2005; YANOS *et al.* 2012). The important role of the mitochondria in determining longevity was conclusively established in these early screens. While there are challenges when comparing RNAi results across labs, primarily due to methodological and RNAi induction variability, these screens are a particularly useful means of generating hypotheses that can be separately validated.

A new program to investigate lifespan extending interventions in nematodes utilizes natural genetic diversity not just within *C. elegans*, but also in closely related species. The *Caenorhabditis* Interventions Testing Program (CITP) is a multi-site effort meant to validate longevity enhancing treatments using worms (PLUMMER *et al.* 2017). This project is modeled after another NIA-supported Interventions Testing Program (ITP) which evaluates well-studied interventions for increased lifespan and healthspan in mice (see below). In addition to their efforts to develop standardized protocols for worm lifespan studies, the CITP is notable for its use of multiple independent strains of genetically diverse *Caenorhabditis* species (KIONTKE *et al.* 2011; LITHGOW *et al.* 2017; LUCANIC *et al.* 2017). In addition to eight different *C. elegans* isolates, the CITP utilizes eight isolates of *C. briggsae* and six isolates of *C. tropicalis*. This is particularly remarkable given historical difficulties culturing *Caenorhabditis* species from the wild (BARRIERE AND FELIX 2005; SCHULENBURG AND FELIX 2017). Whole genome sequences of the CITP strains will be an important resource for investigating intervention efficacy among this set of animals.

Flies

Cost-effective genome sequencing methods have allowed expansion of genetic model systems from a few wild type lab organisms to large panels of organisms representing genetically

diverse natural populations. An example of this is the *Drosophila* Genetic Reference Panel (DGRP) (MACKAY *et al.* 2012). The DGRP is a collection of ~200 inbred *Drosophila melanogaster* lines descended from a population of flies isolated at a farmer's market in Raleigh NC, USA. Even though the parental lines were all isolated from the same location, the DGRP represents a wealth of genetic diversity (HUANG *et al.* 2014). Amongst these 205 lines, over 4.8 million SNPs and 1.2 million larger polymorphisms are captured. Disease phenotypes are screened in the DGRP to identify naturally segregating genetic variants that modify human disease states (CHOW AND REITER 2017; LAVOY *et al.* 2018). The population structure of the DGRP makes this collection well-suited for GWAS studies (MACKAY AND HUANG 2018). While there is substantial variation in survival amongst the DGRP, a GWAS for longevity failed to statistically validate variants associated with longevity within this collection (IVANOV *et al.* 2015). This likely rules out alleles of large effect segregating in this population. Epistatic interactions between multiple alleles, however, may account for a larger amount of variation in aging than currently appreciated (HUANG *et al.* 2012). These researchers suggested expanding the number of lines within the collection to increase power to resolve longevity associated effects of segregating SNPs. Another GWAS study using 800 lines from a different genetically diverse population, the *Drosophila* Synthetic Population Resource (DSPR), identified multiple quantitative trait loci (QTLs) that explain up to 22% of lifespan variation (KING *et al.* 2012a; KING *et al.* 2012b; HIGHFILL *et al.* 2016). Capturing broader genetic variation in sexually isolated populations may reveal novel longevity associated alleles of greater effect (YUKILEVICH AND TRUE 2008; KAO *et al.* 2015). Studies addressing the efficacy of lifespan extending compounds on survival and healthspan have not been completed with the DGRP, but this collection holds promise as a model to investigate how natural genetic variation influences intervention outcomes.

1.8 Age-associated disease models

The promise of targeting aging is not only that we can extend the quantity of our lifespan, but that we can enhance the quality. This is not possible without decreasing the burden of age-associated disease. The core hypothesis of translational geroscience is that there is a fundamental connection between aging and age-associated disease such that, delaying aging will consequently delay the onset of disease. In particular, a major emphasis of translational geroscience is compression of morbidity, meaning that the functional decline and chronic diseases associated with age is pushed back as far as possible toward the end of life (FRIES 1980). A key test of this hypothesis is showing that lifespan extending interventions broadly reduce age-associated disease. There are numerous invertebrate models that attempt to recapitulate aspects of human age-associated diseases. Testing compounds of interest in these disease models is useful for understanding the full utility of lifespan interventions. Interestingly, in some cases, lifespan extending compounds have proven to be effective in disease models not obviously linked to normative aging, such as the ability of rapamycin to suppress severe mitochondrial disease. This lends support for additional studies that screen lifespan extending compounds widely across disease models.

Yeast

Yeast provide a window into fundamental features of normal as well as disease state cell biology that translate to humans in many cases (BASSETT *et al.* 1996). In terms of age-related

diseases, many models of protein aggregation diseases have been developed using yeast (OUTEIRO AND LINDQUIST 2003; GITLER *et al.* 2008; TENREIRO AND OUTEIRO 2010). These have helped elucidate basic mechanisms of the disease state. Yeast are very well-suited for measuring cellular phenotypes associated with a given disease, like mitochondrial dysfunction or protein aggregation (CHEN AND PETRANOVIC 2015). Fundamental drivers of cancer, like genome instability and mutagenesis, are effectively modeled using mutator yeast that are defective for mismatch repair and polymerase proofreading (HANAHAN AND WEINBERG 2011; HERR *et al.* 2011; HERR *et al.* 2014; RAYNER *et al.* 2016; TOMASETTI *et al.* 2017). With few complex behaviors that can be tracked with disease progression, however, yeast are limited beyond understanding cell-intrinsic aspects of basic molecular and cellular biology of disease.

Worms

Multicellularity and tissue differentiation in *C. elegans* provide a more relevant context to study the effects of lifespan extending interventions on age-associated disease. Like yeast, worms are also a popular model system to study protein aggregation diseases (MCCOLL *et al.* 2012; KUMAR *et al.* 2016). With a simple neuromuscular system, age-related paralysis and other behavioral changes provide healthspan related phenotypes that can be measured in the context of these disease models (KEOWKASE *et al.* 2010). Without a circulatory system, worms are less amenable to studying vascular aging. However, the pharynx, an appendage in the head that grinds bacteria as they are consumed, has been described as similar to the heart in its pumping activity and regulation (HAUN *et al.* 1998). Age-associated changes in pharyngeal pumping are another commonly used functional measure of organismal health (HUANG *et al.* 2004; AYYADEVARA *et al.*

2013). Mitochondrial disease and mtDNA genome instability are modeled using Pol gamma proofreading or polymerase dead mutator worms, multiple mutants defective for components of the electron transport chain, and mutants for other critical mitochondrial functions (BRATIC *et al.* 2010; MAGLIONI AND VENTURA 2016; HAROON *et al.* 2018). Worms also provide useful models of conditions involved in dysregulated lipid metabolism, like obesity and related metabolic disorders (MCKAY *et al.* 2003; JONES AND ASHRAFI 2009). While they do not possess a kidney, worms have even proven useful in understanding kidney disease, particularly as its pathogenesis relates to defective ciliary function (BARR 2005; GANNER AND NEUMANN-HAEFELIN 2017).

Flies

Combining genetic disease models with pharmacological interventions is well established in flies (PANDEY AND NICHOLS 2011). Flies are well-suited for studying similar neurodegenerative and protein aggregation diseases as those of yeast and worms (DAWSON *et al.* 2010; LEE *et al.* 2012a; XU *et al.* 2013). Fundamental connections between mitochondrial fission and fusion cycles and Parkinson's disease onset were identified in flies (POOLE *et al.* 2008; MATSUDA *et al.* 2010). Additionally, thanks to their more advanced nervous system and complex behavior, flies allow other neurological and psychiatric diseases to be studied (VAN ALPHEN AND VAN SWINDEREN 2013; GUO *et al.* 2016). Mitochondrial disease models that impact the electron transport chain (ETC) and mitochondrial energetics are also well characterized (BURMAN *et al.* 2014). Interestingly, rapamycin improves survival in a fly model of Leigh syndrome, a disease driven by defects in ETC function (WANG *et al.* 2016). Flies also provide useful models of cardiac aging, cancer, and even

as a model for immunoaging (ZEROFSKY *et al.* 2005; NISHIMURA *et al.* 2011; SONOSHITA AND CAGAN 2017).

1.9 Vertebrates

Validating interventions in vertebrate systems

Invertebrate systems are a discovery engine for longevity interventions. The goal, however, is to translate these interventions into vertebrate systems. Short-lived vertebrate systems are essential for validating interventions in a timely manner, but few options are available. An emerging model for aging research is the African turquoise killifish (*Nothobranchius furzeri*) (HU AND BRUNET 2018). With a median lifespan between 4-6 months, the African turquoise killifish is the shortest lived vertebrate that can be bred in the lab (VALDESALICI AND CELLERINO 2003; DODZIAN *et al.* 2018). In addition to survival, many age-associated phenotypes, including enhanced cognitive decline, can be studied using the killifish (KIM *et al.* 2016). While few longitudinal studies have been reported, resveratrol and low temperature both extend lifespan in this model (VALENZANO *et al.* 2006a; VALENZANO *et al.* 2006b). Interestingly, transfer of gut microbiome from young to old fish extends lifespan, showing the importance of gut flora in regulating aging (SMITH *et al.* 2017). With more genome editing and analysis resources now available (VALENZANO *et al.* 2015; HAREL *et al.* 2016), we can hope to see the killifish develop as a vertebrate discovery and validation engine for lifespan interventions.

While non-mammalian fish models and rats are occasionally used, mouse models are the major vertebrate workhorse in translational geroscience (GENADE *et al.* 2005; SPEAKMAN AND

MITCHELL 2011). Wild type mouse models are genetically well-established and age-associated pathologies are deeply understood. Ever increasing disease models provide complimentary approaches to test interventions. The NIA-sponsored Interventions Testing Program (ITP) is a multi-site effort utilizing genetically heterogeneous mice to validate longevity interventions. These resources establish mice as the major mammalian system for intervention validation.

1.10 WT vertebrate models

If all roads in the ancient world led to Rome, then the mouse, *Mus musculus*, is truly the Rome of the translational geroscientific research pipeline. Mice are ubiquitous in biology of aging research and translational research in general. All of the most promising healthspan interventions are being actively researched using mouse models (BIELAS *et al.* 2018; HOU *et al.* 2018; KARNEWAR *et al.* 2018; LUAN *et al.* 2018). Mice are among the shortest-lived mammals and have a typical lifespan in the lab of 2-3 years (WILKINSON *et al.* 2012). There are multiple common genetic backgrounds that are used for general research (DUTTA AND SENGUPTA 2016). Mice are anatomically and physiologically very well characterized. This allows for detailed pathological analyses to be conducted, even though reporting of this data is sometimes sparse (PETTAN-BREWER AND TREUTING 2011; SNYDER *et al.* 2016). Efforts to standardize pathological grading of aged tissues will allow detailed assessment of organismal aging that can be applied to testing intervention efficacy (LADIGES *et al.* 2017). Assessing cause of death in mice is difficult given care and maintenance requirements, but the most common pathologies that contribute to mortality are cancer, kidney disease, and inflammation (BRAYTON *et al.* 2012). Animal care and maintenance is rigorous (CONOUR *et al.* 2006; LEACH *et al.* 2008). This is necessary to maintain

healthy and humane conditions and it provides a measure of standardization across research sites that is underappreciated. Compared to humans, it is estimated that 9 days is the equivalent of a human year for a mouse (DUTTA AND SENGUPTA 2016). This is interesting to consider in the context of drug studies when thinking about dosing windows and comparing to humans.

As described above for invertebrate models, it is important to carefully consider genetic background when designing and interpreting geroscience studies in mice. Several different WT mouse strains are utilized for such studies, with the most common being inbred C57BL/6J and genetically heterogeneous UMHET3. It is also worth noting that the strain background most commonly provided by the NIA Aging Rodent Colony is C57BL/6Nia, which differs genetically from C57BL/6J. A comparison of longevity and healthspan across 31 different mouse strains at The Jackson Laboratory found substantial differences in morbidity and mortality (YUAN *et al.* 2009; BOGUE *et al.* 2016). Also, as mentioned above, multiple generations of breeding under laboratory conditions is likely to have selected for genotypes that develop rapidly and produce large litter sizes among inbred mouse strains.

1.11 Genetically diverse collections

The relative complexity of mice slows the development of genetic tools compared to invertebrate systems. Efforts are underway to systematically construct the knockout mouse collection, a genome wide set of null mutants for every non-essential mouse gene (AUSTIN *et al.* 2004). This will unlock similar genetic tools for intervention epistasis studies currently used in yeast. Many recombinant lines exist that are produced typically by mating lab strains and establishing diverse lines from progeny. The ILSXISS are a set of recombinant inbred lines

generated by mating mutants isolated within the lab (WILLIAMS *et al.* 2004). These lines provided key insights into the importance of genetic background in mitigating lifespan extension produced by CR (LIAO *et al.* 2010). The largest effort to create diverse genetic models using mice is the Collaborative Cross, a genetic reference panel of recombinant inbred mice descended from an eight-way cross and mating scheme utilizing five lab mouse models and three mouse models representing natural genetic variation (CHURCHILL *et al.* 2004; CHESLER *et al.* 2008). By mating lines from the Collaborative Cross, researchers are now constructing the Diversity Outbred (DO) mouse populations (CHURCHILL *et al.* 2012; LOGAN *et al.* 2013). This set of lines is different than the other genetically diverse organism collections discussed because these lines are kept as heterozygotes instead of being inbred to homozygosity (SVENSON *et al.* 2012). This makes the DO population the closest model to human genetic variation available to biomedical researchers. This will be an important population for testing intervention robustness in genetically diverse mammals.

A key resource for translational geroscience is the NIH-sponsored Interventions Testing Program (ITP). This is a multi-site effort bringing together labs from the NIA, University of Michigan, and University of Texas-San Antonio to test proposed healthspan and lifespan interventions (WARNER *et al.* 2000; NADON *et al.* 2008). The ITP uses a heterogeneous genetic mouse model constructed from crosses of multiple unique mouse strains (in this case, a four-way cross between common lab strains) (JACKSON *et al.* 1999; MILLER *et al.* 1999; MILLER *et al.* 2007). Interventions are selected for ITP testing based on proposal and then evaluated by committee. To date, 42 compounds have been tested, nine of these at different doses, in combination with other compounds, or tested in different aged mice (**Table 1**) (STRONG *et al.* 2008; HARRISON *et al.* 2009; MILLER *et al.* 2011; WILKINSON *et al.* 2012; STRONG *et al.* 2013; HARRISON *et al.* 2014; MILLER

et al. 2014; STRONG *et al.* 2016). Of these, two (rapamycin and acarbose) extend lifespan in both sexes and another four (aspirin, 17αEstradiol, nordihydroguaiaretic acid, and protandim®) extend only in males (NADON *et al.* 2017).

1.12 Disease models

A particular strength of mouse research is the variety of disease models that can be utilized. Multiple reviews are devoted to documenting and comparing the wealth of models for different pathologies available, including age-associated diseases (JANUS AND WELZL 2010; DAY *et al.* 2015; BELLANTUONO AND POTTER 2016). Of particular interest in biology of aging research are mouse progeria models, like the *Zmpste*$^{-/-}$ and *Lmna*$^{L530P/L530P}$ mice (Hutchinson Guilford Syndrome and laminopathy models), *Ercc1*$^{-/-}$ mice (Xeroderma pigmentosum model), and *Bubr1*$^{-/-}$ mice (WEEDA *et al.* 1997; MOUNKES *et al.* 2003; BAKER *et al.* 2004; VARELA *et al.* 2005; OSORIO *et al.* 2009; GURKAR AND NIEDERNHOFER 2015). Mouse models of elevated oxidative stress, like the Cu/Zn superoxide dismutase knockout mouse, are an emerging progeroid model that shows accelerated frailty and molecular damage, especially in the liver, lungs, and kidneys (DEEPA *et al.* 2017; SNIDER *et al.* 2018).

One notable example for the use of lifespan extending interventions beyond impacting age-related survival comes from research into mitochondrial disease that began using yeast. In a screen for yeast deletion mutants that differentially respond to low glucose CR, multiple mitochondrial mutants responded best to the intervention, with some seeing their lifespans more than double (SCHLEIT *et al.* 2013). This led to the hypothesis that CR, or a CR mimetic, may have clinical application in the context of mitochondrial disease. To test this, researchers utilized the *Ndufs4*

knockout mouse model that recapitulates many aspects of Leigh syndrome, a human childhood mitochondrial disease (KRUSE *et al.* 2008). Due to the frail nature of the *Ndufs4* knockout mice and the early onset of disease, rapamycin was administered beginning at postnatal day 10 instead of CR. Impressively, rapamycin treatment nearly doubled median lifespan in this disease model (JOHNSON *et al.* 2013c). This groundbreaking study opened up new interest in utilizing mTOR inhibitors as treatments for mitochondrial disease (ZHENG *et al.* 2016; SIEGMUND *et al.* 2017). It is exciting to consider that this study began in yeast and ended with a successful mammalian disease intervention in little more than a few years. Interestingly, more recent work has shown that hypoxia increases lifespan of *Ndufs4* knockout mice even more robustly than rapamycin (JAIN *et al.* 2016; FERRARI *et al.* 2017). Like rapamycin, hypoxia increases lifespan in *C. elegans* (MEHTA *et al.* 2009; LEISER *et al.* 2013) and may explain longevity among people living at high altitude (LI *et al.* 2017). These observations suggest that this mouse model of severe mitochondrial disease can be used as a short-lived discovery platform for interventions likely to extend lifespan in WT mice and perhaps people.

1.13 Reaching the goal

Applying interventions in companion animals and humans

Using the translational geroscience pipeline, we can go from identifying interventions in diverse invertebrate model systems to validating interventions using mice. From here, where do we go? In studies of CR, the first well-studied longevity extending intervention, substantial efforts were made to validate findings in a non-human primate, the rhesus monkey (MATTISON *et al.*

2017). Parallel studies lasting more than 30 years each at the University of Wisconsin-Madison and NIA ultimately converged on CR having positive effects on primate health and lifespan, despite differences in study design and early controversies about CR having inconsistent effects between sites (COLMAN *et al.* 2009; MATTISON *et al.* 2012; MATTISON *et al.* 2017). Given the exceptionally long lifespan and correspondingly high costs of rhesus monkeys, however, it seems unlikely that additional longevity studies will be performed in these animals. More recently, efforts have been made to establish the common marmoset (*Callithrix jacchus*) as a shorter-lived non-human primate model in geroscience (TARDIF *et al.* 2011; LELEGREN *et al.* 2016; SALMON 2016). This small primate has an average lifespan in the lab of 4-6 years and a maximum lifespan upwards of 16 years (ROSS *et al.* 2012). Efforts are underway now to establish whether rapamycin extends lifespan in this primate (ROSS *et al.* 2015; TARDIF *et al.* 2015)

While primate studies are the intuitive next step for testing putative geroscience interventions from an evolutionary point of view (**Figure 2**), they lack an important component for translational validation: the human environment. In this context an exciting approach is to utilize companion animals for understanding aging biology and intervention testing.

1.14 Companion animals

Companion animals as a non-laboratory model system for translational geroscience represents both a unique scientific model and potentially a realization of the goals of geroscience itself. Companion animals share a number of similarities with humans that are not recapitulated in lab organisms, including their environment and microbiota (SONG *et al.* 2013). These non-genetic factors are critically important to model and understand in translational geroscience as it

is estimated they account for approximately 80% of human lifespan variation (HERSKIND *et al.* 1996; SKYTTHE *et al.* 2003; HJELMBORG *et al.* 2006; PASSARINO *et al.* 2016; DATO *et al.* 2017). In terms of pathology, companion animals share many age-associated diseases with humans, and we have a sophisticated understanding of disease progression for many species through veterinary records (KOL *et al.* 2015; JIN *et al.* 2016; HOFFMAN *et al.* 2018). It is even suggested that studies in companion animals be built into the FDA drug approval process to span the "valley of death" between basic biomedical research and successful human disease treatment (KOL *et al.* 2015; GAMO *et al.* 2017). Beyond their utility as it relates to developing interventions for ourselves, delaying disease and extending lifespan in companion animals is an important end in itself. Considering the important role of pets in our lives and our efforts to care for them to our fullest abilities, it is clear that we generally regard these animals with the same deference as we do other people. Investing in the healthy life of companion animals, then, is an important way that we fulfill an obligation to them that is similar, if not identical, to the obligation we have in biomedical research to help each other.

The Dog Aging Project is a research program designed to develop companion dogs as a model system for aging and test the efficacy of rapamycin as a healthspan intervention in pets (KAEBERLEIN *et al.* 2016). This national study is enrolling dogs for longitudinal and intervention studies. In addition to survival, an important measure of intervention success in the rapamycin trials will be delayed disease onset. Veterinary records provide a good resource to establish breed specific age associated disease risk and life expectancy (BONNETT *et al.* 2005; EGENVALL *et al.* 2005; MATTIN *et al.* 2015; JIN *et al.* 2016; HOFFMAN *et al.* 2018). This allows a comparison of types of morbidities and comorbidities and when they occur between rapamycin treated and historical populations. Middle aged mid and large breed dogs ($\geq$ 40 pounds) were selected for the

first rapamycin experiments. Pilot studies with these dogs identified higher rates of asymptomatic heart valve degeneration than previously understood and provided evidence that short-term rapamycin treatment may improve age-associated cardiac decline (URFER *et al.* 2017a; URFER *et al.* 2017b).

1.15 Humans

The last translational step to humans is the most difficult. The ideal intervention, if started between 40-55 years old, would take decades to clearly assess in terms of delayed morbidity and mortality. This adds to the already substantial challenges associated with longitudinal research in humans (CARUANA *et al.* 2015). Despite its difficulty, clinical research that firmly establishes intervention efficacy in humans is critical to obtain. Proposed and ongoing human studies with metformin and rapamycin analogs (rapalogs) use more proximal measures of human healthspan and resilience in older individuals to assess efficacy. A further challenge is that no validated biomarker of biological age currently exists that can be used to validate and measure intervention success in human populations.

Initial clinical studies

The two best studied pharmacological healthspan and lifespan interventions to date are metformin and rapamycin. Metformin is a biguanide that was initially synthesized in the early 1920's for its potential antidiabetic properties. Interest in biguanides as a diabetes medication originates from early use of French lilac extract as a diabetes treatment (BAILEY AND DAY 1989).

This extract is rich in guanidine, an otherwise toxic compound with long-known antidiabetic properties (WATANABE 1918). Metformin is FDA-approved for type-II diabetes treatment (THOMAS AND GREGG 2017; ADAK *et al.* 2018). There is increasing evidence that metformin also broadly reduces cancer risk (LIBBY *et al.* 2009; BODMER *et al.* 2010; DECENSI *et al.* 2010; LEE *et al.* 2011; ZHANG *et al.* 2011; NOTO *et al.* 2012; SORANNA *et al.* 2012). Epidemiological studies and meta analyses also suggest that diabetics taking metformin have greater survival than age-matched non-diabetic controls (BANNISTER *et al.* 2014; CAMPBELL *et al.* 2017). In the near future, Targeting Aging with Metformin (TAME), a study led by researchers at Albert Einstein College of Medicine, will test metformin as a healthy aging intervention in the elderly (BARZILAI *et al.* 2016). TAME intends to recruit thousands of individuals 65-79 years of age across the US for a randomized, placebo-controlled trial with metformin. Survival, as well as morbidity and comorbidities, will be monitored during and after treatment.

Rapamycin was originally identified as an antifungal compound secreted by soil *Streptomyces* species on Easter Island (Rapa Nui) (VEZINA *et al.* 1975). These effects were known long before the mechanistic target of rapamycin (mTOR) was identified as a kinase complex that acts as a signaling hub in nutrient sensing (SABATINI *et al.* 1994; STAN *et al.* 1994; LORENZ AND HEITMAN 1995; SABERS *et al.* 1995). In the clinic, rapamycin is used in high doses as an immunosuppressive, particularly during organ transplant (SAUNDERS *et al.* 2001; EISEN *et al.* 2003). Like metformin, rapamycin and related analogs (rapalogs) are being explored for their anticancer potential (CLOUGHESY *et al.* 2008; MERIC-BERNSTAM AND GONZALEZ-ANGULO 2009). Current efforts to establish the benefits of rapamycin during human aging are focused on delaying age-associated immunosenescence (MANNICK *et al.* 2014). In an initial study, over 200 elderly (≥65 years old) individuals participated in a study that tested whether administration of the rapalog

everolimus improved immune response to an annual flu vaccination. Those treated with everolimus showed greater antibody response to flu vaccine than placebo treated controls with only minor side effects (mouth ulceration or headache). In another study by this group, combined treatment of everolimus with a catalytic mTOR inhibitor (BEZ235) improved immune response and prevented these side effects (MANNICK *et al.* 2017). Interestingly, a short-term (6 weeks) treatment with BEZ235 resulted in reduced annual rate of infection in the elderly compared to control (MANNICK *et al.* 2017). This suggests that immune changes associated with mTOR inhibition persist long after treatment is stopped.

Unmet needs

A standing challenge for human studies of healthspan intervention is measuring successful intervention. Unlike a traditional clinical trial, geroscience interventions are not aimed at treating or curing a specific disease after diagnosis. Instead, they should keep people healthy and alive longer, more akin to a preventative therapy. Due to the long lifespans of humans, this means that the length of time needed to assess efficacy is much longer than a typical clinical trial. As seen in the rapalog tests in elderly patients, more proximal measures, like immune function, can be used to assess intervention success. While this can be an effective path to FDA approval, it does not really demonstrate that an intervention is impacting the biological aging process.

Perhaps the greatest unmet need for translational geroscience are clinically validated biomarkers of aging that can be measured to assess changes in biological age (which is in contrast to chronological age, typically measured as the time since your birth). The American Federation for Aging Research propose that ideal biomarkers would be non-invasive, accurately measure

cellular health as it relates to age-related physiological decline, and be translatable to other systems in such a way that basic research can be performed utilizing the marker (AFAR 2016). Identifying such biomarkers has proven difficult; however, the advent of relatively inexpensive -omics technologies combined with powerful computational approaches such as machine learning have given new hope to finding predictive biomarkers (FABRIS *et al.* 2017). Recent efforts have focused on developing panels of multiple biomarkers that can be assayed together to meet these proposed guidelines (BURKLE *et al.* 2015; LARA *et al.* 2015). Overall, however, there remains no consensus on what marker(s) reliably predict age at this time.

An emerging biomarker of aging is the epigenetic clock. The epigenetic clock is composed of a set of methylated genomic CpG residues that, taken together, are highly predictive of biological age (HORVATH AND RAJ 2018). DNA methylation (DNAm) patterns are predictive of age in multiple tissues and respond to healthy lifestyle and diet (BOCKLANDT *et al.* 2011; HANNUM *et al.* 2013; HORVATH 2013; QUACH *et al.* 2017). Epigenetic clocks have been characterized for mice (under normal and caloric restricted conditions) and domesticated dogs (STUBBS *et al.* 2017; THOMPSON *et al.* 2017). Understanding methylation age, particularly in mice, provides new means of validating age-associated changes of other interventions that can be related to humans. The epigenetic clock is accelerated in progeroid conditions, like Werner syndrome (MAIERHOFER *et al.* 2017). Interestingly, the epigenetic clock is found to be accelerated in conditions not typically thought of as accelerating aging, like HIV infection and Down syndrome (HORVATH *et al.* 2015; HORVATH AND LEVINE 2015). Lifestyle factors, like stress, are also being recognized as driving accelerated epigenetic aging (PALMA-GUDIEL *et al.* 2015; ZANNAS *et al.* 2015; GASSEN *et al.* 2017).

What to expect

Increased disease-free lifespan is without doubt a great benefit to individuals, but what are the broader societal impacts of extending our healthy lifespan? One answer to this is found in the concept of the longevity dividend (OLSHANSKY *et al.* 2006; OLSHANSKY 2016). The longevity dividend refers to economic and other societal benefits that result from wide improvements in healthspan (OLSHANSKY 2018). Healthcare expenditure, for instance, will be fundamentally changed by breakthroughs in extended healthspan. In 2016, healthcare in the US cost $3.3 trillion dollars and 37% of that was paid through medicare or medicaid (HARTMAN *et al.* 2017). A great deal of these costs (37.9% as of 2013) are generated by treating chronic disease in elderly individuals, like heart disease, hypertension, and diabetes (LASSMAN *et al.* 2014; DIELEMAN *et al.* 2016). Breakthroughs in healthspan interventions that delay or prevent these conditions will likely save considerable money for individuals as well as local, state, and federal governments. Due to the similarities in healthcare between humans and companion animals (CREEVY *et al.* 2016), a key test of the longevity dividend concept as it relates to healthcare economics may be provided by successful geroscience intervention in pet dogs.

Beyond the question of whether interventions will extend human healthspan and lifespan, a related question that is less frequently asked is whether interventions will work the same for everyone. As seen in mice, many interventions preferentially extend lifespan in males (STRONG *et al.* 2008; HARRISON *et al.* 2009; NADON *et al.* 2017). In invertebrate CR studies using genetically diverse models, shorter lived strains tend to reap the largest benefits from the intervention (SCHLEIT *et al.* 2013; WILSON *et al.* 2018). Additionally, in the studies that revealed genotype-dependent responses to CR using the ILSXISS mice lines, the best responders to CR

were also among the shorter lived (RIKKE *et al.* 2010). An explanation proposed for this is that, the closer a population is to its maximum lifespan, the harder it will be to improve upon its lifespan (OLSHANSKY 2015). While this is certainly true, it is unclear if organisms studied in the lab are close to their physiological maximum lifespan. In yeast, for instance, even the longest lived strain tested (*sgf73Δ* median RLS = 42, WT median RLS = 25) showed a small increase in lifespan under CR (SCHLEIT *et al.* 2013). It seems, instead, that interventions like CR are inherently equitable, meaning that those who get the largest benefit from the intervention are those that need it the most.

Another important longevity dividend produced by successful healthy aging intervention may be decreased health disparities between different human populations. In the US, human survival is stratified based on sex, race, and Hispanic origin (**Figure 3**) (ARIAS *et al.* 2017). As of 2014, there is a 12-year difference in median survival between the longest lived group, Hispanic women (median lifespan = 88) and the shortest lived, black men (median lifespan = 76). Black men and women, along with white men, are the three shortest lived groups. We can model idealized human survival by assuming that the maximum human lifespan is close to what we've already witnessed, ~125 years, and that age-associated survival dynamics will be similar to the longest lived subgroup (Hispanic males and females) (**Figure 3a and 3b**). To achieve this ideal, an intervention (or combinations of interventions) would need to extend median lifespan by 30% in the longest lived populations and by closer to 40% in the shortest lived populations (black males and females). In terms of age-associated morbidities, comparing black and white populations (data for other groups is less reliable), the biggest difference in causes of death between these groups is due to diabetes (HERON 2016). If healthspan interventions are similarly equitable in human populations as they are in model systems, we may see the largest benefits in health among those

with the shortest lifespans, particularly black populations. Decreased health disparities that result from healthspan intervention can be thought of as another important longevity dividend.

1.16 Conclusions

Identifying and utilizing lifespan and healthspan extending interventions holds particular promise in extending lifespan and reducing human and companion animal disease burden. Common invertebrate systems provide models for discovery of lifespan extending compounds. Using diverse invertebrate systems, as well as models of genetic diversity and disease models, treatment efficacy can be evaluated in genetically diverse and evolutionarily distant organisms. Vertebrate model systems, particularly mice, provide a mammalian system to validate interventions and understand efficacy as it relates to genetic diversity and disease models. Translating successful interventions to companion pets, particularly dogs, provides a large, genetically diverse mammalian model to better evaluate interventions while potentially extending healthy lifespan of these animals, which is desirable and a biomedical breakthrough in itself. Finally, human healthspan interventions, while promising for all, may yield particular benefits for those already predisposed to shorter lifespan.

1.17 Acknowledgements

We thank Rich Miller and Francesca Macchiarini for datasets and helpful information regarding the Interventions Testing Program. We would like to thank Daniel Promislow, Alessandro Bitto, Benjamin Blue, and Michael Kiflezghi for careful review of the manuscript.

MBL was supported by the Howard Hughes Medical Institute (HHMI) Gilliam Fellowship for Advanced Study, the National Institutes of Health (NIH) Cellular and Molecular Biology training grant (T32GM7270-39), and the University of Washington Graduate Opportunities and Minority Achievement Program (UW GO-MAP) Bank of America Fellowship.

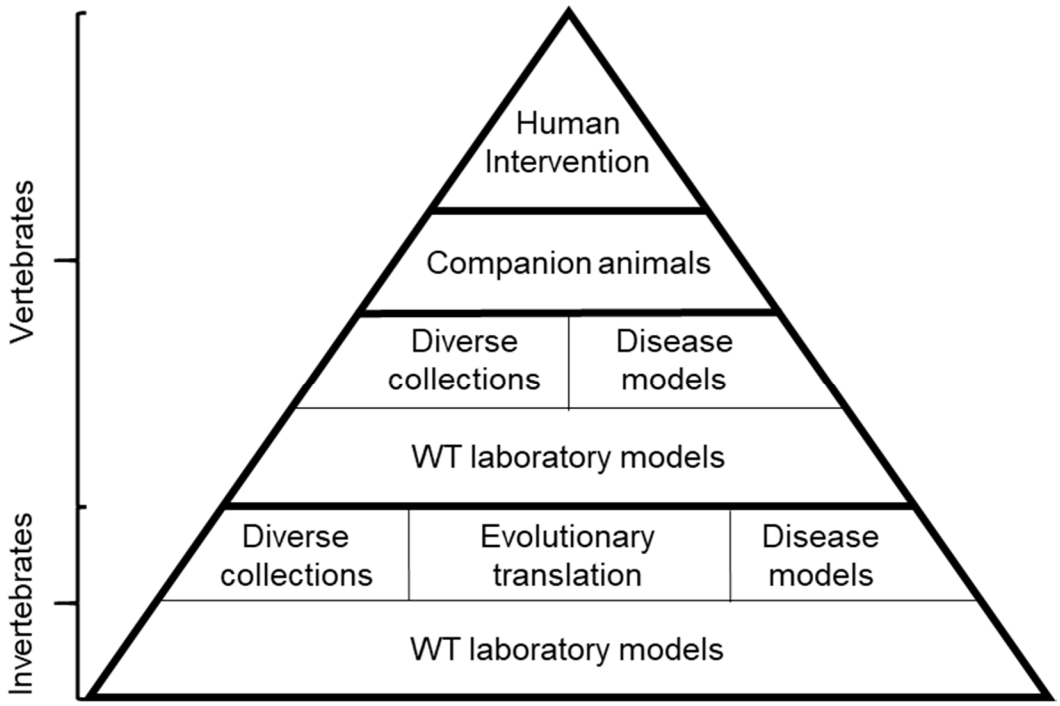

Figure 1.1. The translational pyramid for lifespan and healthspan intervention from invertebrates to companion animals and humans. Interventions are first screened using common laboratory models (either invertebrate or vertebrate). Successful interventions can then be studied for their efficacy among genetically-diverse collections. Disease models and other short-lived backgrounds can also be utilized to identify particular translational opportunities for interventions. Studies in genetically-diverse companion animals can validate interventions that are then tested in humans.

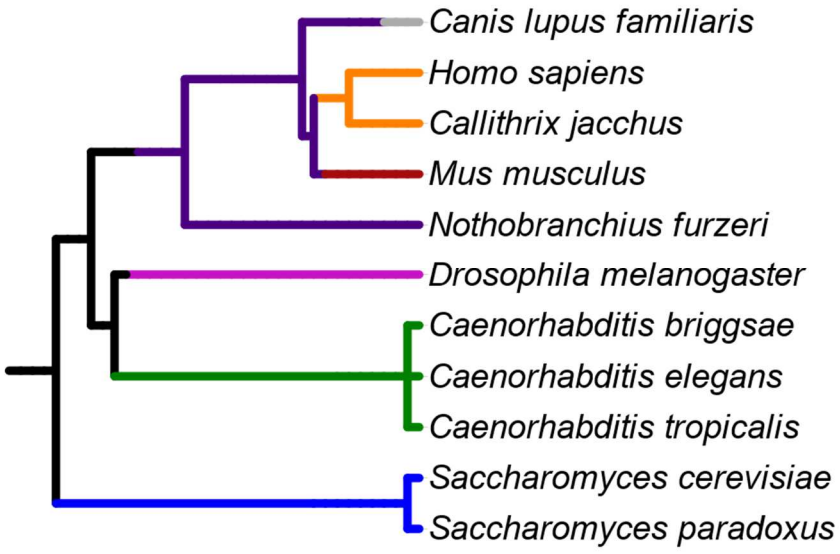

Figure 1.2. Phylogenetic relationships of key organisms used in Translational Geroscience research pyramid. Fungi = blue, nematodes = green, Arthropods = magenta, Vertebrates = dark purple, rodents = dark red, primates = orange, and canines = gray. Phylogenetic tree contructed using NCBI phyloT and Interactive Tree of Life (iTOL) v3 (LETUNIC AND BORK 2016).

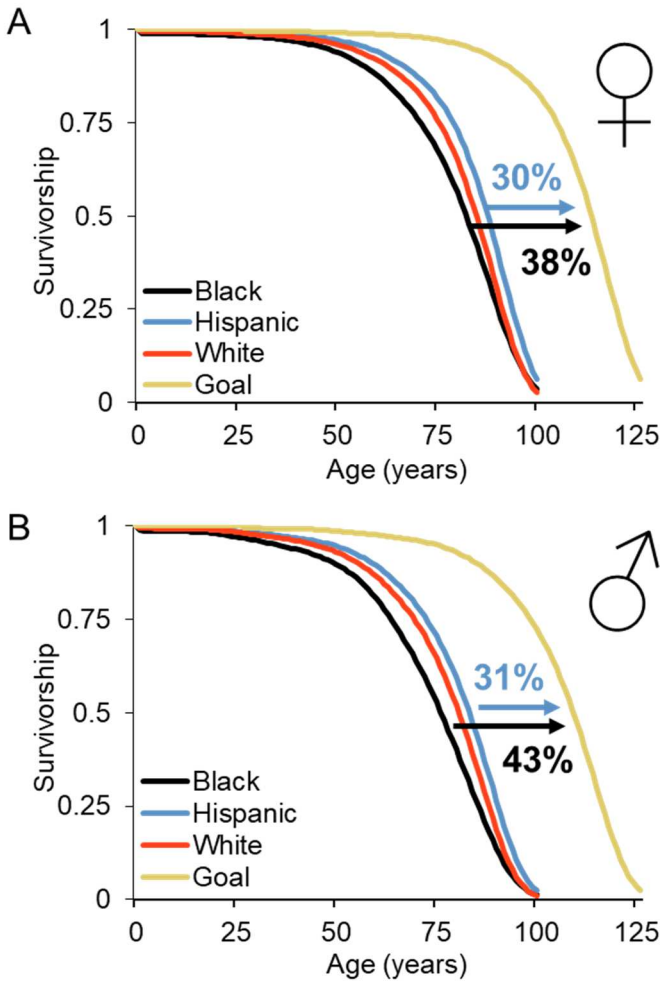

Figure 1.3. Human survival curves separated by sex, race, and Hispanic origin. A) females B) males. Gold curves represent idealized survival based on maximum human lifespan. Data from US life tables, 2014 (Arias et al., 2017).

Table 1.1. Interventions and concentrations tested, age treament started, median lifespan with 95% confidence intervals (CIs), number of animals enrolled (n), and percent change (compared to cohort controls) separated by sex, year enrolled (Cohort), and reference for compounds screened and in progress by the Interventions Testing Program, 2004-2018.

			Median lifespan and 95% CIs (days)							
Intervention	Concentration	Age started	Females	n	% change	Males	n	% change	Cohort	Reference
Control (combined)	NA	NA	886 (875-894)	2269	NA	803 (792-812)	2599	NA	Compiled	NA
Control	NA	NA	892 (860-916)	288	NA	790 (765-819)	379	NA	2004	Strong et al., 2008
4-OH-PBN	315 ppm	4 months	850 (827-905)	144	-4.7	813 (773-866)	180	2.9	2004	Strong et al., 2008
Aspirin	20 ppm	4 months	851 (835-878)	144	-4.6	852 (825-889)	180	7.8*	2004	Strong et al., 2008
Nordihydroguaiaretic acid (NDGA)	2,500 ppm	9 months	895 (862-923)	149	0.3	883 (847-911)	180	11.8*	2004	Strong et al., 2008
Nitrofluribprofen (NFP)	200 ppm	4 months	884 (845-915)	144	-0.9	815 (774-855)	181	3.2	2004	Strong et al., 2008
Control	NA	NA	887 (862-905)	296	NA	797 (769-835)	378	NA	2005	Harrrison et al., 2009
caffeic acid phenethyl ester (CAPE)	30 ppm	4 months	884 (855-920)	144	-0.3	817 (774-875)	180	2.5	2005	Harrrison et al., 2009
caffeic acid phenethyl ester (CAPE)	300 ppm	4 months	926 (886-965)	148	4.4	815 (748-852)	183	2.3	2005	Harrrison et al., 2009
Enalapril Maleate	120 ppm	4 months	868 (839-934)	144	-2.1	849 (807-875)	180	6.5	2005	Harrrison et al., 2009
Rapamycin	14 ppm	20 months	1005 (988-1058)	144	13.3*	952 (902-1004)	177	19.4*	2005	Harrrison et al., 2009
Control	NA	NA	891 (873-911)	272	NA	834 (800-869)	342	NA	2006	Miller et al., 2011
Rapamycin	14 ppm	9 months	1052 (1001-1112)	144	18.1*	902 (854-966)	171	8.2*	2006	Miller et al., 2011
Resveratrol	300 ppm	12 months	906 (870-939)	144	1.7	830 (794-879)	165	-0.5	2006	Miller et al., 2011
Resveratrol	1200 ppm	12 months	905 (867-944)	144	1.6	884 (845-908)	168	6.0	2006	Miller et al., 2011
Simvastatin	12 ppm	10 months	916 (883-952)	143	2.8	858 (809-888)	167	2.9	2006	Miller et al., 2011
Simvastatin	120 ppm	10 months	898 (869-933)	144	0.8	793 (753-853)	168	-4.9	2006	Miller et al., 2011

Control	NA	NA	866 (835-892)	281	NA	786 (749-827)	294	NA	2007	Strong et al., 2013
Curcumin	2000 ppm	4 months	905 (845-936)	132	4.5	808 (758-840)	158	2.8	2007	Strong et al., 2013
Green tea extract	2000 ppm	4 months	923 (898-944)	130	6.6	822 (778-881)	153	4.6	2007	Strong et al., 2013
Medium Chain Triglyceride Oil	60000 ppm	4 months	882 (852-931)	136	1.8	777 (734-853)	153	-1.1	2007	Strong et al., 2013
Oxaloacetic acid	2200 ppm	4 months	892 (855-940)	134	3.0	819 (760-858)	153	4.2	2007	Strong et al., 2013
Resveratrol	300 ppm	4 months	907 (877-939)	131	4.7	813 (767-869)	153	3.4	2007	Strong et al., 2013
Control	NA	NA	891 (869-915)	280	NA	807 (782-841)	300	NA	2009	Harrison et al., 2014
17α-Estradiol	4.8 ppm	10 months	902 (867-930)	136	1.2	900 (852-935)	156	11.5*	2009	Harrison et al., 2014
Acarbose	1000 ppm	4 months	939 (883-985)	136	5.4*	984 (952-1027)	156	21.9*	2009	Harrison et al., 2014
Methylene Blue	28 ppm	4 months	903 (866-945)	136	1.3	790 (738-848)	156	-2.1	2009	Harrison et al., 2014
Rapamycin	42 ppm	9 months	1131 (1115-1174)	136	26.9*	992 (911-1037)	156	22.9*	2009	Miller et al., 2014
Rapamycin	4.7 ppm	9 months	1037 (977-1079)	136	16.4*	834 (767-897)	156	3.3	2009	Miller et al., 2014
Rapamycin	14 ppm	9 months	1084 (1031-1149)	136	21.7*	909 (820-974)	156	12.6*	2009	Miller et al., 2014
Control	NA	NA	902 (873-940)	280	NA	784 (739-819)	300	NA	2010	Strong et al., 2016
Fish Oil	15000 ppm	9 months	863 (834-920)	136	-4.3	812 (771-876)	156	3.6	2010	Strong et al., 2016
Fish Oil	50000 ppm	9 months	923 (883-947)	136	2.3	734 (696-808)	156	-6.4	2010	Strong et al., 2016
Nordihydroguaiaretic acid (NDGA)	5000 ppm	6 months	880 (849-934)	136	-2.4	852 (818-892)	156	8.7*	2010	Strong et al., 2016
Nordihydroguaiaretic acid (NDGA)	800 ppm	6 months	NA	NA	NA	855 (820-931)	156	9.1*	2010	Strong et al., 2016
Nordihydroguaiaretic acid (NDGA)	2500 ppm	6 months	NA	NA	NA	875 (828-917)	156	11.6*	2010	Strong et al., 2016
Control	NA	NA	874 (862-896)	288	NA	785 (749-810)	306	NA	2011	Strong et al., 2016

17α-Estradiol	14.4 ppm	10 months	893 (858-931)	136	2.2	931 (867-966)	156	18.6*	2011	Strong et al., 2016
Bile Acids (ursodeoxycholic acid)	5000 ppm	5 months	884 (848-913)	136	1.1	839 (775-875)	156	6.9	2011	Strong et al., 2016
Metformin	1000 ppm	9 months	875 (839-922)	144	0.1	847 (800-887)	162	7.9	2011	Strong et al., 2016
Protandim®	600 ppm	10 months	887 (868-930)	136	1.5	853 (791-891)	156	8.7*	2011	Strong et al., 2016
Rapamycin + Metformin	14 ppm + 1000 ppm	9 months	1079 (1037-1123)	144	23.5*	955 (906-999)	162	21.7*	2011	Strong et al., 2016
Control	NA	NA	877 (852-914)	284	NA	821 (789-849)	300	NA	2012	Strong et al., 2016
Acarbose	1000 ppm	16 months	903 (873-950)	136	3.0	880 (814-916)	156	7.2*	2012	Strong et al., 2016
2-(2-hydroxyphenyl)-benzoxazole	1 ppm	15 months	856 (832-900)	136	-2.4	822 (790-853)	156	0.1	2012	NA
INT-767 FXR/TG5R agonist	180 ppm	10 months	868 (840-895)	136	-1.0	793 (762-836)	156	-3.4	2012	NA
Control	NA	NA	NA	NA	NA	NA	NA	NA	2013	In progress
Acarbose	2500 ppm	8 months	NA	NA	NA	NA	NA	NA	2013	In progress
Acarbose	1000 ppm	8 months	NA	NA	NA	NA	NA	NA	2013	In progress
Acarbose	400 ppm	8 months	NA	NA	NA	NA	NA	NA	2013	In progress
Ursolic Acid	2000 ppm	10 months	NA	NA	NA	NA	NA	NA	2013	In progress
Control	NA	NA	NA	NA	NA	NA	NA	NA	2014	In progress
Aspirin	60 ppm	11 months	NA	NA	NA	NA	NA	NA	2014	In progress
Aspirin	200 ppm	11 months	NA	NA	NA	NA	NA	NA	2014	In progress
Inulin	600 ppm	11 months	NA	NA	NA	NA	NA	NA	2014	In progress
Glycine	80,000 ppm	9 months	NA	NA	NA	NA	NA	NA	2014	In progress
TM5441	60 ppm	11 months	NA	NA	NA	NA	NA	NA	2014	In progress
Control	NA	NA	NA	NA	NA	NA	NA	NA	2015	In progress
17-DMAG	30 ppm	6 months	NA	NA	NA	NA	NA	NA	2015	In progress
Minocycline	300 ppm	6 months	NA	NA	NA	NA	NA	NA	2015	In progress
MitoQ	100 ppm	7 months	NA	NA	NA	NA	NA	NA	2015	In progress
Rapamycin – intermittent	42 ppm	20 months	NA	NA	NA	NA	NA	NA	2015	In progress

β-guanadinopropionic acid	3300 ppm	6 months	NA	NA	NA	NA	NA	NA	2015	In progress
Control	NA	NA	NA	NA	NA	NA	NA	NA	2016	In progress
17α-Estradiol	14.4 ppm	16 + 20 months	NA	NA	NA	NA	NA	NA	2016	In progress
Canagliflozin	180 ppm	7 months	NA	NA	NA	NA	NA	NA	2016	In progress
Candesartan Cilexetil	30 ppm	8 months	NA	NA	NA	NA	NA	NA	2016	In progress
Geranylgeranyl acetone	600 ppm	9 months	NA	NA	NA	NA	NA	NA	2016	In progress
MIF098	240 ppm	8 months	NA	NA	NA	NA	NA	NA	2016	In progress
Nicotinamide riboside	1000 ppm	8 months	NA	NA	NA	NA	NA	NA	2016	In progress
Control	NA	NA	NA	NA	NA	NA	NA	NA	2017	In progress
1,3-butanediol	100,000 ppm	6 months	NA	NA	NA	NA	NA	NA	2017	In progress
Captopril	180 ppm	5 months	NA	NA	NA	NA	NA	NA	2017	In progress
L-Leucine	40,000 ppm	5 months	NA	NA	NA	NA	NA	NA	2017	In progress
PB125	100 ppm	5 months	NA	NA	NA	NA	NA	NA	2017	In progress
Rapamycin + Acarbose	14.7 ppm + 1000 ppm	9 + 16 months	NA	NA	NA	NA	NA	NA	2017	In progress
Sulindac	5 ppm	5 months	NA	NA	NA	NA	NA	NA	2017	In progress
Syringaresinol	300 ppm	5 months	NA	NA	NA	NA	NA	NA	2017	In progress

* = significantly long-lived compared to cohort matched control.

Chapter 2. Genomic mutation burden decreases lifespan and accelerates aging in mutator yeast

Mitchell B. Lee[a], Ian T. Dowsett[a,b], Daniel T. Carr[a], Brian Wasko[a], Sarah G. Stanton[a], Michael S. Chung[a], Niloufar Ghodsian[a], Anna Bode[a], Michael G. Kiflezghi[a,b], Priya A. Uppal[a], Katherine A. Grayden[a], Yordanos C. Elala[a], Thao T. Tang[a], Ngoc H.B. Tran[a], Thu H.B. Tran[a], Anh B. Diep[a], Michael C. Hope[a], Daniel E. Promislow[a,c], Scott R. Kennedy[a], Matt Kaeberlein[a], Alan J. Herr[a,1]

[a]Department of Pathology, Box 357470, University of Washington, Seattle, WA, 98195-7705, USA.

[b]Molecular Medicine and Mechanisms of Disease (M3D) Program, Box 357470, University of Washington, Seattle, WA, 98195-7705.

[c]Department of Biology, Box 351800, University of Washington, Seattle, WA, 98195-1800, USA.

[1]To whom correspondence may be addressed: Alan J. Herr, Department of Pathology, Box 357470, University of Washington, Seattle, WA, 98195-7705, USA. Telephone: (206)…

Email: alanherr@uw.edu

2.2 Abstract

Mutations accumulate within somatic cells and have been proposed to contribute to aging. It is unclear what level of mutation burden may be required to consistently reduce cellular lifespan. Human cancer cells represent an intriguing model to test this hypothesis, since they carry the highest mutation burdens of any human cell. However, technical limitations make human cell culture ill-equipped to answer questions about single-cell aging. Here, we model the consequences of cancer-related mutator phenotypes on lifespan using yeast defective for mismatch repair (MMR) and/or leading strand (Polε) or lagging strand (Polδ) DNA polymerase proofreading. We show that high rates of active mutagenesis reduce lifespan in both haploid and diploid yeast and that combined defects in proofreading and MMR act synergistically to diminish lifespan. In diploids, we demonstrate that mutagenesis behaves as an accelerant of aging using Weibull Accelerated Failure Time analysis. Strong mutator phenotypes produce a form of genetic anticipation with regards to aging, where the longer a lineage persists the shorter-lived it becomes. Using mutation accumulation lines, we establish a relationship between mutation burden and lifespan, as well as population doubling time. Our observations define a threshold of random mutation burden that consistently decreases cellular longevity in diploid yeast cells. Many human cancer cells carry comparable mutation burdens, suggesting that their lifespan may be limited as well.

2.3 Significance statement

Mutations accumulate throughout life in every cell of the body. A long-standing question is to what extent these changes contribute to aging. Age is the single greatest risk factor for cancer, a disease driven by random mutagenesis and selection for malignant phenotypes. We wondered whether cancer cells age more rapidly, the more they proliferate and accumulate mutations. Human cells are ill-suited for single-cell measurements of aging. So, instead, we engineered diploid yeast to have cancer-associated defects that increase mutagenesis. We then measured lifespan and mutation accumulation. The lifespans of yeast cells decreased as the total number of mutations increased to levels commonly found in human cancers, suggesting that the longevity of cancer cells may be inherently limited.

2.4 Introduction

Accumulated mutation burden, alongside a host of other factors, has long been proposed as a driver of aging (LEPEZ-OTIN *et al.* 2013). Evidence from tumor exome sequencing and whole-genome sequencing of organoids derived from human stem cells show that somatic mutations accumulate during aging (JACOBS *et al.* 2012; LAURIE *et al.* 2012; WELCH *et al.* 2012; TOMASETTI *et al.* 2013; GENOVESE *et al.* 2014; JAISWAL *et al.* 2014; XIE *et al.* 2014; MILHOLLAND *et al.* 2015; BLOKZIJL *et al.* 2016; RISQUES AND KENNEDY 2018). It is unclear what level of mutation burden may be required to impact cellular aging and whether any human cells actually approach that level. Human cancer cells carry higher mutation burdens than any other human cell (ALEXANDROV *et al.* 2013) and therefore represent a biologically relevant system to explore this question. However,

technical limitations make human cell culture ill-equipped to answer questions about cellular aging at the single cell level. Budding yeast share many of the same DNA replication and repair pathways as human cells and are ideally suited to model the impact of mutation burden on cellular aging since there are cost-effective whole-genome sequencing methodologies and well-established single cell lifespan assays available (MORTIMER AND JOHNSTON 1959; EGILMEZ AND JAZWINSKI 1989; KENNEDY *et al.* 2015). Moreover, yeast growth assays provide a simple means to assess how mutation burden impacts cellular health.

Among the most highly mutated human cancers are those that express a "mutator phenotype" due to mutations that diminish DNA polymerase (Pol) proofreading and/or mismatch repair (MMR) (LYNCH *et al.* 2009; PALLES *et al.* 2013; SHLIEN *et al.* 2015). Simultaneous defects in these repair pathways elevate mutation rate synergistically to levels 1000-fold or more above background mutation rates in model systems (HERR *et al.* 2014). Such extreme mutator phenotypes drive extinction of bacteria and haploid yeast through the inactivation of essential genes (FUNCHAIN *et al.* 2000; HERR *et al.* 2011). Diploid yeast cells, which are buffered from this "error-induced extinction" by possessing an additional genome, nevertheless exhibit a catastrophic loss in fitness as mutation rate increases from 1×10^{-3} to 1×10^{-2} Can^r mutants/division (HERR *et al.* 2014). Interestingly, "ultra-mutator" tumors with combined defects in proofreading and MMR rarely surpass ~300 mutations/Mb, suggesting that extreme mutation burden may also limit growth of human cancer cells (SHLIEN *et al.* 2015).

Here, we model the consequences of cancer-related mutator phenotypes on lifespan in yeast defective for MMR and/or leading strand (Polε) or lagging strand (Polδ) polymerase proofreading. We show that high rates of active mutagenesis reduce lifespan in both haploid and diploid yeast and that combined defects in proofreading and MMR act synergistically to diminish lifespan. We

then show that accumulated mutation burden in these strains explain their severely shortened lifespan. To understand how mutation burden impacts cellular aging and population doubling time, apart from an active mutator phenotype, we assessed transiently-mutagenized diploid cells. We find that diploid yeast with mutation burdens past a certain threshold routinely exhibit diminished lifespan and a linear increase in doubling time when decoupled from an active mutator phenotype. Our results suggest that random mutation burden accrued in normal and cancer cells may similarly diminish their longevity and fitness.

2.5 Materials and methods

Media and Growth Conditions

Yeast strains were cultured as previously described (SHERMAN 2002). For standard growth, YPD [1% w/v Bacto™ yeast extract (BD), 2% w/v Bacto™ peptone (BD), 2% w/v dextrose] or synthetic complete (SC) [1.7 g/L Difco™ yeast nitrogen base w/o amino acids and ammonium sulfate (BD), 37.8mM ammonium sulfate, 2% w/v dextrose, 2 g/L synthetic complete amino acid mix (Bufferad)] were used. Unspecified reagents were purchased from Sigma-Aldrich or Fisher Scientific. Amino acid dropout media was used for prototrophic selection and prepared as described (SHERMAN 2002). For haploid mutation rates, Can^r mutants were selected using SC media lacking arginine and supplemented with 60 μg/mL L-canavanine. Diploid mutation rates used the above media with the addition of 100 μg/mL nourseothricin (RPI, Mount Prospect, IL, USA) to maintain counterselection for the *CAN1::natMX* allele and 1g/L monosodium glutamate instead of ammonium sulfate as nitrogen source. Selection against functional *URA3* strains was

performed using SC media supplemented with 1 mg/mL 5-fluorootic acid (FOA) (BOEKE *et al.* 1984). Sporulation in liquid media [1% w/v potassium acetate, 0.1% w/v Bacto™ yeast extract (BD), 0.05% w/v dextrose] was performed as previously described (LUNDBLAD AND STRUHL 2010).

Yeast strains

See **Supplementary Table S1** for a complete list of strains and **Supplementary Table S2** for all primers used in their construction. Strains AH0401 (*CAN1::natMX*/*can1Δ::HIS3*) and AH2801 (*POL2/URA3::pol2-4 MSH6/msh6Δ::LEU2 CAN1::natMX*/*can1Δ::HIS3*) were previously described (HERR *et al.* 2014; KENNEDY *et al.* 2015). To construct AH2601, we first deleted one of the two copies of *MSH6* in AH0401 to obtain AH0502, using a *LEU2* transgene amplified from pRS415 with MSH6GU and MSH6GD primers (*msh6Δ::LEU2*) [Phusion Polymerase (New England Biolabs, Ipswich, MA, USA); 98°C for 1 min. followed by 30 cycles of (98°C, 10 sec.; 54°C, 30 sec.; 72°C, 90 sec.)]. We then integrated the *pol3-01* allele by transformation with a *URA3::pol3-01* DNA fragment amplified from pRS406-pol3-01 with POL3U and pldr6 primers, as described (HERR *et al.* 2014).

Haploid mutator spore clones (**Figure 1**) were outgrown directly from dissected tetrads of AH2601 or AH2801 and genotyped via prototrophic growth and PCR genotyping assays. The *pol3-01* genotyping assay has been previously described (HERR *et al.* 2011). For the *pol2-4* assay, DNA was first PCR-amplified with pol2-4U and pol2-S5 primers (98°C 1 min. followed by 30 cycles of [98°C 10 sec.; 48°C 30 sec.; and 72°C, 1 min.]) and then digested with Alu I. A prominent 824 bp fragment observed in WT cells is cleaved into 447 and 377 bp fragments if the

DNA carries the *pol2-4* mutation. Diploid mutator strains described in **Figures 2-5** were obtained by mating freshly dissected AH2601 or AH2801 haploid spores by placing them adjacent to each other on the agar plate. Mating occurred within 2-4 haploid divisions and the resulting zygotes were moved by microdissection to a defined location on the agar plate to form a colony. We genotyped the *pol2-4* and *pol3-01* alleles, as described above, and assessed the status of *MSH6* using a PCR assay with the primers, msh6-upstream and msh6-downstream (**Supplementary Table S2**), which yielded distinct products for the *MSH6* (3.9 kb) and *msh6Δ::LEU2* (2.5 kb) alleles (98°C 1 min. followed by 30 cycles of [98°C 10 sec.; 60°C 30 sec.; and 72°C, 2.5 min.]). Frozen stocks were prepared by subcloning cells from the initial outgrown zygote colony onto a fresh plate and directly freezing to minimize mutation accumulation. Mutagenically-stable mutation accumulation lines (**Figure 6**) were derived from previously described *POL3/URA3::pol3-01,L612M* strains (HERR *et al.* 2014), which display an ultramutator phenotype due to the *pol3-01,L612M* allele. Ura$^-$ cells that had spontaneously lost the *pol3-01,L612M* allele through mitotic recombination were identified by plating frozen stocks onto FOA plates. We confirmed the absence of the mutator allele via *pol3-01* PCR genotyping as well as by demonstrating WT mutation rates.

Mutation rates via fluctuation analysis

Mutation rates were determined via fluctuation analysis using canavanine-resistance (Can^r). For haploid mutators, individual spore colonies taken directly from the dissection plate were treated as replica colonies and suspended in 200 μLs of water. Twenty μLs of cell suspension were used for 10-fold serial dilutions. The remaining undiluted suspensions, as well as 10 μLs of

each serial dilution, were plated onto canavanine selection plates to determine the number of Can^r mutants in each colony. Dilutions were also plated onto SC plates to estimate the total number of cells per colony (Nt) and onto prototrophic selection plates for genotyping. All plates were grown for two days at 30°C before determining colony counts. At least 12 independent spore clones of each genotype were used for mutation rate calculations. For diploid mutator strains, replica colonies were obtained by streaking frozen stocks onto YPD plates, followed by two days of incubation at 30°C. Colonies were suspended in 100 µLs of water and 20 µLs of cell suspension were used for serial dilutions. The remaining 80 µLs of undiluted cell suspension, as well as 10 µLs of all serial dilutions, were plated onto canavanine selection plates. Dilutions were also plated on SC to determine Nt values and on prototrophic selection plates to confirm genotypes. When possible, we counted Can^r colonies arising from the undiluted cell suspensions. For stronger mutator strains, Can^r mutants were quantified from dilutions. Between six and 12 colonies per genotype were analyzed in each experiment and 2-3 experiments were performed for each strain. Only replica colonies with similar Nt values were used for the final mutation rate calculations. To pool mutation rate data by genotype (**Figure 3**), we combined mutation counts from replicas with similar Nt values from multiple strains. The average number of mutational events occurring during the formation of the colonies (*m*) were estimated by maximum likelihood using newton.LD.plating in the R package rSalvador (ZHENG 2015). *m* was then divided by Nt to obtain Can^r mutants/cell division. The 95% confidence intervals were calculated using confint.LD.plating in rSalvador, and mutation rates were compared by a likelihood ratio test using LRD.LD.plating, which yielded p-values of the comparisons.

Replicative lifespan (RLS)

A modified RLS protocol was developed based on previously described methods (KAEBERLEIN *et al.* 2004; STEFFEN *et al.* 2009) to minimize outgrowth in actively-mutating and mutagenized strains. For haploid mutators, tetrads were dissected directly on lifespan plates and spores were used as mother cells. Early round daughter cells were retained until a small microcolony formed that was transferred to another location on the lifespan plate to outgrow. Once colonies formed, cells were suspended in 50 µLs water and 5 µLs were plated on prototrophic selection plates to determine genotype. For diploid mutator and mutation accumulation lines, frozen stocks were struck for isolates onto YPD and outgrown for two days at 30ºC. Colonies were then patched directly onto lifespan plates and virgin mother cells selected from freshly-divided cells. Survival curves were constructed and Wilcoxon rank sum statistical analyses performed using the RcmdrPlugin.survival package in R commander (FOX 2005; FOX AND CARVALHO 2012). Gompertz parameters were estimated using the R packages survival and flexsurv (THERNEAU 2000; THERNEAU 2015; JACKSON 2016; TEAM 2016).

Growth analysis using Bioscreen C MBR

Outgrowth of yeast was measured using a Bioscreen C MBR (Growth curves USA, Piscataway, NJ, USA) as previously described (MURAKAMI *et al.* 2008). For active mutator lines, colonies were grown out either from dissected haploid spores or from frozen diploid stocks and suspended in 50 µLs without further propagation. For mutation accumulation lines, colonies were outgrown from frozen stocks, then inoculated into five mLs YPD and incubated at 30ºC in a roller drum for 12-16 hours. Two µLs of either cell suspension or outgrown culture was used as

inoculum into 148 μLs YPD for growth analysis. At least three colonies per strain were analyzed in triplicate for each experiment. Doubling times were calculated from the interval $0.2 \leq x \leq 0.5$ $OD_{420\text{-}580nm}$ using the online web tool Yeast Outgrowth Data Analyzer (YODA) (OLSEN *et al.* 2010). Two-tailed t-tests with unequal variance were performed from average doubling time of replicate cultures using R. Bonferroni-corrected p-values were calculated using p-adjust.

Whole-genome sequencing

To estimate the mutation burden of mother cells at the beginning of RLS, frozen stocks of each strain were struck for single colonies on YPD plates and outgrown for two days at 30ºC. Three independent colonies were then patched directly onto fresh plates and one individual virgin mother cell from each patch was moved to a defined location and allowed to form a colony. We inoculated five mLs YPD cultures from these colonies and purified genomic DNA using the ZR Fungal/Bacterial DNA mini-prep Kit (Zymo Research, Irvine, CA, USA). Genomic DNA (200 ng) samples were sheared in a volume of 60 uLs using a Covaris sonicator (peak incident power = 105 (for 96-well format), Intensity = 3 (for single sample cuvettes), Duty factor = 5%, Cycles/burst = 200, 40 sec). After concentrating the DNA with a 0.8x Agencourt AMPure XP bead purification (Beckman Coulter Life Sciences, Indianapolis, IN, USA), we performed one-third volume 3′ End repair reactions using the NEBNext Ultra End Repair/dA-Tailing module (New England Biolabs, Ipswich, MA, USA) followed by ligation to annealed DNA adapter oligos (**Supplementary Table S2**) using the NEBNext Ultra Ligation Module. Following another 0.8x AMPure bead purification, the resulting libraries were single or dual-indexed by quantitative PCR (QPCR) (for primers see **Supplementary Table S2**) (program: Initial denature: 98ºC, 45 seconds; cycle

denature: 98°C, 15 seconds; annealing: 65°C, 30 seconds; elongation: 72°C, 30 seconds) with Kapa HiFi Hotstart Ready Mix (KAPA Biosystems, Wilmington, MA, USA). The indexed DNA samples were purified using a double bead purification procedure in which we first removed fragments larger than ~1000 bp by performing a 0.55x AMPure bead purification. We then precipitated fragments larger than ~500 bp in the resulting supernatant by bringing the total volume of bead suspension added to 0.65x. We quantified the DNA using a Qubit dsDNA HS Assay Kit (Life Technologies Waltham, MA, USA) and pooled the samples by mass before sequencing the mixture on either a HiSeq 2500 [reagents: TruSeq Rapid SBS Kit v2 (500 cycle) (Illumina, FC-402-4023), TruSeq Rapid PE Cluster Kit v2 -HS (Illumina, PE-402-4002)] or NextSeq 500 [reagents: Mid-Output Kit V2 (Illumina, FC-404-2003)]. An established computational pipeline was used to align sequencing reads and identify mutations within individual strains (KENNEDY *et al.* 2015). As part of this pipeline, polymorphisms present in the parental strain (AH0401), as well as recurring mapping artifacts, were identified and excluded from our analyses. We also documented and followed the inheritance of strain-specific variants present in AH2601 and AH2801. The total number of mutations present in each strain was divided by the total number of bases scored and multiplied by 10^6 to obtain the number of mutations/Mb. For **Figure 3**, the mutation burden was averaged among isolates of the same mutator genotypes and standard error of the mean (SEM) used to express the variance in the data.

2.6 Results

Diminished replicative lifespan negatively correlates with increased mutation rate in haploid mutator yeast

To investigate how mutator phenotypes influence cellular aging, we first measured replicative lifespan (RLS) of haploid spores with mutations affecting base-base MMR (*msh6Δ*) and/or Polε proofreading (*pol2-4*) or Polδ proofreading (*pol3-01*). The spores were freshly dissected from diploid yeast strains that were heterozygous for the mutator alleles (AH2601 and AH2801). We reasoned that the low mutation rate of these diploid strains would ensure that the haploid spores began life with a modest mutation burden. Any background mutations with lifespan effects would be expected to segregate equally to each genotype, controlling for any adverse effects on lifespan. Spores defective for Polδ proofreading (*pol3-01*) exhibited a 30% decrease in median lifespan (median RLS = 18, n = 74), compared to WT (median RLS = 24, n = 161) (**Figure 1a**, Wilcoxon rank sum test, $p < 0.001$). In the absence of Msh6, Polδ proofreading deficiency (*pol3-01 msh6Δ*) reduced median lifespan by 65% (median RLS = 9, n = 78) (Wilcoxon rank sum test, $p < 0.001$). Neither Msh6- nor Polε-proofreading-defective spores (*pol2-4*) were short-lived relative to WT (**Figure 1a**). However, *pol2-4 msh6Δ* double mutant spores were as short-lived as *pol3-01* spores (median RLS = 17, n = 83) (Wilcoxon rank sum test, $p < 0.001$). Thus, alone, individual mutator alleles compromise RLS to a variable extent, but in combination, they consistently impose a marked reduction in lifespan.

The mutator phenotypes of the strains used for the RLS analyses conformed to the reported values from previous studies (HERR *et al.* 2011) (**Figure 1b**). Lack of Polε proofreading (*pol2-4*) or Msh6 elevated mutation rates 2-6-fold, while lack of Polδ proofreading (*pol3-01*) increased mutation rates 32-fold. Combined defects to Msh6 and Polε proofreading (*pol2-4 msh6Δ*) increased mutation rates synergistically to 200-fold greater than WT. A mutation rate for *pol3-01 msh6Δ* haploids could not be determined since they failed to form macroscopic colonies due to

error-induced extinction. Mutation rates for these spores can be estimated at ~$1x10^{-3}$ Can^r mutants/cell division based on our previous work on the haploid error-threshold (HERR *et al.* 2011) and the measured mutation rates of *pol3-01 msh2Δ* diploid strains (HERR *et al.* 2014). A linear model of the relationship between mutation rate and median RLS reveals a strong negative correlation (**Figure 1c**) (adjusted R-squared = 0.81, p = 0.009), suggesting that random mutagenesis drives reduced lifespan in these spores.

We previously found that *pol2-4 msh6Δ* cells accumulate an average of 2.6 mutations per division (KENNEDY *et al.* 2015). Given a median lifespan of 17 divisions, *pol2-4 msh6Δ* mother cells would have an average of ~44 mutations at the time of death. In contrast, *msh6Δ* and *pol2-4* cells, whose mutation rates are ~100 times less than *pol2-4 msh6Δ* haploids would be expected to accumulate less than one mutation over a lifetime (0.026 mutations/division x 25 median RLS). Assuming 0.5 mutations/division and a lifespan of 18 divisions, *pol3-01* cells would die with an average of 9 mutations, while *pol3-01 msh6Δ* cells may have as many as 234 mutations (26 mutations/division x median RLS of 9). Thus, mutator spores with reduced lifespan are those that have the greatest opportunity to accumulate mutations within their average lifespan.

Repair of DNA replication errors is required for normal lifespan in diploid yeast

Since diploidy likely buffers human cells from the consequences of mutagenesis during cancer and aging, we sought to model the influence of mutation burden on diploid yeast cells. We created various diploid mutator strains by randomly mating haploid spores dissected from tetrads from the same parental strains used for our haploid RLS studies. For each genotype, we isolated and froze multiple independent strains. From frozen stocks, single colonies were isolated and

patched onto fresh plates to isolate mother cells for 20-cell aging cohorts (**Figure 2A**). Multiple independent cohorts were used for lifespan measurements of each strain. To interpret our lifespan data, we assessed mutation rates (**Figure 2B**), and mutation burden (**Figure 2C**).

To facilitate mutation rate measurements in diploid cells, the parental strains were engineered to be hemizygous for the *CAN1* gene (*CAN1::natMX/can1Δ::HIS3*). We screened all mated diploid strains for this hemizygous configuration. We observed that *CAN1* hemizygous strains (designated WT for our studies) were longer-lived than BY4743, the diploid background strain (**Supplementary Figure S1**) (WT median RLS = 39, n = 761; BY4743 median RLS = 34.5, n = 660, $p < 0.001$, Wilcoxon rank sum test). Loss of *CAN1* extends lifespan in haploid yeast (BEAUPERE *et al.* 2017). Our data suggests that this longevity phenotype depends on gene dosage in diploids. Our strict use of *CAN1::natMX/can1Δ::HIS3* strains eliminates this potential source of variation in our aging measurements.

To estimate the mutation burden at the beginning of lifespan analysis, we sequenced three independent clones patched and isolated identically to those used in our lifespan cohorts. As controls, we sequenced the genomes of three independent isolates of the parental strains, AH2601 and AH2801. We found that AH2601 isolates shared nine clonal mutations that segregated in AH2601-derived strains. AH2801 isolates had no common mutations. Every AH2601 and AH2801 isolate carried 5-13 unique variants. Unique mutations in the haploid spores used for mating contribute to starting mutation burdens in our diploid strains, along with any additional mutations that arose in the few haploid divisions prior to mating haploid spores.

Mutations continually arise in our mutator lines. Clonal mutations affect cells in all lifespan cohorts and will have the largest potential impact on survival demographics. Subclonal variants arise during the initial propagation of the diploid strain and are fixed by isolating single

colonies from frozen stocks. These are most likely to influence lifespan of individual cohorts. Subclonal variants that arise after this single cell bottleneck will be largely private to individual cells within the cohort and likely generate greater variability within survival cohorts. However, the probability of deleterious mutations and synthetic interactions increases as a function of aggregate mutation burden. There may be a level of mutation burden where every cell carries subclonal or private lifespan-limiting mutations, giving the appearance of a uniform effect across the entire population.

WT, *MSH6/msh6Δ*, *POL2/pol2-4*, and *POL2/pol2-4 MSH6/msh6Δ* strains derived from our mating experiments exhibited similar median lifespans, mutation rates, and mutation burdens as the WT parental strain (yML046) used to construct AH2601 and AH2801 (**Supplementary Table S1**). Importantly, the WT strain derived from AH2601 (AH3251) contained all nine AH2601 mutations (six nonsynonymous changes), suggesting that none of these variants in the heterozygous state influence lifespan. Strains lacking Msh6 (*msh6Δ/msh6Δ*) or Polε proofreading (*pol2-4/pol2-4* and *pol2-4/pol2-4 MSH6/msh6Δ*) displayed a 10-fold increase in mutation rate relative to WT (**Figure 2B**) and a fractional increase in mutation burden (**Figure 2C**). Seven out of the nine isolates of these three genotypes displayed moderate declines in median lifespan even though deficiencies in Polε proofreading or Msh6 failed to reduce lifespan in haploids. The genotypes of the two strains with normal lifespans, yML262 (*msh6Δ/msh6*Δ) and yML268 (*pol2-4/pol2-4 MSH6/msh6Δ*) suggests that reduced RLS derives from strain-specific mutations rather than the *msh6Δ/msh6Δ* or *pol2-4/pol2-4* mutator genotypes.

A review of the history of each strain and their genomic sequence supports the hypothesis that strain-specific mutations, and not genotype, reduce lifespan. yML268 is derived from the same AH2801 culture from which we isolated WT (yML279), *MSH6/msh6Δ* (yML280, yML281),

and *POL2/pol2-4 MSH6/msh6Δ* (yML267, yML271, and yML274) strains. A different AH2801 culture served as the source for short-lived *msh6Δ/msh6Δ* (yML337 and yML338), *pol2-4/pol2-4* (yML329 and yML332), and *pol2-4/pol2-4 MSH6/msh6Δ* strains (yML326). These strains carried two nonsynonymous mutations (*yel020c-A58V*, and *vid30-P18Q*). Deletion of *VID30* reduces chronological lifespan (BURTNER *et al.* 2011; MAREK AND KORONA 2013). Although the RLS of yML338, yML329, and yML332 were the same, yML337 and yML326 were shorter-lived. yML337 carried two additional heterozygous nonsynonymous mutations while yML326 had a different set of five heterozygous nonsynonymous mutations. The remaining short-lived *pol2-4/pol2-4 MSH6/msh6Δ* strains (AH4703 and AH4713) came from a different AH2801 culture and shared two different heterozygous nonsynonymous mutations (*ade6-G445R* and *stt4-K1223N*) and one homozygous mutation (*bcp1-A4D*). Variation in lifespan was also observed among the *POL3/pol3-01* strains (AH3203, AH3228, AH3240, and AH3241), which were all derived from the same AH2601 culture. One strain (AH3228) had a significantly shorter median lifespan than the others and carried three unique heterozygous nonsynonymous mutations (*hnm1-W372L*, *ypl068C-N98I*, *mms1-K861Q*). Taken together, these observations suggest that relatively small numbers of heterozygous mutations, acting alone or in combination, can reduce diploid yeast lifespan.

Clonal mutation did not explain reduced RLS in the six *POL3/pol3-01 MSH6/msh6Δ* strains. These strains exhibited similar mutation rates as the *POL3/pol3-01* strains. Some of these strains had higher clonal mutation burdens, which likely indicates that a WT and a strongly mutagenic *pol3-01 msh6Δ* spore were mated to generate those strains. All six strains were isolated from the same AH2601 culture. Two nonsynonymous mutations segregated among these strains, but neither variant was present in all six isolates. Reduced lifespan in *POL3/pol3-01 MSH6/msh6Δ*

cells may be due to a shared mutation missed by our analysis, different clonal mutations specific to each strain, or the *POL3/pol3-01 MSH6/msh6Δ* genotype itself.

Evidence for an effect of mutation burden on diploid longevity grew more pronounced as we analyzed strains with increasingly stronger mutator phenotypes. Despite a ~10-fold increase in mutation rate and mutation burden (10 mutations/Mb), the two *POL2/pol2-4 msh6Δ/msh6Δ* strains (AH4730 and yML275) exhibited similar lifespans as the *msh6Δ/msh6Δ*, *pol2-4/pol2-4*, and *pol2-4/pol2-4 MSH6/msh6Δ* strains. Mutation rate and burden increased an additional three- to four-fold in the six *pol2-4/pol2-4 msh6Δ/msh6Δ* strains. These strains displayed consistently lower median lifespans than weaker mutator strains with the same shared inherited variants (compare yML272 with yML268; AH4712 and AH4737 with AH4703; and yML327, yML335 and yML340 with yML329). AH2601-derived strains with similar mutation rates and burdens as the *pol2-4/pol2-4 msh6Δ/msh6Δ* strains displayed similar reductions in lifespans (*pol3-01/pol3-01*, *pol3-01/pol3-01 MSH6/msh6Δ*, and *POL3/pol3-01 msh6Δ/msh6Δ*). Variability in RLS was apparent among isolates of the same genotype, but was not explained by inherited mutations segregating among these strains. Since the effect of mutation burden on lifespan appears to lack uniformity, each strain may contain only a limited number of mutations (or combinations of mutations) that reduce lifespan. A further 10-fold increase in mutation burden produced a dramatically shortened RLS in every *pol3-01/pol3-01 msh6Δ/msh6Δ* strain (combined median RLS = 6, n = 240, $p<0.001$, Wilcoxon rank sum test), suggesting that lifespan declines dramatically when mutation burden exceeds a certain threshold.

Decreased lifespan strongly correlates with increased mutation rate and mutation burden in diploid mutator yeast

We performed linear modeling to characterize the relationship between mutagenesis and reduced lifespan in diploid mutator strains. First, we compared the relationship between increased mutation rate and mutation burden after pooling the data on the basis of genotype (**Figure 3a**). As expected, a strong log-log linear relationship exists between increased mutation rate and average mutation burden in diploid mutators (adjusted R-squared = 0.9, $p < 0.001$). Next, we compared mutator median RLS to mutation rate (**Figure 3b**). In this and subsequent correlation studies, *pol3-01/pol3-01 msh6Δ/msh6Δ* strains were identified as outliers by analyzing residuals and not included in the linear models. Median RLS decreased linearly as mutation rates increased across three orders of magnitude (adjusted R-squared = 0.82, $p < 0.001$). We also compared median RLS to mutation burden (**Figure 3c**). To improve resolution, instead of pooling by genotype, we analyzed all individual strains where RLS and mutation burden had been quantified. Again, a strong negative relationship was observed between increased mutation burden and decreased RLS (adjusted R-squared = 0.55, $p < 0.001$).

Mutator-driven mutagenesis is an accelerant of cellular aging

Progeria syndromes, including Werner, Bloom, Xeroderma pigmentosum, Cockayne, trichothiodystrophy, and the collection of syndromes known as the laminopathies, all share some form of genome instability as a unifying disease driver (RAMIREZ *et al.* 2007). To understand if polymerase proofreading and MMR defects are sufficient to promote a progeria-like phenotype at the single cell level, we modeled increased mutation rate (**Figure 4a**) and burden (**Figure 4b**) as an accelerant of aging using Weibull Accelerated Failure Time (AFT) analysis. We identified

appropriate mutator genotypes to use for this analysis by comparing their log-transformed cumulative hazard plots to that of the WT control (**Supplementary Figure S3**). Genotypes that satisfied the assumptions for Weibull proportional hazards analysis were linear and did not change the slope of the cumulative hazard relative to WT. We found decreased Weibull acceleration factor correlated with increased mutation rate (adjusted R-squared = 0.79, $p < 0.001$) and mutation burden (adjusted R-squared = 0.60, $p < 0.001$), supporting the hypothesis that increased numbers of point mutations promote a progeria-like phenotype during cellular aging.

Genetic anticipation in the lifespan reduction of mutator diploid cells

Most lifespan cohorts experience a period of low early-life mortality before deaths increase with age. The *pol3-01/pol3-01 msh6Δ/msh6Δ* cells, however, began to die at a constant rate from the very first division, which produced a Weibull cumulative hazard plot with a very different intercept and slope than any other plots in our analysis. Even *pol3-01 msh6Δ* haploids underwent several divisions before mortality became apparent (**Figure 1a and 2a**). Combined deficiencies in Pol δ proofreading and MMR could conceivably increase early mortality independent of the mutator phenotype in diploid cells. Alternatively, early deaths in *pol3-01/pol3-01 msh6Δ/msh6Δ* cells may derive from elevated mutation burden combined with a strong mutator phenotype. Haploid lifespans were measured from the very first division of the full mutator phenotype, whereas diploid lifespan measurements began after a period of propagation and thus accumulated variable mutation burdens (**Figure 2c and Extended Dataset 2**). If reduced lifespan in *pol3-01/pol3-01 msh6Δ/msh6Δ* diploids depends on mutation burden, then this phenotype should

display a form of genetic anticipation, evidenced by replicative lifespan growing ever shorter the longer a lineage persists.

To test for genetic anticipation, we measured lifespans of freshly-isolated *pol3-01/pol3-01 msh6Δ/msh6Δ* diploid cells (**Figure 5**). We first dissected tetrads from the *POL3/pol3-01 MSH6/msh6Δ* parent strain (AH2601) onto media that selected for double mutant haploid spores. We mated the haploids after 2-3 divisions, manually isolated the resulting zygotes, and then used the first or second diploid daughters as mother cells for lifespan analysis. Daughter cells from each zygote were transferred to separate locations on the plates to form colonies for genotyping. To test for genetic anticipation, we patched six of these colonies onto lifespan plates, selecting cells after an overnight incubation (d3 series). Cells from these patches were patched onto a second set of lifespan plates and cells were again selected after an overnight incubation (d4 series). In each lifespan measurement, we set aside three mother cells to form colonies for whole genome sequencing. As controls, we measured lifespans of cells from one of our previous diploid *pol3-01/pol3-01 msh6Δ/msh6Δ* strains, as well as the AH2601 parent strain.

AH2601 displayed a similar lifespan (median RLS = 27, n = 60) as *POL3/pol3-01 MSH6/msh6Δ* strains derived from mating (median RLS = 30, n = 720), which provides further evidence that the *POL3/pol3-01 MSH6/msh6Δ* genotype inherently limits lifespan (**Figure 5**). Freshly-isolated double mutant cells appear shorter-lived (median RLS = 22, n = 21) than AH2601, especially over the last quartile, but this did not rise to the level of significance after a multiple-testing correction ($p = 0.075$, Wilcoxon rank sum test, Bonferroni-corrected). The freshly-isolated double mutant cells, however, were substantially longer-lived than their passaged descendants (Median RLS = 8, n = 240 for both passaged lines) and the previously isolated control diploid mutator strain (median RLS = 6, n = 60) ($p < 0.001$, Wilcoxon rank sum test, Bonferroni-

corrected). Mutation burden in the new passaged lines averaged 176 mutations/Mb, which was significantly higher than the average of 40 clonal mutations/Mb present in the mother cells near the beginning of their lifespan, as estimated by sequencing DNA extracted from pooled cells from each patch. Thus, reduced RLS due to strong mutator phenotypes shows genetic anticipation, further defining the impact of mutation burden on cellular lifespan.

Effect of random mutation burden on cellular lifespan and doubling time in the absence of an active mutator phenotype

Although mutation certainly explains the variation in lifespan among strains of the same genotype and underlies the genetic anticipation of lifespan reduction in strong mutator strains, we found evidence to suggest that the mutator genotypes in some cases may contribute to reduced lifespan. To explore the effects of mutation burden on lifespan decoupled from an ongoing mutator phenotype, we generated diploid yeast mutation accumulation (MA) lines mutagenized by transient expression of a powerful mutator allele (*pol3-01,L612M*) (HERR *et al.* 2014). In a previous study, we used a *URA3* transgene to select for integration of the *pol3-01,L612M* allele at the *POL3* locus (HERR *et al.* 2014) and archived the transformants. We recovered *POL3/URA3::pol3-01,L612M* lines from frozen stocks by streaking for single colonies on Ura$^-$ plates and then plated the cells onto 5-fluoroorotic acid (5-FOA)-media to select for mitotic recombinants that had spontaneously lost the *URA3*::*pol3-01,L612M* allele (BOEKE *et al.* 1984). In this manner, we obtained eleven transiently-mutagenized *POL3/POL3* lines, each derived from an independently isolated *POL3/URA3::pol3-01,L612M* diploid strain. All strains exhibited WT

mutation rates, suggesting that the accumulated mutation burden had not introduced additional mutator alleles (data not shown).

Whole-genome sequencing of the MA lines revealed a wide range of mutation burdens from 0.4 mutations/Mb to 100 mutations/Mb (**Figure 6a**). Four of the five least mutagenized MA lines (MA1, 2, 4, and 5) retained a normal lifespan and had mutation burdens ranging between 0.9 and 31.1 mutations/Mb, respectively). The lone exception (MA3) had 12.4 mutations/Mb and a 43% reduction in median RLS (Wilcoxon rank sum test, $p < 0.001$, Bonferroni-corrected for multiple tests). All strains with a mutation burden greater than 31.6 mutations/Mb showed at least a 29% decrease in lifespan (**Figure 6b**, $p < 0.001$ for all strains, Wilcoxon rank sum test, Bonferroni-corrected). The most severely affected strain (MA7), with a 63% decrease in median lifespan, had a mutation burden of 39.7 mutations/Mb. Thus, increased mutation burden apart from an ongoing mutator phenotype consistently produced diminished lifespan above a threshold. The MA3 and MA7 replicative lifespans suggest that even with large mutation burdens, rare mutations (or combinations of mutations) can still exert a disproportionate effect on RLS.

In addition to survival, we sought to understand how mutation accumulation impacted overall population health. One way to assess health in a microbial culture is to quantify peak doubling time (minutes/cell division) in an outgrowing population (LEE *et al.* 2017). We measured growth of the MA lines with a Bioscreen C MBR reader/shaker/incubator and calculated doubling time using Yeast Outgrowth Data Analyzer (YODA) (OLSEN *et al.* 2010). Linear modeling revealed a strong correlation between mutation burden and population health as measured by doubling time (adjusted R-squared = 0.87, $p < 0.001$) (**Figure 6c**).

The role of accumulated mutation burden in driving diminished lifespan and increased doubling time in mutagenic diploid yeast

Combining data from the genetic anticipation and mutation accumulation studies **(Figures 5 and 6)** with our diploid mutator dataset, we re-examined the relationship between accumulated mutation burden and diminished lifespan in all of our diploid strains (**Figure 7a**). At the lowest burdens (0.04-0.4 mutations/Mb), median RLS was unchanged. Intermediate mutation burdens (0.4-35 mutations/Mb) were variable with regard to their impact on lifespan. This variability suggests that individual mutations and synthetic interactions between mutations drive diminished survival in modestly mutagenized populations. Above 35 mutations/Mb, lifespan is consistently and severely diminished (at least a 42% reduction in median RLS). Interestingly, this is true in transiently-mutagenized diploids as well as active mutator strains, suggesting that all strains carry sufficient numbers of these lifespan-limiting mutations.

To better characterize how mutation burden impacted health of our yeast populations, we expanded our analysis of peak doubling time to include all diploid strains (**Figure 7b**). Using untransformed data, linear modeling revealed a strong correlation between increased mutation burden and doubling time (adjusted R-squared = 0.85, $p < 0.001$). Interpretation of this correlation is challenged, however, by the large number of data points from strains with very low mutation burdens. We log-transformed mutation burden data (**Figure 7c**) and found that doubling time was consistent across mutation burdens for three orders of magnitude (0.04-30 mutations/Mb). Above 30 mutations/Mb, doubling time exponentially increased. As we saw with median RLS, transiently-mutagenized populations behaved similarly to populations with an active mutator phenotype. Strikingly, the threshold for increased doubling time corresponds to the level at which

mutation burden severely impacts RLS. This shows a clear link between decreased cellular lifespan and degraded population health resulting from elevated mutation burden.

2.7 Discussion

Accumulated somatic mutation burden has long been theorized to drive aging (FAILLA 1958; SZILARD 1959; FREITAS AND DE MAGALHAES 2011). It is clear that a variety of mutations, from single basepair changes to large chromosomal translocations, accumulate with age in flies, mice, and humans (VIJG AND DOLLE 2002; GARCIA *et al.* 2010; JACOBS *et al.* 2012; LAURIE *et al.* 2012). Yet the contribution of mutation load to the age-related decline of the soma remains difficult to assess. A full accounting of the total mutation burden of individual aged cells is obscured by technical limitations of accurately sequencing single cells. Moreover, the field has lacked clear functional tests to distinguish the effects of age-associated mutation burden from the effects of other types of damage that accrue over a lifetime. Testing this hypothesis has relevance not only for normal aging but also for understanding the intrinsic longevity of cancer cells. To bridge the gap in our understanding of how mutation burden influences aging, we elevated random mutation burden using mutator alleles in the well-established model of cellular aging, budding yeast.

In haploids, prior research showed that mutations accumulate too slowly (less than one per replicative lifespan) to play a causative role in yeast aging (KAYA *et al.* 2015a). A mutator strain with a 10-fold elevation in mutation rate driven by oxidative damage engineered by this group also failed to decrease replicative lifespan. Our results confirm and expand upon this finding by showing that mutation rates must be 3-5 times greater than those previously tested before

consistent lifespan reduction is seen in haploid cells. Yeast require one sixth of all genes for macroscopic growth. Since an estimated 15-20% of all mutations within an average gene compromise function (HERR *et al.* 2014), it is not surprising that sufficient levels of active mutagenesis can curtail the lifespan of haploid cells (**Figure 1**).

Diploids, however, are generally thought to be buffered against mutation accumulation. We present evidence indicating that a wide range of mutation burdens can impact longevity of diploid cells. First, we show that diploid strains with modest mutation rates and low mutation burdens exhibit variation in lifespan that can be explained by the presence or absence of just a few random heterozygous mutations (**Figure 2**). Second, we show that lifespan declines in a linear fashion as mutation burden increases (**Figure 3**). Third, we show that mutagenesis acts as an accelerant of aging via Weibull AFT analysis (**Figure 4**). Fourth, we show that the loss of longevity due to mutator phenotypes displays genetic anticipation, with later generations having shorter lifespans than earlier ones (**Figure 5**). Finally, we find that mutation accumulation lines that lack an active mutator phenotype nevertheless exhibit reductions in lifespan that correlate with mutation burden (**Figure 6**). Combined analysis of all diploid strains tested show a threshold for severely diminished cellular lifespan and increased population doubling time driven by mutation burdens >10 mutations/Mb (**Figure 7**).

Several lines of evidence suggest that rare mutations or combinations of mutations underlie the diminished lifespan observed in our study. We fortuitously isolated several sets of related strains with reduced lifespan and low mutation burdens (<1 mutation/Mb). Reduced lifespan in these groups likely indicates heterozygous driver mutations that erode longevity of diploids in an additive fashion. Throughout our study we found that mutation burdens greater than 4 mutations/Mb generally reduced cellular lifespan. However, there were exceptional strains with

significant mutation burdens that lived as long as WT. We cannot exclude the possibility that such strains acquired lifespan extending mutations that mask the deleterious effects of mutation burden. However, such exceptions, combined with variation in lifespan among strains of the same mutator genotype and similar mutation loads, argue that reductions in lifespan derive from a few discrete genetic changes rather than a general effect of mutation load. The probability of lifespan-reducing mutations increases with mutation burden, which likely explains the genetic anticipation observed with *pol3-01/pol3-01 msh6Δ/msh6Δ* strains (**Figures 2 and 5**). Mutation burdens in the nine passaged *pol3-01/pol3-01 msh6Δ/msh6Δ* strains ranged from 120 to 235 mutations/Mb, which corresponded to between 1000 and 2500 nonsynonymous mutations in verified protein-coding genes. These strains displayed a high mortality rate from their very first divisions, evidenced in Kaplan-Meier and cumulative hazard plots. This reflects the total effect of accrued lifespan-reducing mutations and the compounding influence of the continued strong mutator phenotype that can directly generate lethal mutations through synthetic interactions or biallelic inactivation of essential genes.

The phenotypic consequences of accumulated mutation burden in multicellular organisms are realized in a complex milieu of multiple lineages with variable mutation burdens. Recent work using data from the Cancer Genome Atlas project reveal a six-fold increase (0.37-2.21 mutations/Mb in samples from individuals under 20 yr and over 80 yr, respectively) in somatic mutation frequency occurring with age (MILHOLLAND *et al.* 2015). Our observations suggest that mutation burdens of some human stem cells could plausibly restrict their longevity or functionality. Stem cell attrition due to cell death places a demand on other stem cell lineages to expand. Under these dynamic conditions, dividing cells with new mutations are subject to the evolutionary forces of selection and genetic drift. Thus, seemingly-normal looking tissues contain

clonal expansions where the phenotypic consequences of particular mutation burdens may predominate (RISQUES AND KENNEDY 2018). In the context of cancer, where selection for rare driver mutations favors cells with higher mutation burdens, maintaining replicative potential is paramount. Exome sequencing from tumor populations show that mutation burdens range from <1 to over 100 mutations/Mb, depending on cancer type (ALEXANDROV *et al.* 2013; MARTINCORENA AND CAMPBELL 2015). This indicates that many tumors carry mutation loads that may impact their longevity or replicative capacity. Our findings suggest that cells from the most extreme mutator-driven tumors with mutation burdens greater than 200 mutations/Mb likely possess a profoundly shortened lifespan.

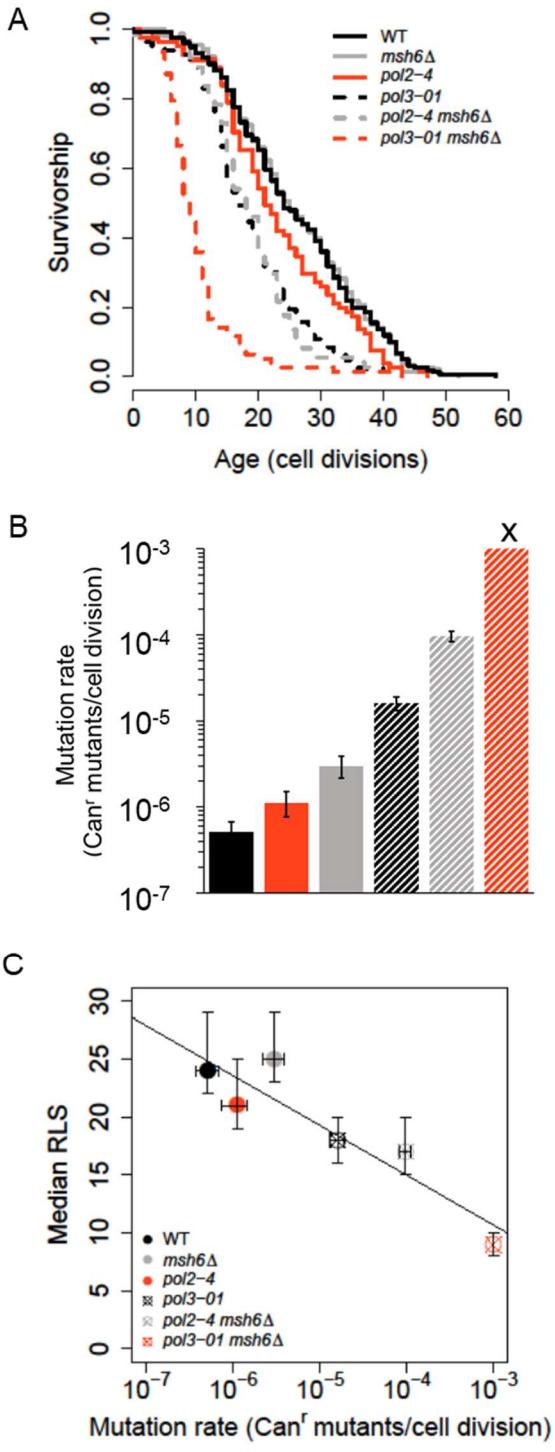
A
Survivorship
Age (cell divisions)
WT
msh6Δ
pol2−4
pol3−01
pol2−4 msh6Δ
pol3−01 msh6Δ
B
Mutation rate
(Canr mutants/cell division)
X
C
Median RLS
Mutation rate (Canr mutants/cell division)

Figure 2.1. Mutation rate negatively correlates with RLS in haploid mutator yeast. A) RLS of freshly dissected haploid spores. Mutator spores compared to WT using Wilcoxon rank sum tests with Bonferroni-corrected p-values using p-adjust in R. WT (cells from both AH2601 and AH2801 backgrounds), median RLS = 24, n = 161; *pol3-01*, median RLS = 18, n = 74, p < 0.001; *pol2-4*, median RLS = 21, n = 81, p = 0.43, *msh6*Δ (cells pooled from both AH2601 and AH2801 backgrounds), median RLS = 25, n = 156, p=1; *pol2-4 msh6*Δ n = 83, p < 0.001. *pol3-01 msh6*Δ, n = 78, p < 0.001. B) Mutation rates for haploid spores. Colonies from independent spores served as replica cultures for fluctuation analysis using canavanine-resistance (Can^r) [WT, n = 32 (combined from both genetic backgrounds); *pol2-4*, n = 14; *msh6*Δ, n = 15 (combined from both genetic backgrounds), *pol3-01*, n = 22; *pol2-4 msh6*Δ, n = 19]. *pol3-01 msh6*Δ spores failed to form colonies; mutation rate was estimated from the synthetic relationship between proofreading and MMR in haploids (23) and confirmed by measurements of *pol3-01/pol3-01 msh6Δ/msh6Δ* diploids (see Figure 2). Error bars represent 95% confidence intervals (CI). Mutation rates of viable mutator strains were compared to WT cells using a Likelihood Ratio Test (all strains, p<0.005). C) Scatterplot of median replicative lifespan (RLS) as a function of mutation rate (horizontal error bars, 95% CI; vertical error bars, standard error of the mean (SEM)). Linear model adjusted R-squared = 0.81, p = 0.009.

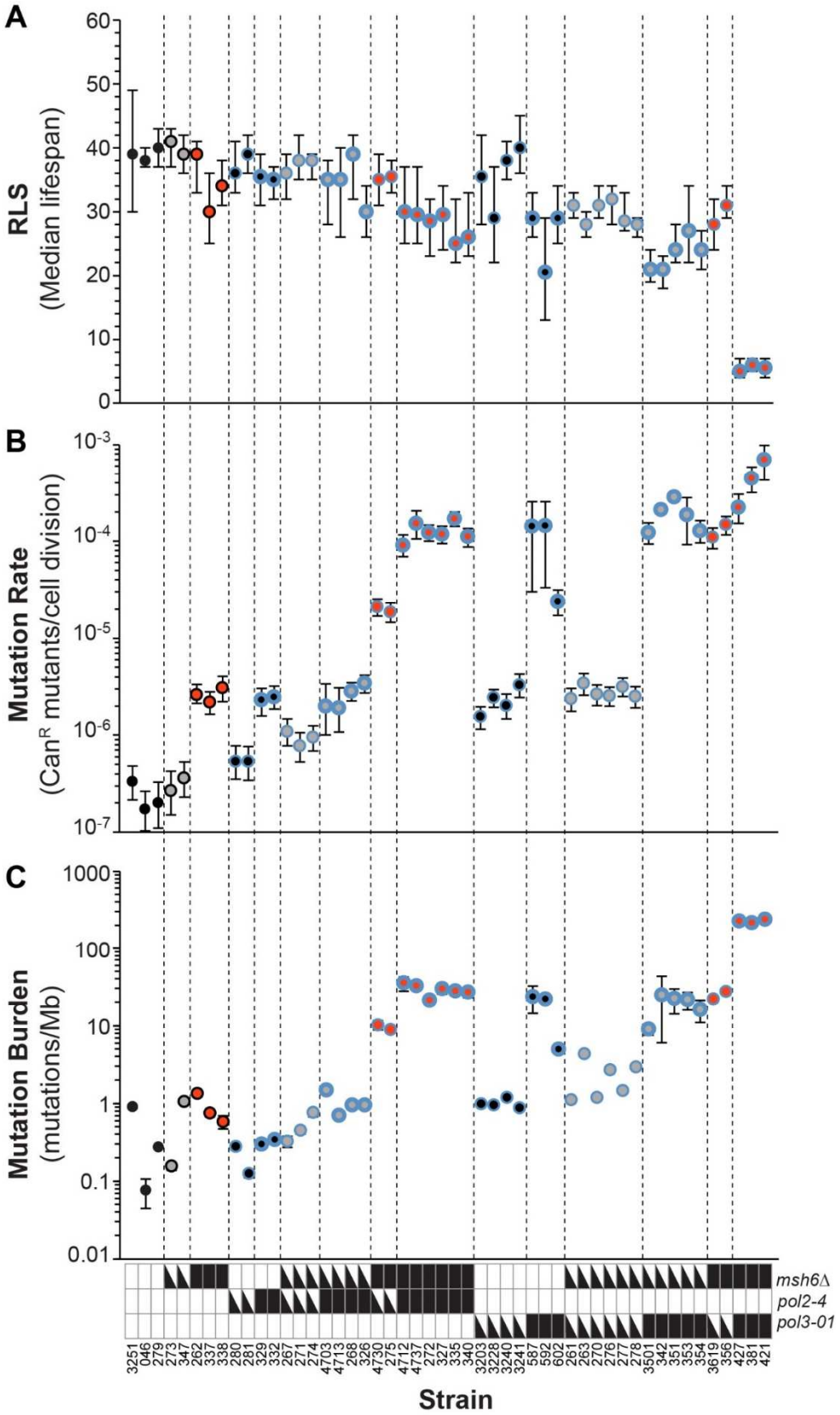
A
RLS
(Median lifespan)
60
50
40
30
20
10
0
B
Mutation Rate
(Can^R mutants/cell division)
10^-3
10^-4
10^-5
10^-6
10^-7
C
Mutation Burden
(mutations/Mb)
1000
100
10
1
0.1
0.01
msh6Δ
pol2-4
pol3-01
3251
046
279
273
347
262
337
338
280
281
329
332
267
271
274
4703
4713
268
326
4730
275
4712
4737
272
327
335
340
3203
3228
3240
3241
587
592
602
261
263
270
276
277
278
3501
342
351
353
354
3619
356
427
381
421
Strain

Figure 2.2. Lifespan, mutation rates, and mutation burden of polymerase proofreading and/or mismatch repair defective diploid mutator yeast. A) Median RLS of diploid mutator strains separated by genotype. Error bars = 95% CI. B) Mutation rates of diploid mutators. All strains were hemizygous for *CAN1* (*CAN1::natMX/can1Δ::HIS3*), which facilitated canavanine-resistance (Can^r) mutation rate measurement. Error bars represent 95% CI. Mutation rates compared to WT using the log-rank test; p-values were corrected for multiple testing ($p < 0.001$ for all strains except *MSH6/msh6Δ*). C) Mutation burdens (mutations/Mb) of diploid mutator yeast measured using whole-genome sequencing. Sequenced populations were age-matched to cells analyzed in RLS. Three independent isolates sequenced for each strain. Error bars = SEM.

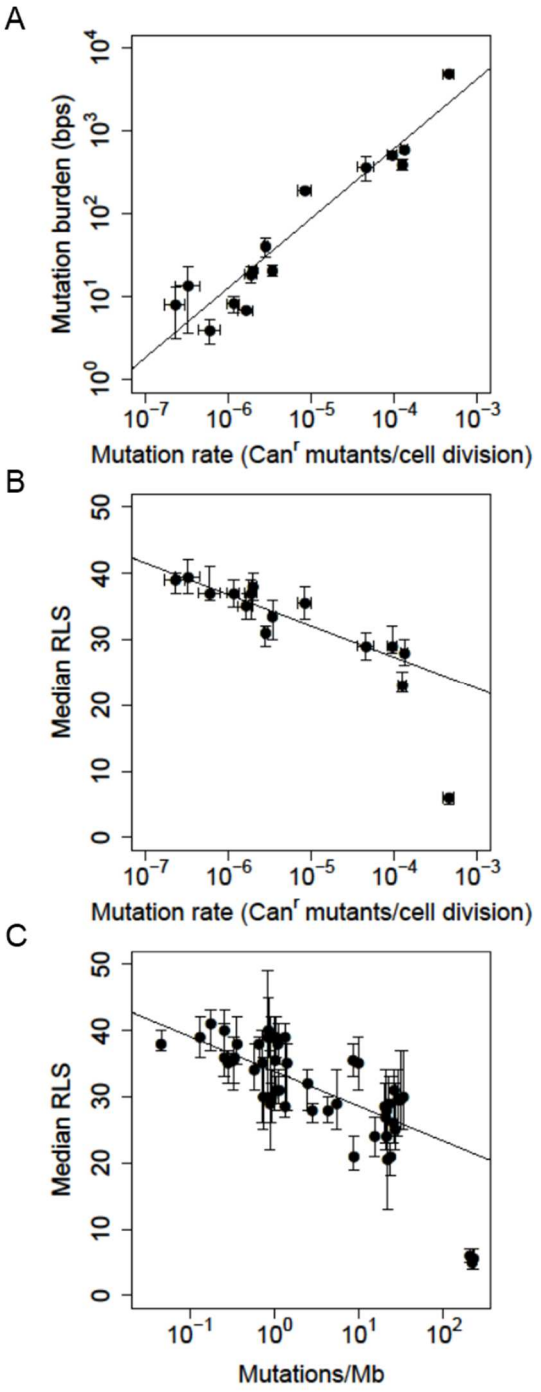
A
Mutation burden (bps)
10^0
10^1
10^2
10^3
10^4
10^{-7}
10^{-6}
10^{-5}
10^{-4}
10^{-3}
Mutation rate (Can^r mutants/cell division)
B
Median RLS
0
10
20
30
40
50
10^{-7}
10^{-6}
10^{-5}
10^{-4}
10^{-3}
Mutation rate (Can^r mutants/cell division)
C
Median RLS
0
10
20
30
40
50
10^{-1}
10^0
10^1
10^2
Mutations/Mb

Figure 2.3. Decreased lifespan negatively correlates with increased mutagenesis in diploid yeast. For genotype comparisons, data from multiple mutator diploid strains pooled. Outliers within genotype were identified and removed using two methods: from RLS data, ANOVA of strains by genotype combined with pairwise t-tests where ANOVA $p < 0.05$. From mutation rate data, pairwise likelihood ratio tests were used to identify and remove outliers. All strain data removed from genotype analysis if found to be an outlier using either method. A) Correlation between mutation rate and mutation burden. Horizontal error bars = 95% CIs. Vertical error bars = SEM. Linear model adjusted R-squared = 0.90, $p < 0.001$. B) Median RLS as a function of mutation rate. Horizontal error bars = 95% CIs. Vertical error bars = SEM. Linear model adjusted R-squared = 0.82, $p < 0.001$. C) Median RLS as a function of mutation burden (in mutations/Mb of gDNA sequenced) in diploid mutators. Instead of pooling on the basis of mutator genotype, individual mutator strains plotted. Error bars = SEM. Linear model adjusted R-squared = 0.55, $p < 0.001$. For B) and C), linear regression modeling performed excluding outlier genotype (*pol3-01/pol3-01 msh6Δ/msh6Δ*).

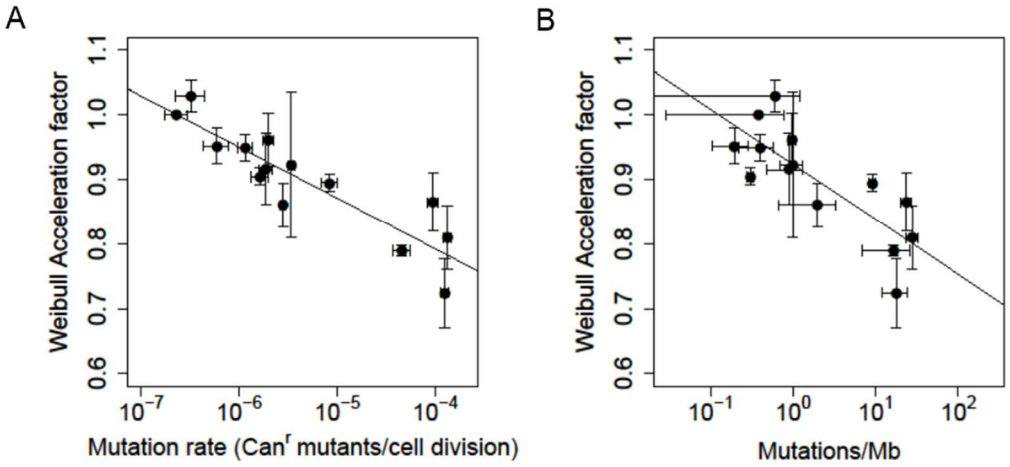

Figure 2.4. Mutator-driven mutagenesis is an accelerant of cellular aging in diploid yeast. A) Correlation between Weibull AFT acceleration factor and mutation rate in yeast separated by mutator genotype (adjusted R-squared = 0.73, $p < 0.001$). Horizontal and vertical error bars = 95% CI. B) Correlation between Weibull AFT acceleration factor and mutation burden (mutations/Mb) (adjusted R-squared = 0.60, $p < 0.001$). Horizontal error bars = standard deviation and vertical error bars = 95% CI.

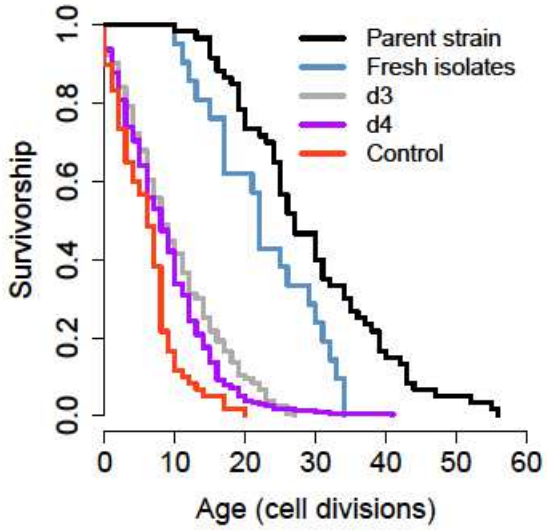

Figure 2.5. Mutation accumulation erodes replicative lifespan in strong diploid mutators. RLS of *pol3-01/pol3-01 msh6Δ/msh6Δ* cells decline with propagation. *pol3-01/pol3-01 msh6Δ/msh6Δ* zygotes were manually isolated from a cross of *pol3-01 msh6Δ* haploid cells that had undergone ≤ 3 cell divisions after tetrad dissection. First or second diploid cells from zygotes were used as mother cells for RLS measurements. The RLS of these cells (Fresh isolates, blue) (median RLS = 22, n = 21) was compared to the RLS of concurrently measured *pol3-01/pol3-01 msh6Δ/msh6Δ* cells previously passaged for ~40-60 cell divisions (Control, red) (median RLS = 6, n = 60, $p < 0.001$) as well as that of the parent strain (Parent strain, black) (*POL3/pol3-01 MSH6/msh6Δ*, median RLS = 27, n = 60, $p = 0.075$) using a Wilcoxon rank sum test Bonferroni-corrected for multiple tests. Daughter cells dissected from mothers were set aside to grow into colonies and subcloned to generate d3 passaged cells (d3, gray). Cells from d3 patches were subcloned again to generate d4 passaged cells (d4, purple) (both passaged lines median RLS = 8, n = 240, $p < 0.001$).

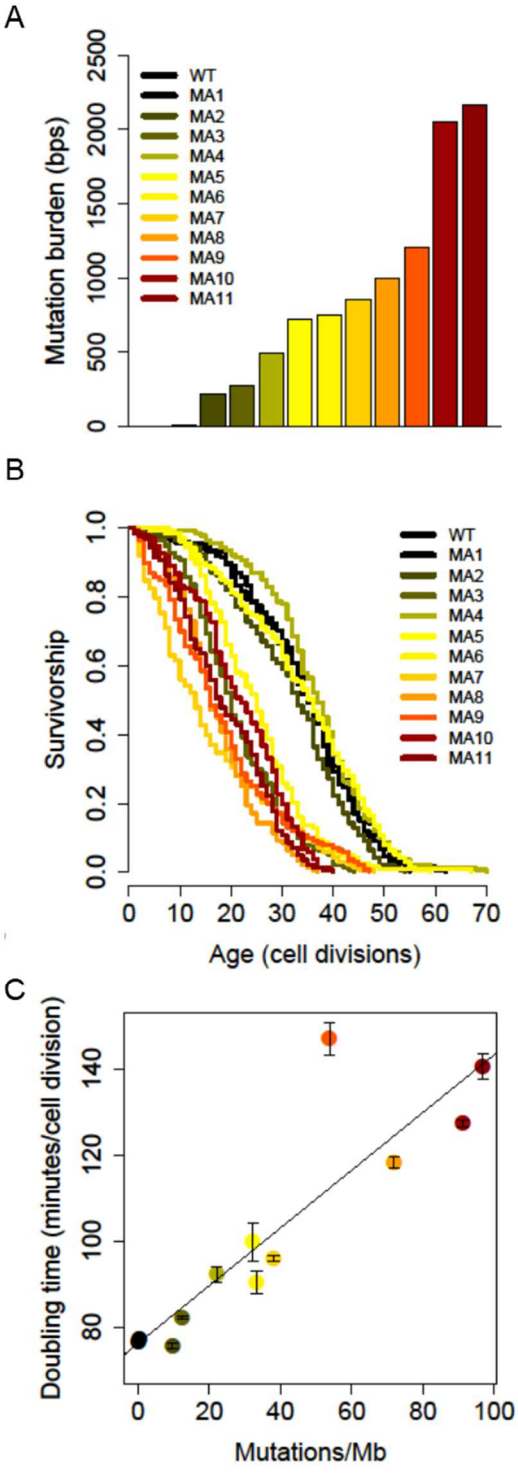
A
Mutation burden (bps)
0
500
1000
1500
2000
2500
WT
MA1
MA2
MA3
MA4
MA5
MA6
MA7
MA8
MA9
MA10
MA11
B
Survivorship
0.0
0.2
0.4
0.6
0.8
1.0
0
10
20
30
40
50
60
70
Age (cell divisions)
C
Doubling time (minutes/cell division)
80
100
120
140
0
20
40
60
80
100
Mutations/Mb

Figure 2.6. Mutation accumulation in the absence of active mutagenesis erodes replicative lifespan in diploid yeast. A) Total mutation burdens (bps) of diploid yeast mutation accumulation (MA) lines transiently-mutagenized using the *pol3-01,L612M* strong mutator allele. B) Kaplan-Meier plots of survival of MA lines. C) Peak doubling time (minutes/cell division) of MA lines as a function of mutation burden. Error bars = SEM. Linear model adjusted R-squared = 0.75, $p < 0.001$.

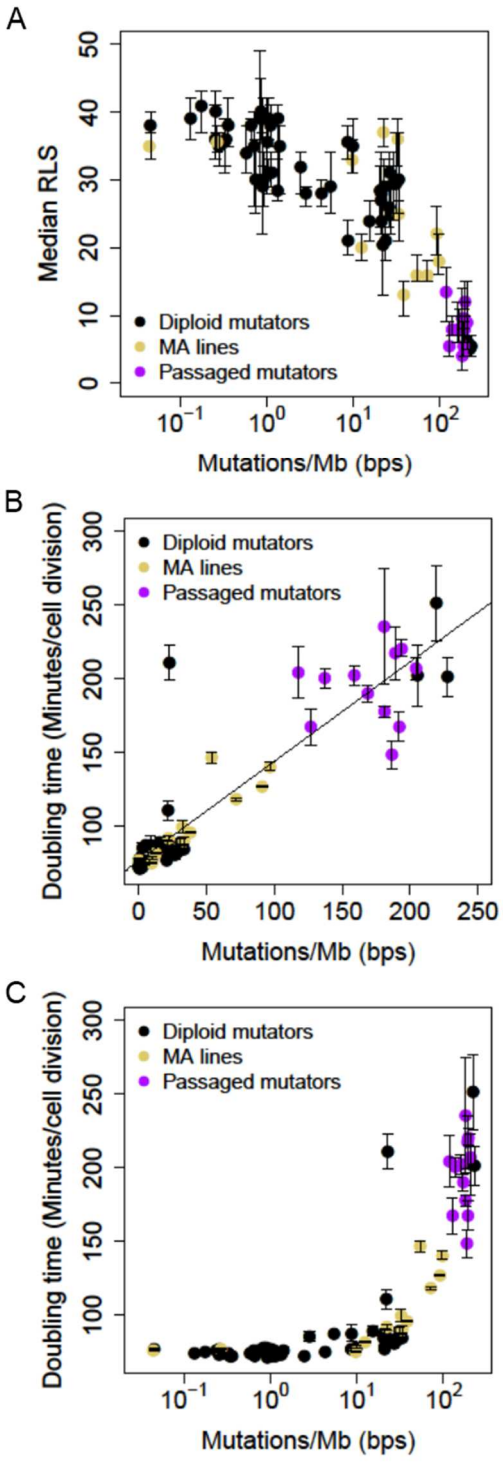
A
Median RLS
0
10
20
30
40
50
Diploid mutators
MA lines
Passaged mutators
10^{-1}
10^{0}
10^{1}
10^{2}
Mutations/Mb (bps)
B
Doubling time (Minutes/cell division)
100
150
200
250
300
Diploid mutators
MA lines
Passaged mutators
0
50
100
150
200
250
Mutations/Mb (bps)
C
Doubling time (Minutes/cell division)
100
150
200
250
300
Diploid mutators
MA lines
Passaged mutators
10^{-1}
10^{0}
10^{1}
10^{2}
Mutations/Mb (bps)

Figure 2.7. The role of accumulated mutation burden in driving diminished lifespan and increased doubling time in diploid yeast. A) Scatterplot showing the relationship between mutation burden (Mutations/Mb gDNA sequenced) and median RLS in diploid mutator yeast (figures 2-4, black), passaged *pol3-01/pol3-01 msh6Δ/msh6Δ* strong mutators (figure 5, purple), and transiently-mutagenized mutation accumulation (MA) lines (figure 6, gold). Error bars = 95% CIs. B) Correlation between mutation burden (Mutations/Mb) and peak doubling time (Minutes/cell division) in diploid mutagenized yeast. Error bars = SEM. Linear model adjusted R-squared = 0.85, $p < 0.001$. C) Correlation between log-transformed mutation burden (Mutations/Mb) and peak doubling time.

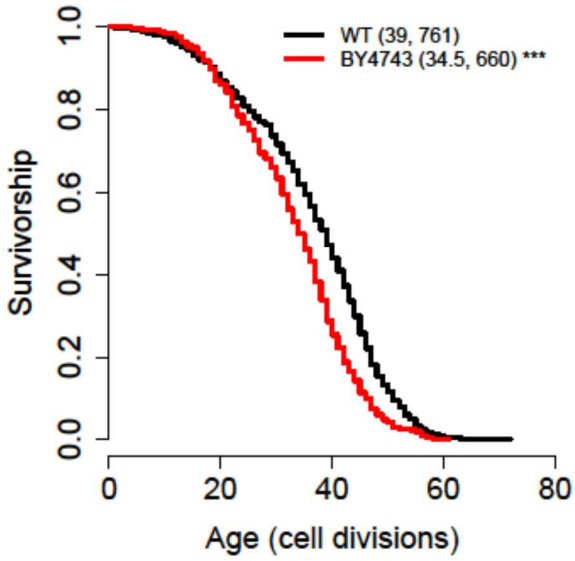

Supplementary figure S2.1. RLS of AH0401 (WT) and BY4743 (median RLS and mother's dissected in parentheses). *** = $p < 0.001$, Wilcoxon rank sum test.

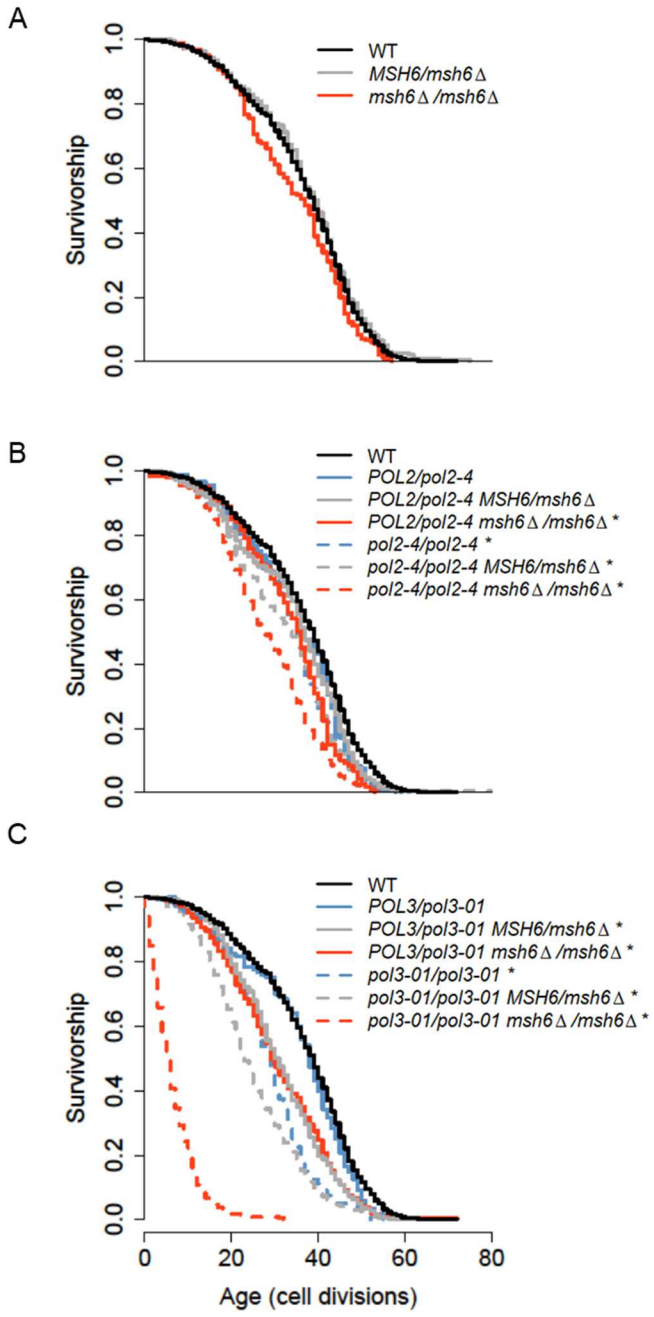

Supplementary figure S2.2. RLS of diploid mismatch repair and polymerase proofreading deficient mutator strains. A) *MSH6* deficient (*msh6Δ*) mutators. B) Polε proofreading-deficient (*pol2-4*) with and without *MSH6*. C) Polδ proofreading-deficient (*pol3-01*) with and without *MSH6*. * = $p < 0.05$, Wilcoxon rank sum test, Bonferroni-corrected.

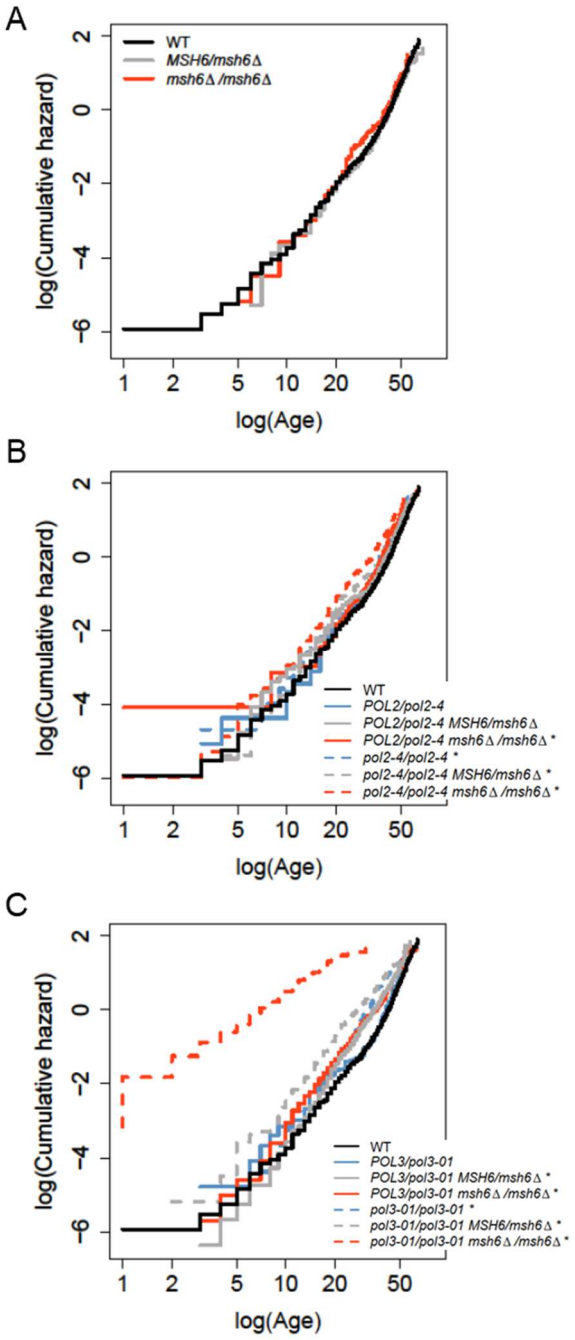

Supplementary figure S2.3. Cumulative hazard plots of diploid mismatch repair and polymerase proofreading deficient mutator strains. A) *MSH6* deficient (*msh6Δ*) mutators. B) Polε proofreading-deficient (*pol2-4*) with and without *MSH6*. C) Polδ proofreading-deficient (*pol3-01*) with and without *MSH6*. * = $p < 0.05$, Wilcoxon rank sum test, Bonferroni-corrected.

Supplementary Table S2.1. Yeast strains.

Strain	Genetic background	Relevant genotype	Source
AH0401	BY4743	*CAN1::natMX/can1Δ::HIS3*	Herr et al., 2014
AH2601	AH0401	*CAN1::natMX/can1Δ::HIS3 MSH6/msh6Δ::LEU2 POL3/URA3::pol3-01*	This study
AH2801	AH0401	*CAN1::natMX/can1Δ::HIS3 MSH6/msh6Δ::LEU2 POL2/pol2-4::URA3*	Herr et al., 2011
AH3203	AH2601	*CAN1::natMX/can1Δ::HIS3 MSH6/MSH6 POL3/URA3::pol3-01*	This study
AH3228	AH2601	*CAN1::natMX/can1Δ::HIS3 MSH6/MSH6 POL3/URA3::pol3-01*	This study
AH3240	AH2601	*CAN1::natMX/can1Δ::HIS3 MSH6/MSH6 POL3/URA3::pol3-01*	This study
AH3241	AH2601	*CAN1::natMX/can1Δ::HIS3 MSH6/MSH6 POL3/URA3::pol3-01*	This study
AH3251	AH2601	*CAN1::natMX/can1Δ::HIS3 MSH6/MSH6 POL3/POL3*	This study
AH3501	AH2601	*CAN1::natMX/can1Δ::HIS3 MSH6/msh6Δ::LEU2 URA3::pol3-01/URA3::pol3-01*	This study
AH3619	AH2601	*CAN1::natMX/can1Δ::HIS3 msh6Δ::LEU2/msh6Δ::LEU2 POL3/URA3::pol3-01*	This study
AH4703	AH2801	*CAN1::natMX/can1Δ::HIS3 MSH6/msh6Δ::LEU2 pol2-4::URA3/pol2-4::URA3*	This study
AH4712	AH2801	*CAN1::natMX/can1Δ::HIS3 msh6Δ::LEU2/msh6Δ::LEU2 pol2-4::URA3/pol2-4::URA3*	This study
AH4713	AH2801	*CAN1::natMX/can1Δ::HIS3 MSH6/msh6Δ::LEU2 pol2-4::URA3/pol2-4::URA3*	This study
AH4730	AH2801	*CAN1::natMX/can1Δ::HIS3 msh6Δ::LEU2/msh6Δ::LEU2 POL2/pol2-4::URA3*	This study
AH4737	AH2801	*CAN1::natMX/can1Δ::HIS3 msh6Δ::LEU2/msh6Δ::LEU2 pol2-4::URA3/pol2-4::URA3*	This study
yML033*	AH0401	MA1, CAN1::natMX/can1Δ::HIS3	This study
yML034*	AH0401	MA2, CAN1::natMX/can1Δ::HIS3	This study
yML036*	AH0401	MA7, *CAN1::natMX/can1Δ::HIS3*	This study
yML037*	AH0401	MA9, *CAN1::natMX/can1Δ::HIS3*	This study
yML038*	AH0401	MA4, *CAN1::natMX/can1Δ::HIS3*	This study
yML039*	AH0401	MA6, *CAN1::natMX/can1Δ::HIS3*	This study
yML040*	AH0401	MA10, *CAN1::natMX/can1Δ::HIS3*	This study
yML041*	AH0401	MA5, *CAN1::natMX/can1Δ::HIS3*	This study
yML042*	AH0401	MA11, *CAN1::natMX/can1Δ::HIS3*	This study
yML043*	AH0401	MA8, *CAN1::natMX/can1Δ::HIS3*	This study
yML044*	AH0401	MA3, *CAN1::natMX/can1Δ::HIS3*	This study

yML261	AH2601	*CAN1::natMX/can1Δ::HIS3 MSH6/msh6Δ::LEU2 POL3/URA3::pol3-01*	This study
yML262	AH2601	*CAN1::natMX/can1Δ::HIS3 msh6Δ::LEU2/msh6Δ::LEU2 POL3/POL3*	This study
yML263	AH2601	*CAN1::natMX/can1Δ::HIS3 MSH6/msh6Δ::LEU2 POL3/URA3::pol3-01*	This study
yML267	AH2801	*CAN1::natMX/can1Δ::HIS3 MSH6/msh6Δ::LEU2 POL2/pol2-4::URA3*	This study
yML268	AH2801	*CAN1::natMX/can1Δ::HIS3 MSH6/msh6Δ::LEU2 pol2-4::URA3/pol2-4::URA3*	This study
yML270	AH2601	*CAN1::natMX/can1Δ::HIS3 MSH6/msh6Δ::LEU2 POL3/URA3::pol3-01*	This study
yML271	AH2801	*CAN1::natMX/can1Δ::HIS3 MSH6/msh6Δ::LEU2 POL2/pol2-4::URA3*	This study
yML272	AH2801	*CAN1::natMX/can1Δ::HIS3 msh6Δ::LEU2/msh6Δ::LEU2 pol2-4::URA3/pol2-4::URA3*	This study
yML273	AH2801	*CAN1::natMX/can1Δ::HIS3 MSH6/msh6Δ::LEU2 POL2/POL2*	This study
yML274	AH2801	*CAN1::natMX/can1Δ::HIS3 MSH6/msh6Δ::LEU2 POL2/pol2-4::URA3*	This study
yML275	AH2801	*CAN1::natMX/can1Δ::HIS3 msh6Δ::LEU2/msh6Δ::LEU2 POL2/pol2-4::URA3*	This study
yML276	AH2601	*CAN1::natMX/can1Δ::HIS3 MSH6/msh6Δ::LEU2 POL3/URA3::pol3-01*	This study
yML277	AH2601	*CAN1::natMX/can1Δ::HIS3 MSH6/msh6Δ::LEU2 POL3/URA3::pol3-01*	This study
yML278	AH2601	*CAN1::natMX/can1Δ::HIS3 MSH6/msh6Δ::LEU2 POL3/URA3::pol3-01*	This study
yML279	AH2801	*CAN1::natMX/can1Δ::HIS3 MSH6/MSH6 POL2/POL2*	This study
yML280	AH2801	*CAN1::natMX/can1Δ::HIS3 MSH6/MSH6 POL2/pol2-4::URA3*	This study
yML281	AH2801	*CAN1::natMX/can1Δ::HIS3 MSH6/MSH6 POL2/pol2-4::URA3*	This study
yML326	AH2801	*CAN1::natMX/can1Δ::HIS3 MSH6/msh6Δ::LEU2 pol2-4::URA3/pol2-4::URA3*	This study
yML327	AH2801	*CAN1::natMX/can1Δ::HIS3 msh6Δ::LEU2/msh6Δ::LEU2 pol2-4::URA3/pol2-4::URA3*	This study
yML329	AH2801	*CAN1::natMX/can1Δ::HIS3 MSH6/MSH6 pol2-4::URA3/pol2-4::URA3*	This study
yML332	AH2801	*CAN1::natMX/can1Δ::HIS3 MSH6/MSH6 pol2-4::URA3/pol2-4::URA3*	This study

yML335	AH2801	*CAN1::natMX/can1Δ::HIS3 msh6Δ::LEU2/msh6Δ::LEU2 pol2-4::URA3/pol2-4::URA3*	This study
yML337	AH2801	*CAN1::natMX/can1Δ::HIS3 msh6Δ::LEU2/msh6Δ::LEU2 POL2/POL2*	This study
yML338	AH2801	*CAN1::natMX/can1Δ::HIS3 msh6Δ::LEU2/msh6Δ::LEU2 POL2/POL2*	This study
yML340	AH2801	*CAN1::natMX/can1Δ::HIS3 msh6Δ::LEU2/msh6Δ::LEU2 pol2-4::URA3/pol2-4::URA3*	This study
yML342	AH2601	*CAN1::natMX/can1Δ::HIS3 MSH6/msh6Δ::LEU2 URA3::pol3-01/URA3::pol3-01*	This study
yML347	AH2601	*CAN1::natMX/can1Δ::HIS3 MSH6/msh6Δ::LEU2 POL3/POL3*	This study
yML351	AH2601	*CAN1::natMX/can1Δ::HIS3 MSH6/msh6Δ::LEU2 URA3::pol3-01/URA3::pol3-01*	This study
yML353	AH2601	*CAN1::natMX/can1Δ::HIS3 MSH6/msh6Δ::LEU2 URA3::pol3-01/URA3::pol3-01*	This study
yML354	AH2601	*CAN1::natMX/can1Δ::HIS3 MSH6/msh6Δ::LEU2 URA3::pol3-01/URA3::pol3-01*	This study
yML356	AH2601	*CAN1::natMX/can1Δ::HIS3 msh6Δ::LEU2/msh6Δ::LEU2 POL3/URA3::pol3-01*	This study
yML381	AH2601	*CAN1::natMX/can1Δ::HIS3 msh6Δ::LEU2/msh6Δ::LEU2 URA3::pol3-01/URA3::pol3-01*	This study
yML421	AH2601	*CAN1::natMX/can1Δ::HIS3 msh6Δ::LEU2/msh6Δ::LEU2 URA3::pol3-01/URA3::pol3-01*	This study
yML427	AH2601	*CAN1::natMX/can1Δ::HIS3 msh6Δ::LEU2/msh6Δ::LEU2 URA3::pol3-01/URA3::pol3-01*	This study
yML587	AH2601	*CAN1::natMX/can1Δ::HIS3 MSH6/MSH6 URA3::pol3-01/URA3::pol3-01*	This study
yML592	AH2601	*CAN1::natMX/can1Δ::HIS3 MSH6/MSH6 URA3::pol3-01/URA3::pol3-01*	This study
yML602	AH2601	*CAN1::natMX/can1Δ::HIS3 MSH6/MSH6 URA3::pol3-01/URA3::pol3-01*	This study

* = mutation accumulation line

Table S2.2: Primers

Primer Name	Sequence
AH2601 Strain Construction	
MSH6GU	TTTAATTGGAGCAACTAGTTAATTTTGACAAAGCCAATTTGAACT CCAAAAGATTGTACTGAGAGTGCAC
MSH6GD	ACTTTAAAAAAAATAAGTAAAAATCTTACATACATCGTAAATGAA AATACCTGTGCGGTATTTCACACCG
POL3U	ATATTGAGCACTTGCTATTAAGCATTAATCTTTATACATATACGCA CAGCAAGATTGTACTGAGAGTGCAC
pldr6	AAACCACAACGGCATCGTGC
Genotyping Assays	
pol2-4U	CCTTCTTTGCTAACAGATAAGATTT
pol2-S5	ATAACACTCTCAGGGGACAAGTATAT
msh6-upstream	CCTTCTTTGCTAACAGATAAGATTT
msh6-downstream	CAGCTATTAATGTTCAACTTATTCC
Illumina Adapter Primers	
MWS51	AATGATACGGCGACCACCGAGATCTACACTCTTTCCCTACACGAC GCTCTTCCGATCT
MWS55	5'/Phos/GATCGGAAGAGCACACGTCTGAACTCCAGTCAC
Illumina I5 index primers for QPCR	
P5	AATGATACGGCGACCACCGAGATCTACAC
I5index1	AATGATACGGCGACCACCGAGATCTACACTATAGCCTACACTCTT TCCCTACACGACG
I5index2	AATGATACGGCGACCACCGAGATCTACACATAGAGGCACACTCTT TCCCTACACGACG
I5index3	AATGATACGGCGACCACCGAGATCTACACCCTATCCTACACTCTT TCCCTACACGACG
I5index4	AATGATACGGCGACCACCGAGATCTACACGGCTCTGAACACTCTT TCCCTACACGACG
I5index5	AATGATACGGCGACCACCGAGATCTACACAGGCGAAGACACTCT TTCCCTACACGACG
I5index6	AATGATACGGCGACCACCGAGATCTACACTAATCTTAACACTCTT TCCCTACACGACG
Illumina I7 Index Primers for QPCR	
I7index1	CAAGCAGAAGACGGCATACGAGATACAAGCTGTGACTGGAGTTC AGACGTGTGC
I7index2	CAAGCAGAAGACGGCATACGAGATAAACATCGTGACTGGAGTTC AGACGTGTGC
I7index3	CAAGCAGAAGACGGCATACGAGATACATTGGGTGACTGGAGTTC AGACGTGTGC

I7index4	CAAGCAGAAGACGGCATACGAGATACCACTGGTGACTGGAGTTC AGACGTGTGC
I7index5	CAAGCAGAAGACGGCATACGAGATAACGTGAGTGACTGGAGTTC AGACGTGTGC
I7index6	CAAGCAGAAGACGGCATACGAGATCGCTGATGTGACTGGAGTTC AGACGTGTGC
I7index7	CAAGCAGAAGACGGCATACGAGATCAGATCTGTGACTGGAGTTC AGACGTGTGC
I7index8	CAAGCAGAAGACGGCATACGAGATATGCCTAGTGACTGGAGTTC AGACGTGTGC
I7index9	CAAGCAGAAGACGGCATACGAGATCTGTAGCGTGACTGGAGTTC AGACGTGTGC
I7index10	CAAGCAGAAGACGGCATACGAGATAGTACAAGTGACTGGAGTTC AGACGTGTGC
I7index11	CAAGCAGAAGACGGCATACGAGATCATCAAGGTGACTGGAGTTC AGACGTGTGC
I7index12	CAAGCAGAAGACGGCATACGAGATAGTGGTCGTGACTGGAGTTC AGACGTGTGC
I7index13	CAAGCAGAAGACGGCATACGAGATAACAACCGTGACTGGAGTTC AGACGTGTGC
I7index14	CAAGCAGAAGACGGCATACGAGATAACCGAGGTGACTGGAGTTC AGACGTGTGC
I7index15	CAAGCAGAAGACGGCATACGAGATAACGCTTGTGACTGGAGTTC AGACGTGTGC
I7index16	CAAGCAGAAGACGGCATACGAGATAAGACGGGTGACTGGAGTTC AGACGTGTGC
I7index17	CAAGCAGAAGACGGCATACGAGATAAGGTACGTGACTGGAGTTC AGACGTGTGC
I7index18	CAAGCAGAAGACGGCATACGAGATACACAGAGTGACTGGAGTTC AGACGTGTGC
I7index19	CAAGCAGAAGACGGCATACGAGATACAGCAGGTGACTGGAGTTC AGACGTGTGC
I7index20	CAAGCAGAAGACGGCATACGAGATACCTCCAGTGACTGGAGTTC AGACGTGTGC
I7index21	CAAGCAGAAGACGGCATACGAGATACGCTCGGTGACTGGAGTTC AGACGTGTGC
I7index22	CAAGCAGAAGACGGCATACGAGATACGTATCGTGACTGGAGTTC AGACGTGTGC
I7index23	CAAGCAGAAGACGGCATACGAGATACTATGCGTGACTGGAGTTC AGACGTGTGC
I7index24	CAAGCAGAAGACGGCATACGAGATAGAGTCAGTGACTGGAGTTC AGACGTGTGC
I7index25	CAAGCAGAAGACGGCATACGAGATAGATCGCGTGACTGGAGTTC AGACGTGTGC
I7index26	CAAGCAGAAGACGGCATACGAGATAGCAGGAGTGACTGGAGTTC AGACGTGTGC

I7index27	CAAGCAGAAGACGGCATACGAGATAGTCACTGTGACTGGAGTTC AGACGTGTGC
I7index28	CAAGCAGAAGACGGCATACGAGATATCCTGTGTGACTGGAGTTC AGACGTGTGC
I7index29	CAAGCAGAAGACGGCATACGAGATATTGAGGGTGACTGGAGTTC AGACGTGTGC
I7index30	CAAGCAGAAGACGGCATACGAGATCAACCACGTGACTGGAGTTC AGACGTGTGC
I7index31	CAAGCAGAAGACGGCATACGAGATCAAGACTGTGACTGGAGTTC AGACGTGTGC
I7index32	CAAGCAGAAGACGGCATACGAGATCAATGGAGTGACTGGAGTTC AGACGTGTGC
I7index33	CAAGCAGAAGACGGCATACGAGATCACTTCGGTGACTGGAGTTC AGACGTGTGC
I7index34	CAAGCAGAAGACGGCATACGAGATCAGCGTTGTGACTGGAGTTC AGACGTGTGC
I7index35	CAAGCAGAAGACGGCATACGAGATCATACCAGTGACTGGAGTTC AGACGTGTGC
I7index36	CAAGCAGAAGACGGCATACGAGATCCAGTTCGTGACTGGAGTTC AGACGTGTGC
I7index37	CAAGCAGAAGACGGCATACGAGATCCGAAGTGTGACTGGAGTTC AGACGTGTGC
I7index38	CAAGCAGAAGACGGCATACGAGATCCGTGAGGTGACTGGAGTTC AGACGTGTGC
I7index39	CAAGCAGAAGACGGCATACGAGATCCTCCTGGTGACTGGAGTTC AGACGTGTGC
I7index40	CAAGCAGAAGACGGCATACGAGATCGAACTTGTGACTGGAGTTC AGACGTGTGC
I7index41	CAAGCAGAAGACGGCATACGAGATCGACTGGGTGACTGGAGTTC AGACGTGTGC
I7index42	CAAGCAGAAGACGGCATACGAGATCGCATACGTGACTGGAGTTC AGACGTGTGC
I7index43	CAAGCAGAAGACGGCATACGAGATCTCAATGGTGACTGGAGTTC AGACGTGTGC
I7index44	CAAGCAGAAGACGGCATACGAGATCTGAGCCGTGACTGGAGTTC AGACGTGTGC
I7index45	CAAGCAGAAGACGGCATACGAGATCTGGCATGTGACTGGAGTTC AGACGTGTGC
I7index46	CAAGCAGAAGACGGCATACGAGATGAATCTGGTGACTGGAGTTC AGACGTGTGC
I7index47	CAAGCAGAAGACGGCATACGAGATGACTAGTGTGACTGGAGTTC AGACGTGTGC
I7index48	CAAGCAGAAGACGGCATACGAGATGAGCTGAGTGACTGGAGTTC AGACGTGTGC
I7index49	CAAGCAGAAGACGGCATACGAGATGATAGACGTGACTGGAGTTC AGACGTGTGC

I7index50	CAAGCAGAAGACGGCATACGAGATGCCACATGTGACTGGAGTTC AGACGTGTGC
I7index51	CAAGCAGAAGACGGCATACGAGATGCGAGTAGTGACTGGAGTTC AGACGTGTGC
I7index52	CAAGCAGAAGACGGCATACGAGATGCTAACGGTGACTGGAGTTC AGACGTGTGC
I7index53	CAAGCAGAAGACGGCATACGAGATGCTCGGTGTGACTGGAGTTC AGACGTGTGC
I7index54	CAAGCAGAAGACGGCATACGAGATGGAGAACGTGACTGGAGTTC AGACGTGTGC
I7index55	CAAGCAGAAGACGGCATACGAGATGGTGCGAGTGACTGGAGTTC AGACGTGTGC
I7index56	CAAGCAGAAGACGGCATACGAGATGTACGCAGTGACTGGAGTTC AGACGTGTGC
I7index57	CAAGCAGAAGACGGCATACGAGATGTCGTAGGTGACTGGAGTTC AGACGTGTGC
I7index58	CAAGCAGAAGACGGCATACGAGATGTCTGTCGTGACTGGAGTTC AGACGTGTGC
I7index59	CAAGCAGAAGACGGCATACGAGATGTGTTCTGTGACTGGAGTTCA GACGTGTGC
I7index60	CAAGCAGAAGACGGCATACGAGATTAGGATGGTGACTGGAGTTC AGACGTGTGC
I7index61	CAAGCAGAAGACGGCATACGAGATTATCAGCGTGACTGGAGTTC AGACGTGTGC
I7index62	CAAGCAGAAGACGGCATACGAGATTCCGTCTGTGACTGGAGTTCA GACGTGTGC
I7index63	CAAGCAGAAGACGGCATACGAGATTCTTCACGTGACTGGAGTTCA GACGTGTGC
I7index64	CAAGCAGAAGACGGCATACGAGATTGAAGAGGTGACTGGAGTTC AGACGTGTGC
I7index65	CAAGCAGAAGACGGCATACGAGATTGGAACAGTGACTGGAGTTC AGACGTGTGC
I7index66	CAAGCAGAAGACGGCATACGAGATTGGCTTCGTGACTGGAGTTC AGACGTGTGC
I7index67	CAAGCAGAAGACGGCATACGAGATTGGTGGTGTGACTGGAGTTC AGACGTGTGC
I7index68	CAAGCAGAAGACGGCATACGAGATTTCACGCGTGACTGGAGTTC AGACGTGTGC
I7index69	CAAGCAGAAGACGGCATACGAGATAACTCACGTGACTGGAGTTC AGACGTGTGC
I7index70	CAAGCAGAAGACGGCATACGAGATAAGAGATGTGACTGGAGTTC AGACGTGTGC

Chapter 3. A system to identify inhibitors of mTOR signaling using high-resolution growth analysis in *Saccharomyces cerevisiae*

Published in *GeroScience* (2017) 39**:** 419-428

Mitchell B. Lee[1], Daniel T. Carr[1], Michael G. Kiflezghi[1,2], Yan Ting Zhao[1], Deborah B. Kim[1], Socheata Thon[1], Margarete D. Moore[1], Mary Ann K. Li,[1], Matt Kaeberlein[1]

1. Department of Pathology, University of Washington, Seattle, WA, USA.

2. Molecular Medicine and Mechanisms of Disease (M3D) Program, University of Washington, Seattle, WA, USA.

3.2 Abstract

The mechanistic target of rapamycin (mTOR) is a central regulator of growth and proliferation and mTOR inhibition is a promising therapy for a variety of diseases and disorders. Inhibition of mTOR complex I (mTORC1) with rapamycin delays aging and increases healthy longevity in laboratory animals and is used clinically at high doses to prevent organ transplant rejection and to treat some forms of cancer. Clinical use of rapamycin is associated with several unwanted side effects, however, and several strategies are being taken to identify mTORC1 inhibitors with fewer side effects. We describe here a yeast-based growth assay that can be used to screen for novel inhibitors of mTORC1. By testing compounds using a wild type strain and isogenic cells lacking either *TOR1* or *FPR1*, we can resolve not only whether a compound is an inhibitor of mTORC1, but also whether the inhibitor acts through a mechanism similar to rapamycin by binding Fpr1. Using this assay, we show that rapamycin derivatives behave similarly to rapamycin, while caffeine and the ATP competitive inhibitors Torin 1 and GSK2126458 are mTORC1 inhibitors in yeast that act independently of Fpr1. Some mTOR inhibitors in mammalian cells do not inhibit mTORC1 in yeast, and several nutraceutical compounds were not found to specifically inhibit mTOR but resulted in a general inhibition of yeast growth. Our screening method holds promise as a means of effectively assaying drug libraries for mTOR-inhibitory molecules *in vivo* that may be adapted as novel treatments to fight diseases and extend healthy longevity.

3.3 Introduction

The budding yeast, *Saccharomyces cerevisiae*, is a premier model system for identifying conserved genetic and pharmacological interventions that extend lifespan (KAEBERLEIN 2010; LONGO *et al.* 2012). A particularly good example of this is the mechanistic target of rapamycin (mTOR) pathway that was first genetically implicated in aging in yeast (FABRIZIO *et al.* 2001) and has since emerged as an important target for delaying aging in multicellular invertebrates and mice (JOHNSON *et al.* 2013b; JOHNSON *et al.* 2015). Likewise, the small molecule mTOR inhibitor, rapamycin, was first shown to extend lifespan in yeast (POWERS *et al.* 2006) and has since been shown to have similar pro-longevity effects in nematodes (ROBIDA-STUBBS *et al.* 2012), fruit flies (BJEDOV *et al.* 2010), and mice (HARRISON *et al.* 2009).

In addition to increased lifespan, rapamycin maintains organismal health during aging in mice, evidenced by decreased occurrence of multiple age-related diseases (JOHNSON *et al.* 2013a). Rapamycin treatment in aging mice reduces cancer (ANISIMOV *et al.* 2011; POPOVICH *et al.* 2014), prevents cognitive dysfunction (HALLORAN *et al.* 2012; MAJUMDER *et al.* 2012), attenuates declining renal and hepatic function (NEFF *et al.* 2013), improves muscle and visual performance (NEFF *et al.* 2013), and reverses cardiac (FLYNN *et al.* 2013; DAI *et al.* 2014) and immune decline (CHEN *et al.* 2009). Improved cardiac function from rapamycin treatment has recently been similarly observed in middle-aged companion dogs (URFER *et al.* 2017b), while improved immune function has been observed in healthy elderly people treated with the rapamycin derivative everolimus (RAD001) (MANNICK *et al.* 2014). Transient rapamycin treatment regimens lasting as few as twelve weeks and initiated late in life are also effective at increasing lifespan and healthspan in mice (BITTO *et al.* 2016). These findings place rapamycin and other mTOR inhibitors among

the leading candidates for translational interventions to promote healthy aging in people and companion animals (BLAGOSKLONNY 2010; KAEBERLEIN *et al.* 2015; KAEBERLEIN *et al.* 2016).

The mechanistic target of rapamycin (mTOR) is a nutrient and growth factor responsive kinase that functions in two distinct protein complexes: mTOR complex 1 (mTORC1) and mTOR complex 2 (mTORC2) (LOEWITH *et al.* 2002; WULLSCHLEGER *et al.* 2006). Rapamycin binds to the FK506 binding protein FKPB12 (Fpr1 in yeast), and the FKBP12-rapamycin complex inhibits the activity of mTORC1 by disrupting the physical interaction between the mTOR protein and a second mTORC1 component, raptor (Kog1 in yeast) (HEITMAN *et al.* 1991; LORENZ AND HEITMAN 1995). Deletion of *FPR1* confers resistance to rapamycin in yeast (HEITMAN *et al.* 1991; BENTON *et al.* 1994). The mTORC1 complex regulates a variety of downstream cellular processes including mRNA translation, autophagy, and mitochondrial metabolism, all of which are affected by rapamycin treatment (SAXTON AND SABATINI 2017). Unlike mTORC1, mTORC2 activity is not directly inhibited by rapamycin (JACINTO *et al.* 2004). The mTORC2 complex is less well characterized than mTORC1, but is similarly involved in regulating a variety of cellular processes including cytoskeleton organization and regulation of metabolism. Long-term treatment with rapamycin in mammals is reported to cause indirect inhibition of mTORC2, which is implicated in metabolic defects including insulin resistance and glucose intolerance (LAMMING *et al.* 2012). Both mTOR complexes are essential for viability in yeast and multicellular eukaryotes.

Budding yeast contain two genes that encode the mTOR kinase: *TOR1* and *TOR2*. Tor1 functions exclusively in mTORC1, while Tor2 functions in both complexes (HELLIWELL *et al.* 1994). Consistent with this, deletion of *TOR2* leads to inviability due to the complete lack of mTORC2 activity (KUNZ *et al.* 1993), while deletion of *TOR1* results in viable cells that are long-lived and sensitive to rapamycin, due to reduced mTORC1 activity (HEITMAN *et al.* 1991;

KAEBERLEIN *et al.* 2005c). Despite their sensitivity to rapamycin, *tor1*Δ yeast cells do not show a substantial reduction in mRNA translation or doubling time (MCCORMICK *et al.* 2015; BEAUPERE *et al.* 2017), indicating that Tor2 provides sufficient mTORC1 activity for relatively normal growth in rich medium.

Multiple pharmaceutical mTORC1 and general mTOR inhibitors are used as chemotherapeutic agents (FOLKES *et al.* 2008; CHRESTA *et al.* 2010; KNIGHT *et al.* 2010; LIU *et al.* 2012; O'DONNELL *et al.* 2017). Additionally, several natural products and natural product mixtures are reported to inhibit mTOR signaling in cell culture and rodent models, including: curcumin (BEEVERS *et al.* 2006; BEEVERS *et al.* 2009), green tea extract (ZHANG *et al.* 2006), epigallocatechin-3-gallate (ZHANG *et al.* 2006; VAN ALLER *et al.* 2011), caffeine (REINKE *et al.* 2006; SAIKI *et al.* 2011), genistein (ANASTASIUS *et al.* 2009), lycopene and eicosapentaenoic acid (LIU *et al.* 2012), sulforaphane (WICZK *et al.* 2012), alpha-lipoic acid (XIE *et al.* 2012; LI *et al.* 2014), glucosamine (JIANG *et al.* 2014), quercetin (LU *et al.* 2015; MENG *et al.* 2015), berberine (FAN *et al.* 2015) and resveratrol (PARK *et al.* 2016). In most cases, the mechanistic basis for inhibition of mTOR via these natural products is unknown, and it remains unclear whether these compounds act via direct inhibition of mTOR, mTORC1, or through indirect effects on components of the mTOR/nutrient response network.

To facilitate identification of new small molecule mTOR inhibitors *in vivo*, we have developed a simple yeast-based assay that quantifies differential growth inhibition in rapamycin-sensitized and rapamycin-resistant genetic backgrounds using a Bioscreen C MBR plate reader/shaker/incubator. We have previously optimized the Bioscreen C MBR machine to obtain high-resolution growth curves of budding yeast cells for chronological lifespan analysis (MURAKAMI *et al.* 2008; MURAKAMI AND KAEBERLEIN 2009) and assessing differential

sensitivities of yeast strains to different chemical and environmental stressors (DELANEY *et al.* 2013). Here we extend this method by assessing the impact of rapamycin and several other small molecules on doubling time and outgrowth in rich media for wild type BY4742 cells and isogenic *tor1Δ* and *fpr1Δ* cells. Our method relies on the fact that deletion of *TOR1* confers sensitivity to rapamycin due to diminished mTORC1 activity, while deletion of *FPR1* confers resistance to rapamycin due to the necessary role of Fpr1 in rapamycin-mediated mTORC1 inhibition. Given this, we predict that mTORC1 inhibitors with mechanisms similar to rapamycin will display similar differential growth inhibition across the three genotypes, while compounds that inhibit mTORC1 by a mechanism distinct from rapamycin will have a greater inhibitory effect on growth of *tor1Δ* cells relative to WT or *fpr1Δ* cells, but that WT and *fpr1Δ* cells will show similar inhibition of growth at a given drug concentration. Drugs that do not inhibit mTORC1 will either have no effect on growth in any of the genotypes or will similarly inhibit growth across all three genotypes. We report the validation of this assay using rapamycin, rapamycin derivatives, and mTOR catalytic inhibitors. We also report the effect of several natural product compounds on mTORC1 inhibition and outgrowth, finding that among the natural products tested, only caffeine displays the outgrowth profile expected for an *in vivo* inhibitor of mTORC1 in yeast.

3.4 Methods

Yeast strains and culture conditions

All yeast strains used were in the BY4742 genetic background (*MATα his3Δ1 leu2Δ0 lys2Δ0 ura3Δ0*). BW1121 (BY4742) was purchased from Thermo Fisher Scientific (Waltham,

MA). GS668 (*fpr1Δ::kanMX4*) and GS983 (*tor1Δ::kanMX4*) were obtained from the haploid *MATα* yeast deletion collection (WINZELER *et al.* 1999). PCR was used to confirm knockout identity. For GS983, 5'-TTGAATCCTAATTTCTTGCTCAATC-3' and 5'-AAGGCATATATTGATGCTCAAAAAG-3' primers were used to confirm knockout. For GS668, 5'-GTTACTTGATGATATTAAGCACGGG-3' and 5'-ACAAAAATGAACCATTAGCAAAGAG-3' primers were used to confirm knockout. The *tor1Δ fpr1Δ* double deletion strain was constructed by mating *tor1Δ::URA3* (gift of Lindsay Fox) and *fpr1Δ::kanMX4* and selecting for Ura^+ $G418^r$ haploid spores after sporulation and tetrad dissection. PCR was used to verify presence of gene deletions. For overnight culture and growth analysis, YPD (1% w/v Bacto™ yeast extract (BD), 2% w/v Bacto™ peptone (BD), 2% w/v dextrose) media was used. Yeast were cultured at 30°C for all experiments.

Growth analysis using Bioscreen C MBR

Growth analysis of yeast strains was performed using a Bioscreen C CMB (Growth curves USA, Piscataway NJ, USA) as previously described (MURAKAMI *et al.* 2008). Briefly, colonies outgrown from frozen stocks were inoculated into 5 mL YPD and incubated at 30°C in a roller drum for 12-16 hours. Two μL of outgrown culture was used to inoculate 148 μL YPD into 100-well honeycomb plates for growth analysis. At least three colonies per strain were analyzed in triplicate for each drug treatment. Doubling times were calculated identifying the slope of the inflection point along growth curves using the online web tool Yeast Outgrowth Data Analyzer (YODA) (OLSEN *et al.* 2010). Welch's (unequal variance) t-test was used to assess statistical significance.

Drug preparation and suppliers

All drugs except caffeine and cycloheximide were suspended in DMSO (these drugs suspended in H_2O). Rapamycin, everolimus, and temsirolimus, were purchased from LC Laboratories (Woburn MA, USA). Cycloheximide and berberine were purchased from Sigma-Aldrich (St. Louis MO, USA). Torin 1 was purchased from Cayman Chemical (Ann Arbor MI, USA). AZD8055, GDC-0941, and GSK2126458 were kind gifts from Jason Pitt. Caffeine was purchased from MP Biomedicals (Santa Ana CA, USA). Resveratrol was purchased from AstaTech Inc. (Bristol PA, USA). Alpha-lipoic acid, broccoli concentrate, glucosamine, lycopene, and quercetin were provided by USANA Health Sciences, Inc. (Salt Lake City UT, USA).

3.5 Results

TOR1 mutants are hypersensitive and FPR1 mutants are resistant to rapamycin and rapalogs

We tested the effect of known mTORC1 inhibitors on growth kinetics in three haploid yeast strains: wild type (WT) BY4742 and isogenic *tor1Δ*, and *fpr1Δ* single-gene deletion mutants. We began by analyzing dose responses for rapamycin and two rapalogs, everolimus and temsirolimus. As expected, all concentrations of rapamycin tested reduced *tor1Δ* outgrowth to a greater extent than WT cells, while *fpr1Δ* cells were resistant to growth inhibition (**Figures 1 and 2**). Everolimus and rapamycin produced remarkably similar growth inhibitory responses, while

higher concentrations of temsirolimus were necessary to achieve growth inhibition comparable to the other two drugs.

Sensitivity of the *tor1Δ* strain to mTORC1 inhibitors can been seen at 2.5 ng/mL rapamycin or everolimus and at 20 ng/mL temsirolimus, where deletion of *TOR1* results in a significantly greater increase in doubling time relative to WT (**Figure 2 and Supplemental table 1**). Resistance of the *fpr1Δ* strain is most evident at the highest concentration of each drug tested, where both WT and *tor1Δ* strains have doubling times exceeding 200 minutes, while the *fpr1Δ* cells are still growing as rapidly as in the vehicle control (doubling time 80-90 minutes).

One consequence of diminished mTORC1 signaling is diminished protein translation (BERETTA *et al.* 1996; STEFFEN *et al.* 2008). To determine if diminished protein translation is sufficient to recapitulate rapamycin-like patterns of growth inhibition, we tested concentrations of the general protein translation inhibitor cycloheximide (CHX) ranging from 1-500 ng/mL. Cycloheximide treatment potently and similarly inhibits growth of all three strains at concentrations of 50 ng/mL and greater (**Supplemental figure 1),** demonstrating that general translation inhibition does not recapitulate the differential effects of rapamycin on growth of these three yeast strains.

ATP competitive inhibitors of mTORC1 produce a distinct growth inhibitory profile compared to rapamycin treatment

In addition to rapamycin-like compounds that inhibit mTORC1 signaling via interaction with Fpr1, several drugs have been developed that act as ATP-competitive inhibitors of mTOR in mammalian cells. To understand how these compounds differentially impact growth in our yeast

strains, we tested dose responses for Torin 1, GSK2126458, GDC-0941, and AZD8055 (**Figure 3**, **Supplemental figure 2**, and **Supplemental table 2**). All of the ATP-competitive inhibitors required micromolar concentrations to inhibit growth, compared to nanomolar concentrations when using rapamycin and rapalogs. At 10 μM Torin 1, *tor1Δ* cells were strongly growth inhibited, while WT cells or *fpr1Δ* cells were less strongly affected (**Figure 3** and **Supplemental table 2**). At 25 μM Torin 1, growth of all three strains was severely impacted, with WT and *fpr1Δ* cells showing similar reductions in growth rate, as expected for a catalytic inhibitor of mTOR that does not act through Fpr1.

GSK2126458, another catalytic inhibitor of mTOR, only weakly impacted yeast growth (**Supplemental figure 2** and **Supplemental table 2**). Doubling time was modestly increased by 100 μM GSK2126458 in all three strains, while growth of only the *tor1Δ* cells was impacted by lower concentrations. Interestingly, neither GDC-0941 nor AZD8055 produced a measurable change in growth in any yeast strains (**Supplemental figure 2** and **Supplemental table 2**).

Among several putative mTORC1 inhibitory nutraceuticals, caffeine shows specificity for mTORC1 in yeast

Many nutraceutical compounds are described as having an mTORC1 inhibitory effect, particularly in the context of human cancer cell culture models. To identify and validate mTORC1-modulating nutraceuticals in yeast, we tested a subset of these compounds in our Bioscreen C MBR assay (**Table 1**). Most of the tested nutraceuticals produced no effect on growth at concentrations up to 100 μg/mL (**Table 1**). Quercetin significantly inhibited WT and *tor1Δ* doubling time by 23% and 25%, respectively, at the highest concentration tested ($p < 0.01$, Welch's

t-test), but did not produce a significant difference in *fpr1Δ* doubling time (p = 0.24, Welch's t-test) even though a trend toward increased doubling time is seen in the strain. Two compounds tested, berberine and lycopene, inhibited growth in a genotype-independent manner. Lycopene only modestly impacted growth, while berberine strongly inhibited growth at 100 μg/mL.

Among the nutraceuticals tested, caffeine was the only compound that showed growth inhibition consistent with an mTOR inhibitory effect, increasing doubling time specifically in the *tor1Δ* mutant cells at 100 μg/mL (**Figure 4**). Caffeine also increased WT and *fpr1Δ* doubling times at concentrations greater than 750 μg/mL. To assess epistatic relationships between Fpr1 and mTORC1, we constructed a *tor1Δ fpr1Δ* double mutant. Growth inhibitory profiles in *tor1Δ fpr1Δ* were identical to those of *tor1Δ* in our caffeine dose response (**Figure 3C**), confirming that Fpr1 is not required for caffeine-mediated growth inhibition in yeast.

3.6 Discussion

Rapamycin and other mTOR inhibitors have emerged as one of the most promising classes of molecules for treating a variety of diseases and promoting healthy longevity (KAEBERLEIN 2013b). The largest barrier to clinical utilization of these compounds for such purposes is the perceived risk of adverse side effects. While it remains unclear how significant an issue this is in relatively healthy people at lower doses, the perception that mTOR inhibitors are risky drugs remains a significant challenge. Thus, there is utility in developing or identifying novel mTOR inhibitors that are effective *in vivo* and which may have fewer side effects. Of particular interest are natural product "nutraceutical" mTOR inhibitors.

By utilizing yeast strains with differential sensitivity to mTORC1 inhibition, we developed an *in vivo* screening platform that allows us to preliminarily categorize compounds as growth inhibitory, mTOR inhibitory, and/or rapamycin mimetics. Compounds that inhibit WT, *tor1Δ*, and *fpr1Δ* cells similarly are general growth inhibitors, but are unlikely to be either direct or indirect mTOR inhibitors, at least in yeast. Compounds that induce growth inhibition preferentially or specifically in *tor1Δ* cells are candidate mTOR inhibitors, and if *fpr1Δ* cells are resistant to these compounds, then they are likely inhibiting mTOR by a mechanism similar to rapamycin. The assay system performed as expected here for rapamycin, the rapalogs everolimus and temsirolimus, the catalytic mTOR inhibitors Torin 1 and GSK2126458, and the natural product mTOR inhibitor caffeine. Therefore, we conclude that this assay system is likely to be suitable for identification of novel, unknown pharmaceutical and natural product mTOR inhibitors.

Our analyses also confirmed previously observed cases of differential sensitivity between yeast and mammals with regard to the catalytic mTOR inhibitors AZD8055 and GDC-0941, which may be due to sequence differences between the mammalian and yeast proteins (Wu *et al.* 2015). It is also likely that equivalent doses of some compounds will yield different intracellular concentrations in yeast cells relative to mammalian cells, and that yeast may be able to clear or otherwise detoxify certain compounds more or less effectively. Thus, it is important to recognize that any hits identified in the yeast-based screening system described here will need to be validated in mammalian cells to confirm similar mTOR-inhibitory effects, and that failure to detect mTOR inhibition in this system for a given compound does not rule out the possibility that the compound could inhibit mTOR in mammalian cells. Nonetheless, given the biochemical and mechanistic similarities between yeast and mammalian mTORC1 and mTORC2, we anticipate that many

compounds will behave similarly in both systems, as is the case for several examples reported here.

It is of particular interest that, among the nutraceutical compounds tested, only caffeine demonstrated growth kinetics consistent with mTORC1 inhibition in our yeast assay. This supports prior studies of caffeine on mTOR activity in budding yeast (REINKE *et al.* 2006; WANKE *et al.* 2008) and fission yeast (RALLIS *et al.* 2013), and is of interest in light of numerous reports that caffeine can extend lifespan in invertebrate models (SUTPHIN *et al.* 2012; BRIDI *et al.* 2015) and that coffee consumption is associated with reduced mortality in people (JE AND GIOVANNUCCI 2014; LOFTFIELD *et al.* 2015). It is intriguing to speculate that these effects could be related to caffeine's mTOR inhibitory activities.

The absence of effects from the other nutraceutical compounds tested suggests that they may not be true mTOR inhibitors. One potential explanation is that some of these compounds, which were generally reported to inhibit mTOR in cancer cell culture models, act via indirect mechanisms through targets that are not present or not similarly affected in yeast. Another possibility is that some of these compounds inhibit mammalian cell growth or nutrient uptake, perhaps specifically in the context of cancer cell culture models, which could have indirect effects on mTOR signaling in response. One interesting example is resveratrol, which is reported to have numerous targets in mammalian cells and to inhibit mTOR through both direct and indirect mechanisms. In one study, resveratrol was found to enhance the physical interaction between mTOR and its inhibitor DEPTOR (LIU *et al.* 2010), which has no obvious yeast ortholog. Resveratrol has also been suggested to inhibit mTOR by indirect mechanisms including regulation of phosphoinositide 3-kinase (PI3K), Akt (BRITO *et al.* 2009), and AMP-activated protein kinase (AMPK) (TILLU *et al.* 2012). We found no evidence here to support an mTOR-inhibitory role for

resveratrol in yeast, nor any effect on growth at all, consistent with prior work showing that resveratrol does not impact yeast growth or replicative lifespan (KAEBERLEIN *et al.* 2005b).

Overall, the system described here represents a sensitive, high-throughput, and inexpensive approach to identify growth inhibitory molecules with specificity for mTOR *in vivo*. It may be possible to further optimize this system, for example by screening compounds in a drug sensitized background or by humanizing the system through expression of human proteins in the mTOR signaling pathway in yeast. Additionally, this method is easily adapted for testing drug interactions by adding a mixture of two or more compounds, as well as for investigating the impact of genetic diversity on mTORC1 inhibition through use of large-scale genetic libraries or wild isolate yeast strains (FAY AND BENAVIDES 2005; LITI *et al.* 2009). The identification of new mTOR inhibitors and genetic variants that impact sensitivity to mTOR inhibition will facilitate the development of new therapies and personalized approaches for a breadth of conditions where mTOR signaling is perturbed.

3.7 Acknowledgments

This work was supported by the University of Washington Nathan Shock Center of Excellence in the Basic Biology of Aging Invertebrate Longevity and Healthspan Core **(**P30AG013280) and a grant to MK from USANA Health Sciences. MBL was supported by the Howard Hughes Medical Institute (HHMI) Gilliam Fellowship for Advanced Study, the National Institutes of Health (NIH) Cellular and Molecular Biology training grant (T32GM7270-39), and the University of Washington Graduate Opportunities and Minority Achievement Program (UW GO-MAP) Bank of America Fellowship.

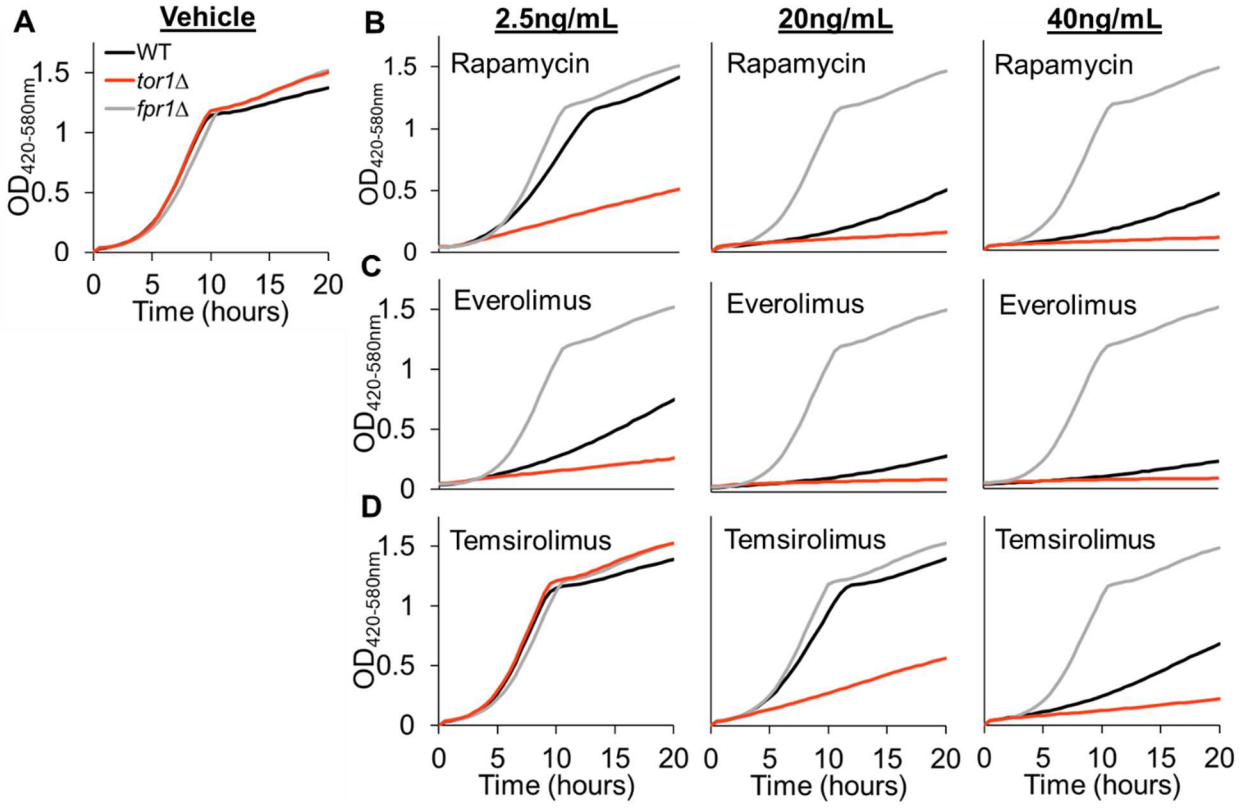

Figure 3.1. Differential growth of wild type (WT), *tor1Δ* and *fpr1Δ* strains in the presence of rapamycin and rapalogs. *tor1Δ* mutants are hypersensitive and *fpr1Δ* mutants are resistant to rapamycin and rapalogs. Representative growth curves of WT (black), *tor1*Δ (red), and *fpr1*Δ (gray) yeast grown in YPD with A) 1.5% DMSO (vehicle) or 2.5-40 ng/mL (left to right) B) rapamycin, C) everolimus, or D) temsirolimus.

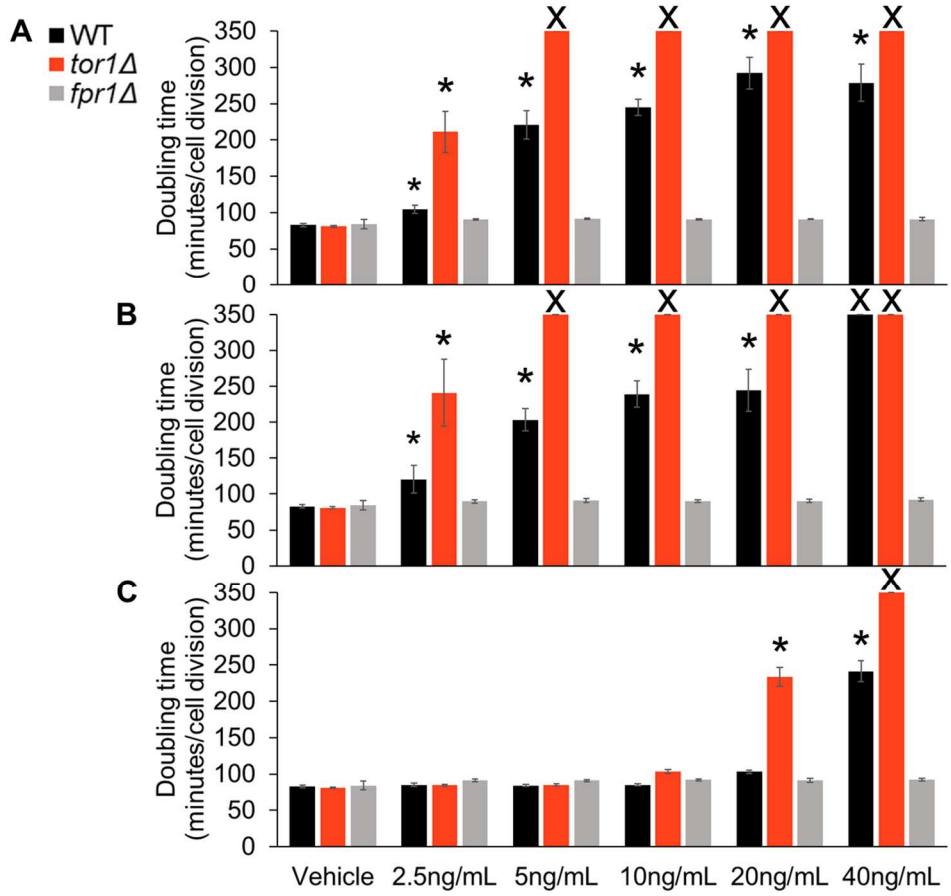

Figure 3.2. Effect of rapamycin and rapalogs on maximal doubling time of wild type (WT), *tor1*Δ, and *fpr1*Δ yeast cells. Peak doubling times of wild type (black), *tor1*Δ (red), and *fpr1*Δ (gray) in vehicle or 2.5-40 ng/mL A) rapamycin, B) everolimus, or C) temsirolimus (n=3-5 for each treatment). Error bars = SEM. * = significantly different from 1.5% DMSO control (vehicle) ($p < 0.05$, Welch's t-test). x = doubling time could not be calculated due to no growth, indicated by OD $\leq$ 0.3 after 20 hours.

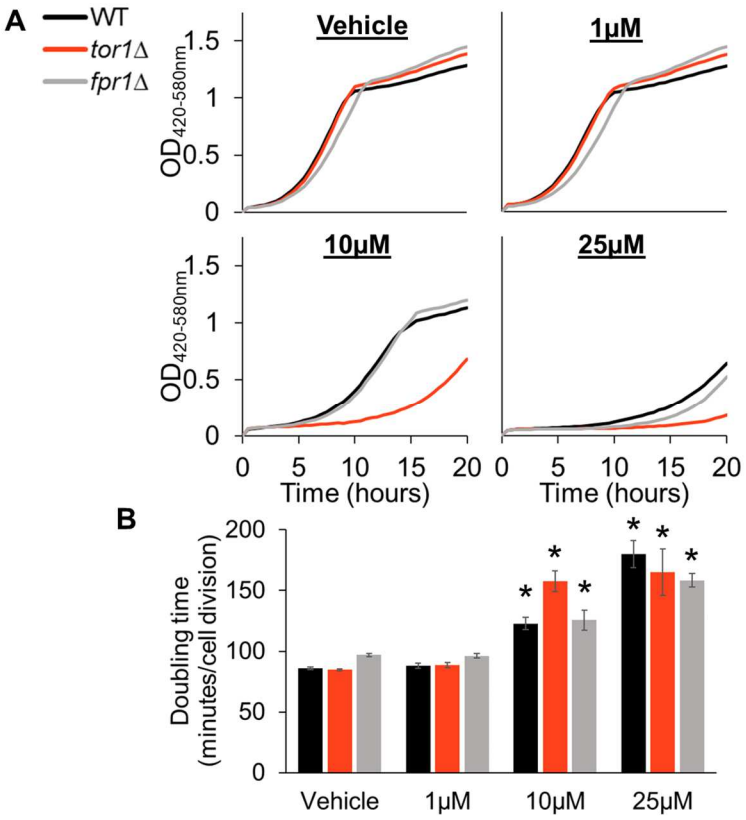

Figure 3.3. The catalytic mTOR inhibitor Torin 1 produces a distinct growth inhibitory profile relative to rapamycin. tor1Δ mutants are hypersensitive to Torin 1 and fpr1Δ mutants are not resistant. A) Representative growth curves of WT, tor1Δ, and fpr1Δ outgrown in the presence of 2.5% DMSO (vehicle) (top left), 1μM Torin 1 (top right), 10μM Torin 1 (bottom left), or 25μM Torin 1 (bottom right). B) Maximal doubling time (minutes/cell division) for WT, tor1Δ, and fpr1Δ strains grown in either 2.5% DMSO (vehicle control) (n=9 for WT and fpr1Δ, and n=10 for tor1Δ) or 1-25μM Torin 1 (n=4 for each strain in 1μM Torin 1 and n=5 for each strain in 10 and 25μM Torin 1). * = significantly different from vehicle ($p < 0.05$, Welch's t-test).

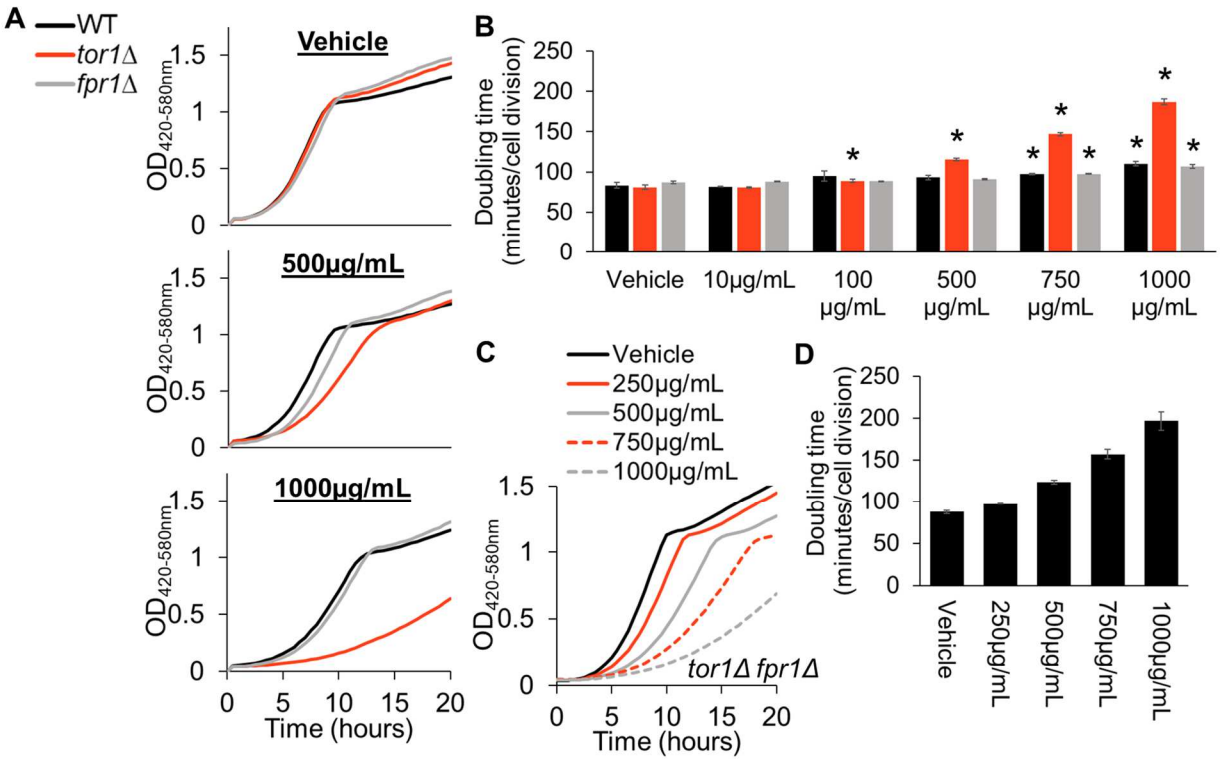

Figure 3.4. Caffeine inhibits yeast growth in *tor1Δ* cells independently of Fpr1. A) Representative growth curves of 6.67% H_2O (vehicle) (top left), 500µg/mL (middle), and 1000µg/mL (bottom). B) Maximal doubling time (minutes/cell division) for WT, *tor1Δ*, and *fpr1Δ* yeast grown in vehicle or 10-1000µg/mL caffeine (n=3-5 independent cultures for each strain*treatment tested). * = significantly different from vehicle control ($p < 0.05$, Welch's t-test). C) *tor1Δ fpr1Δ* are sensitive to caffeine, indicating that caffeine-mediated growth inhibition in *tor1Δ* cells is independent of Fpr1. D) Peak doubling times for *tor1Δ fpr1Δ* grown in vehicle or 250-1000µg/mL caffeine (n=6 independent cultures for each strain*treatment tested).

Table 1. Maximum doubling time of wild type (WT), *tor1Δ* , and *fpr1Δ* cells grown in rich YPD medium supplemented with the indicated neutraceuticals. Doubling time (DT) (minutes/cell division), standard error of the mean (SEM), percent change, and number of cultures tested (n) for putative mTOR-inhibitory neutraceutical compounds.

	WT			*tor1Δ*			*fpr1Δ*		
Treatment	DT (SEM)	% change	n	DT (SEM)	% change	n	DT (SEM)	% change	n
1% DMSO	83.3 (0.9)	-	13	82.8 (0.9)	-	13	90.8 (1.0)	-	13
100µg/mL alpha lipoic acid	85.4 (2.3)	2.6	3	85.2 (1.2)	2.9	3	91.7 (2.1)	-6.2	3
100µg/mL Broccoli concentrate	83.3 (1.1)	0	3	82.7 (2.8)	-0.2	3	89.2 (1.9)	-1.8	3
100µg/mL Glucosamine	81.0 (2.5)	-2.8	4	81.2 (2.1)	-2	4	87.5 (2.6)	-3.6	4
100µg/mL Lycopene	95.8 (0.3)	15.0*	3	101.1 (2.8)	22.2*	3	107.7 (0.7)	18.6*	3
100µg/mL Quercetin	104.1 (3.1)	25.0*	4	102.0 (6.0)	23.2*	4	105.4 (10.2)	16.1	4
100µg/mL Resveratrol	82.7 (0.8)	-0.7	3	82.4 (0.5)	-0.5	3	87.0 (1.5)	-4.2	3
1µg/mL Berberine	80.2 (2.4)	-3.7	3	79.7 (2.6)	-3.7	3	87.0 (4.2)	-4.2	3
10µg/mL Berberine	102.2 (1.9)	22.7*	3	95.2 (1.8)	14.9*	3	101.8 (2.3)	12.1*	3
100µg/mL Berberine	227.1 (6.7)	172.6*	3	228.6 (2.9)	176.1*	3	238.1 (2.5)	162.3*	3

*= $p < 0.05$, compared to 1% DMSO, Welch's (unequal variance) t-test.

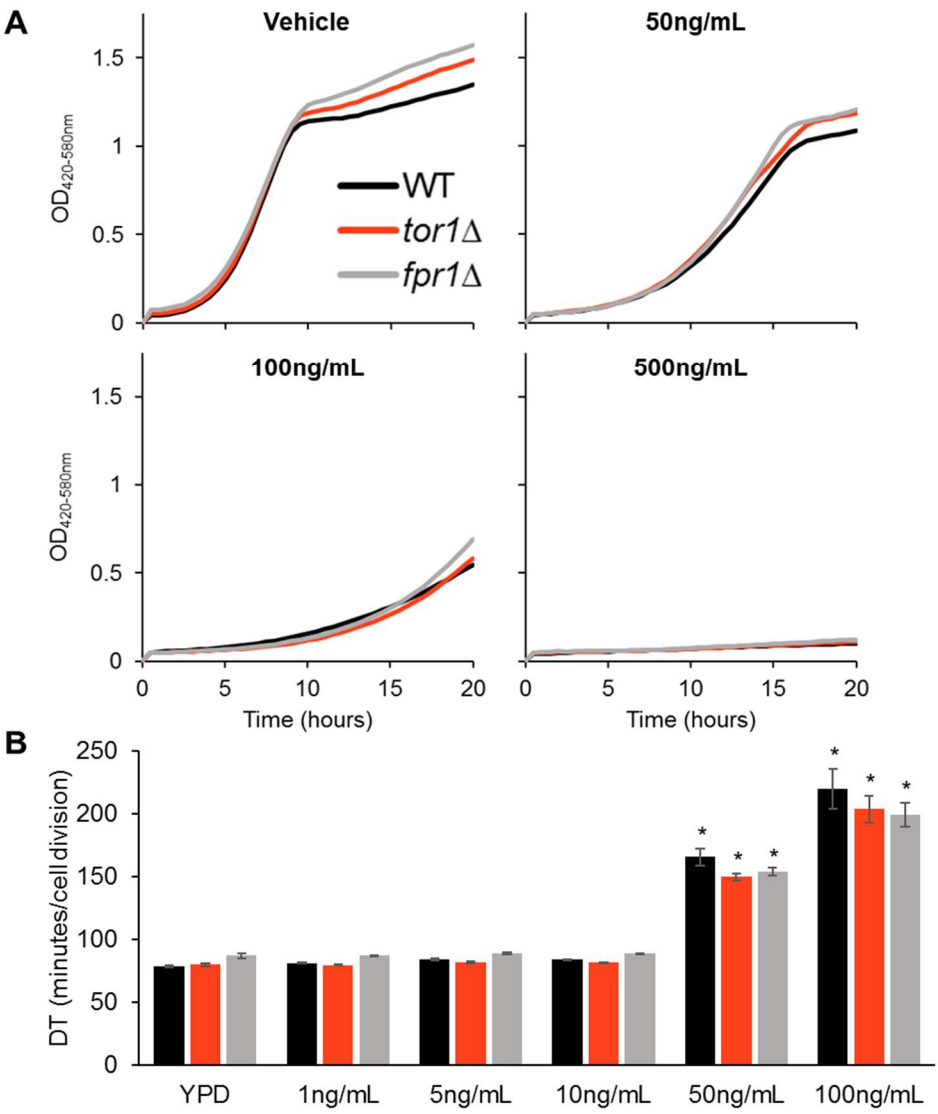

Supplemental figure 3.1. Cycloheximide (CHX) is a general growth inhibitor in yeast. A) WT (black), *tor1Δ* (red), and *fpr1Δ* (gray) grown in YPD with vehicle (top left), 50ng/mL (top right), 100ng/mL (bottom left), and 500ng/mL (bottom right) CHX. B) Peak doubling time (DT) (minutes/cell division) of WT, *tor1Δ*, *fpr1Δ* cells outgrown in the presence of 1-100ng/mL CHX (n=3-5 biological replicate cultures tested for each strain and treatment). *significantly different from 1.5% DMSO control ($p < 0.05$, Welch's t-test). Error bars = SEM. 500ng/mL CHX treatment could not be calculated because outgrowing cultures failed to reach OD = 0.3 after 20 hours.

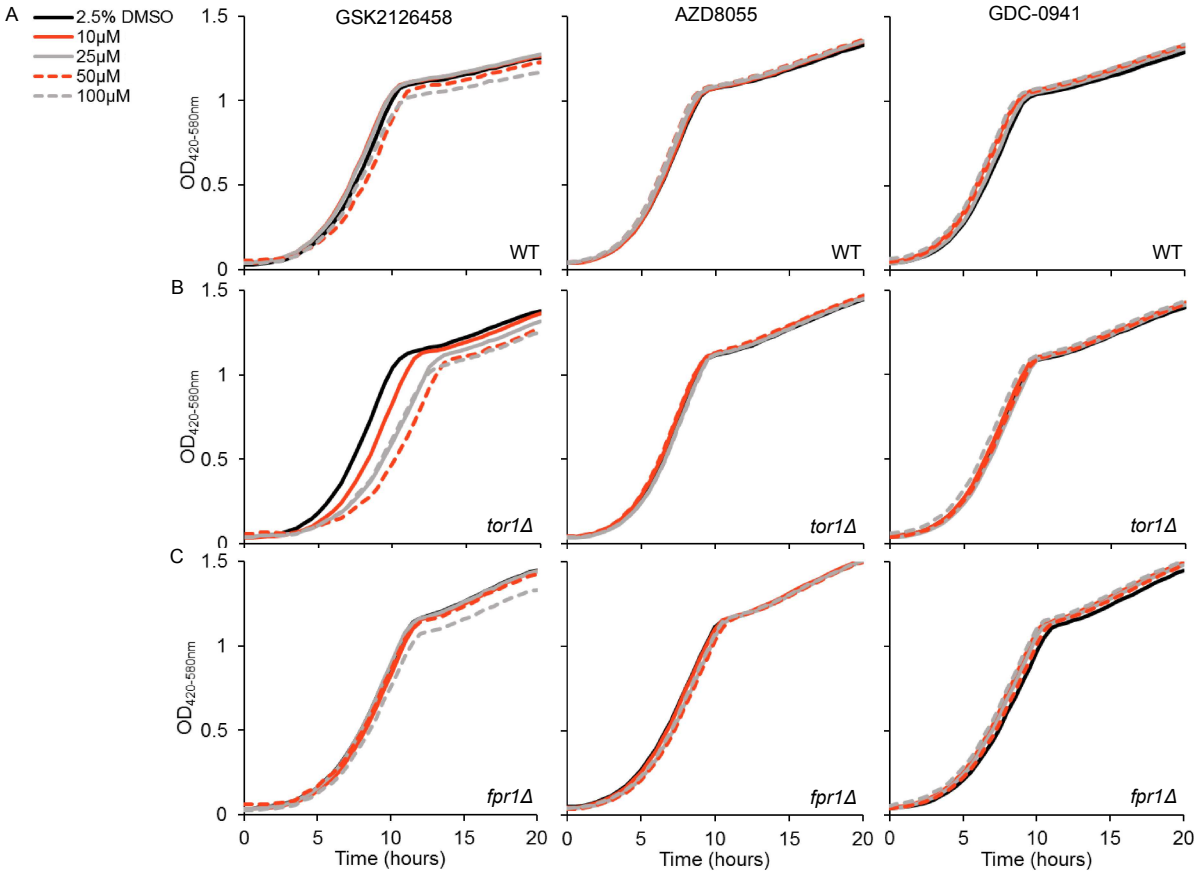

Supplemental figure 3.2. Many mTOR catalytic inhibitors have limited or no effect on yeast growth. GSK2126458, but not AZD8055 or GDC-0941, impacts growth of tor1Δ mutant yeast. Outgrowth of WT (A), tor1Δ (B), and fpr1Δ (C) in 2.5% DMSO (vehicle control) or 10-100μM GSK2126458 (left), AZD8055 (middle), or GDC-0941 (right). n=3-5 biological replicate cultures tested for each strain and treatment.

Supplemental Table 1. Doubling time (DT) (minutes/cell division), standard error of the mean (SEM),

	WT			*tor1Δ*			*fpr1Δ*		
Treatment	DT (SEM)	% change	n	DT (SEM)	% change	n	DT (SEM)	% change	n
1.5% DMSO	82.8 (2.2)	-	5	80.9 (1.2)	-	5	84.3 (6.4)	-	5
2.5ng/mL Rapamycin	104.6 (5.6)	26.3*	4	211.4 (28.3)	161.3*	4	90.6 (1.0)	7.5	4
5ng/mL Rapamycin	221.3 (19.5)	167.2*	4	NG	-	4	91.5 (0.8)	8.5	4
10ng/mL Rapamycin	245.1 (11.0)	196.1*	4	NG	-	4	91.0 (0.9)	7.9	4
20ng/mL Rapamycin	292.0 (22.2)	252.7*	4	NG	-	4	91.1 (0.6)	8.1	4
40ng/mL Rapamycin	278.9 (25.5)	236.9*	4	NG	-	4	90.9 (2.2)	7.8	4
2.5ng/mL Everolimus	120.5 (2.2)	45.5*	4	241.0 (46.3)	198.0*	4	89.7 (2.2)	6.4	4
5ng/mL Everolimus	203.4 (19.1)	145.7*	3	NG	-	3	91.2 (2.7)	8.2	3
10ng/mL Everolimus	239.1 (18.4)	188.7*	3	NG	-	3	90.0 (1.7)	6.7	3
20ng/mL Everolimus	244.8 (29.2)	195.7*	3	NG	-	3	90.3 (2.4)	7.1	3
40ng/mL Everolimus	NG	-	3	NG	-	3	92.2 (2.4)	9.4	3
2.5ng/mL Temsirolimus	85.1 (2.2)	2.8	3	84.4 (1.5)	4.3	3	91.3 (1.8)	8.3	3
5ng/mL Temsirolimus	84.2 (1.4)	1.7	3	85.2 (1.5)	5.3	3	91.2 (1.4)	8.2	3
10ng/mL Temsirolimus	84.9 (1.3)	2.5	3	103.4 (3.2)	27.8*	3	92.1 (1.5)	9.2	3
20ng/mL Temsirolimus	103.0 (2.5)	24.4*	3	233.6 (13.1)	188.8*	3	91.2 (2.6)	8.2	3
40ng/mL Temsirolimus	241.3 (14.7)	191.4*	3	NG	-	3	92.4 (1.9)	9.6	3

* = $p < 0.05$, compared to 2.5% DMSO, Welch's (unequal variance) t-test.

NG = DT could not be calculated due to no growth, indicated by OD ≤ 0.3 after 20 hours.

Supplemental Table 2. Doubling time (DT) (minutes/cell division), standard error of the mean (SEM), percent change, and number of cultures tested (n) for catalytic mTOR inhibitors.

	WT			*tor1Δ*			*fpr1Δ*		
Treatment	DT (SEM)	% change	n	DT (SEM)	% change	n	DT (SEM)	% change	n
2.5% DMSO	85.9 (0.9)	-	12	84.6 (1.0)	-	13	96.9 (1.1)	-	12
10μM AZD8055	92.4 (8.4)	7.5	4	93.0 (7.5)	9.9	4	104.4 (10.8)	7.7	4
25μM AZD8055	86.2 (1.4)	0.3	3	87.3 (2.2)	3.1	3	95.7 (1.1)	-1.2	3
50μM AZD8055	87.6 (2.6)	1.9	3	89.5 (2.6)	5.8	3	96.9 (3.2)	0.0	3
100μM AZD8055	87.7 (3.3)	2.1	3	89.6 (2.3)	5.9	3	98.6 (2.8)	1.8	3
10μM GDC-0941	85.7 (2.0)	-0.3	3	84.2 (2.1)	-0.5	3	95.9 (2.4)	-1.0	3
25μM GDC-0941	84.6 (1.6)	-1.6	3	82.5 (1.0)	-2.6	3	95.2 (1.2)	-1.7	3
50μM GDC-0941	86.8 (2.8)	1.0	3	85.8 (2.1)	1.4	3	96.8 (2.9)	-0.1	3
100μM GDC-0941	94.3 (3.3)	9.7	3	93.1 (2.6)	10.0	3	102.5 (4.4)	5.8	3
10μM GSK2126458	85.4 (1.5)	-0.6	6	92.5 (1.6)	9.3*	6	97.8 (2.9)	1.0	6
25μM GSK2126458	89.9 (2.5)	4.6	7	105.7 (2.6)	24.9*	7	96.7 (2.3)	-0.1	7
50μM GSK2126458	80.6 (6.3)	-6.2	6	93.2 (4.1)	10.1	6	95.6 (1.6)	-1.3	6
100μM GSK2126458	103.8 (5.4)	20.8*	6	117.3 (6.8)	38.6*	6	112.4 (5.3)	16.0*	6
1μM Torin 1	88.1 (2.0)	2.6	4	88.7 (2.1)	4.9	4	96.2 (2.0)	-0.7	4
10μM Torin 1	122.7 (5.0)	42.8*	5	157.5 (8.6)	86.2*	5	125.5 (8.3)	29.6*	5
25μM Torin 1	179.9 (11.2)	109.4*	5	165.1 (19.1)	95.1*	5	158.4 (5.6)	63.5*	5

*= $p < 0.05$, compared to 2.5% DMSO, Welch's (unequal variance) t-test.

Chapter 4. *Pterocarpus marsupium* extract extends replicative lifespan independent of pterostilbene or (-)-epicatechin in *Saccharomyces cerevisiae*

Mitchell B. Lee[1], Michael G. Kiflezghi[1,2], Mitsuhiro Tsuchiya[1], Brian Wasko[1], Daniel T. Carr[1], Priya A. Uppal[1], Katherine A. Grayden[1], Yordanos C. Elala[1], Tu Anh Nguyen[1], Jesse Wang[1], Priya Ragosti[1], Sunny Nguyen[1], Yan Ting Zhao[1], Deborah Kim[1], Socheata Thon[1], Irika Sinha[1], Thao T. Tang[1], Ngoc H.B. Tran[1], Thu H.B. Tran[1], Margarete D. Moore[1], Mary Ann K. Li[1], Matt Kaeberlein[1]

1. Department of Pathology, University of Washington, Seattle, WA, USA.

2. Molecular Medicine and Mechanisms of Disease (M3D) Program, University of Washington, Seattle, WA, USA.

4.2 Abstract

Once merely the fodder of science fiction, our understanding of aging has progressed to the point that evidence-based, anti-aging interventions are now being tested in humans and large mammals. Concerns about intervention side effects and efficacy across genetically-diverse organisms create a need for additional compounds that can be developed into healthspan- and lifespan-extending interventions. In order to identify novel natural product compounds and extracts that extend cellular lifespan, we screened a set of nutraceuticals with proposed mTOR inhibitor activity using yeast replicative lifespan (RLS). Of these, only *Pterocarpus marsupium* extract (PME) extended lifespan. *Pterocarpus marsupium* (a deciduous tree found in southeast Asia) is used in ayurvedic medicine to treat numerous conditions, including diabetes. Within this extract are at least two compounds previously proposed to have longevity benefits: pterostilbene and (-)-epicatechin. We tested concentrations of pterostilbene similar to those found in PME and found that it does not extend lifespan. We tested a broader dose response of (-)-epicatechin and found that it also does not extend lifespan. Identifying novel, inexpensive compounds that extend healthspan and lifespan will allow more individuals to reap the benefits of longevity research and may lead to the development of combinatorial treatments that can be used to maximize healthy human and companion pet lifespan.

4.3 Introduction

Compounds that protect our health as we age and delay the onset of age-associated disease hold unparalleled promise as translatable healthy aging interventions. Numerous small molecules

have been reported to extend lifespan in invertebrate and vertebrate model systems (BARARDO *et al.* 2017). Rapamycin, an inhibitor of mechanistic Target Of Rapamycin (mTOR) signaling, is reported to extend lifespan in yeast, nematode, fly, and multiple mouse backgrounds (HARRISON *et al.* 2009; RALLIS *et al.* 2013; MILLER *et al.* 2014; BITTO *et al.* 2016). In humans, elderly patients given the rapamycin analog everolimus (RAD001) showed improved immune function (MANNICK *et al.* 2014) and short-term rapamycin treatment in pet dogs improves cardiac function (URFER *et al.* 2017b). Future studies will monitor survival and age-associated disease onset in a large cohort of pet dogs given rapamycin as a first-of-its-kind attempt to increase companion pet healthy lifespan (KAEBERLEIN *et al.* 2016). Other compounds, like metformin, nicotinamide mononucleotide (NMN), resveratrol, and pterostilbene, are either being tested in clinical trials, or are already being marketed without clinical validation, as healthy aging interventions for humans (ANISIMOV *et al.* 2008; YOSHINO *et al.* 2011; CABREIRO *et al.* 2013; BARZILAI *et al.* 2016; DELLINGER *et al.* 2017; GUAN *et al.* 2017).

While current small molecule interventions are clearly capable of increasing lifespan and, in some cases, improving healthspan in laboratory model systems, concerns about efficacy and safety within genetically-diverse populations create a need to identify additional interventions. Side effects from clinical use of rapamycin as an immunomodulator or cancer therapy, for example, include oral stomatitis and other oral pathologies, altered blood chemistry (particularly dyslipidemia and hyperglycemia), peripheral edema, and proteinuria (VERHAVE *et al.* 2014; FERNANDES-SILVA *et al.* 2017; LO MUZIO *et al.* 2018). It is less well-understood what side effects would manifest in healthy individuals given lower doses, or different dosing regimens, of rapamycin (JOHNSON AND KAEBERLEIN 2016). Other proposed healthy aging interventions, like metformin, can cause side effects that include intestinal distress, diarrhea, and in rare cases, lactic

acidosis (DANDONA *et al.* 1983; BAILEY AND TURNER 1996). Additionally, metformin has contraindications that would preclude use in many individuals (INZUCCHI 2002). Other putative healthy aging interventions that are not yet clinically validated have little information regarding their efficacy and safety in non-laboratory, genetically heterogeneous organisms, making an assessment of their broad translatability difficult.

Multiple efforts are currently underway to validate pharmacological healthy aging interventions. The Interventions Testing Program (ITP) is a multi-site effort to perform confirmatory tests of healthy aging compounds using a genetically-heterogeneous mouse model (WARNER *et al.* 2000; NADON *et al.* 2017). Instead of broadly screening potential small molecules, compounds are tested based on prior evidence and peer review. This endeavor has tested over 40 interventions in mice and found that six (including rapamycin) extend lifespan in at least one gender (STRONG *et al.* 2008; MILLER *et al.* 2011; WILKINSON *et al.* 2012; STRONG *et al.* 2013; HARRISON *et al.* 2014; STRONG *et al.* 2016). A similar effort geared toward examining more compounds at higher throughput is the *Caenorhabditis* Intervention Testing Program (CITP). While similar in concept to the ITP, the CITP utilizes over 20 genetically-distinct strains encompassing three species of *Caenorhabditis* (LITHGOW *et al.* 2017; LUCANIC *et al.* 2017; PLUMMER *et al.* 2017). With these standardized programs in place to independently test and replicate putative healthy aging interventions, the identification of high priority candidates for future testing in humans or companion animals is becoming streamlined. This creates a need for discovery-based studies aimed at identifying new potential lifespan-extending interventions.

To identify new compounds and extracts that extend lifespan in budding yeast, we screened 15 nutraceuticals for their impact on yeast replicative lifespan (RLS). This work follows up on previous results that tested many of these compounds for mTOR inhibitor activity (LEE *et al.*

2017). We report that one extract, *Pterocarpus marsupium* extract (PME), extends replicative lifespan. Further, PME effect is not mediated by pterostilbene or (-)-epicatechin, two compounds thought to confer PME its health benefits.

4.4 Methods

Yeast strains and culture conditions

Strains BW1121 (wild type) and GS983 (*tor1Δ::kanMX4*) were the same as previously described (LEE *et al.* 2017). All yeast were from BY4742 background (BRACHMANN *et al.* 1998). Yeast were cultured using 1% yeast extract (Bacto™ BD), 2% peptone (Bacto™ BD), and 2% dextrose (YPD) media with 2% agar added when solid media prepared.

Drug preparation and suppliers

All drugs, except berberine, were suspended in DMSO. Berberine was suspended in H_2O. Pterostilbene was purchased from AstaTech, Inc. (Bristol, PA, USA). (-)-Epicatechin was purchased from AdooQ Bioscience (Irvine, CA, USA). Berberine was purchased from Sigma Aldrich (St. Louis, MO, USA). All other compounds were provided by USANA Health Sciences, Inc. (Salt Lake City, UT, USA).

Replicative lifespan analysis

Survival of yeast was quantified using replicative lifespan (RLS) analysis, as previously described (STEFFEN *et al.* 2009). To do this, yeast colonies struck from frozen stocks and outgrown on YPD were prepatched onto YPD plates, either with drug of interest or vehicle alone, and grown at 30^{o}C overnight. From prepatched plates, cells were transferred onto RLS plates with treatment maintained and, after overnight growth, were selected for RLS analysis. In the screen, all drugs (except berberine) were screened at 100 μg/mL concentration. Berberine was screened in a dose response from 1-50 μg/mL.

Outgrowth analysis using Bioscreen C MBR

Bioscreen-based growth assays combined with analysis using Yeast Outgrowth Data Analyzer (YODA) was used to quantify doubling time as previously described (MURAKAMI *et al.* 2008; OLSEN *et al.* 2010). To identify whether PME is mTOR inhibitory, we used our mTOR inhibitors screening strategy (LEE *et al.* 2017). Briefly, WT, *tor1Δ*, and *fpr1Δ* cells were outgrown in YPD, with and without drug, in 100-well honeycomb plates. *tor1Δ* sensitivity was compared to that of WT and *fpr1Δ* in the presence of compound to assess whether the treatment preferentially inhibited outgrowth.

4.5 Results

A screen of nutraceuticals reveal that Pterocarpus marsupium extract extends RLS

We tested 15 compounds and extracts for their impact on WT haploid yeast (BY4742) replicative lifespan (RLS) (**Table 1**). Two 20-cell sets were initially assayed for each treatment, then follow-up experiments were performed on 20-cell sets to validate potential lifespan-extending treatments. All compounds were tested at 100 μg/mL and compared to 1% DMSO (vehicle) except berberine, which was dissolved in water and tested 1-50 μg/mL. DMSO alone did not impact lifespan (**Supplemental figure S1**). Most treatments (12/15) did not significantly change lifespan. Green tea extract and berberine both significantly reduced median RLS (29% and 52%, respectively, Wilcoxon rank sum test, Bonferroni-corrected, $p = 0.03$ and <0.001). Only one treatment, *Pterocarpus marsupium* extract (PME), extended RLS (**Figure 1**). *Pterocarpus marsupium*, a deciduous tree found in India and Sri Lanka, is used as an anti-inflammatory and anti-diabetic in Ayurvedic medicine. 100 μg/mL PME increased median lifespan 33% ($n = 104$, $p < 0.001$, Wilcoxon rank sum test, Bonferroni-corrected). Using a yeast outgrowth-based mTOR inhibitor assay we developed (LEE *et al.* 2017), we found that PME does not impact yeast growth, either in WT or in *tor1Δ* mutants (**Supplemental figure S2**). From this, we conclude that PME is not a mTOR inhibitor.

Pterostilbene or (-)-epicatechin alone does not extend replicative lifespan

At least two compounds within PME have reported healthspan benefits that may influence cellular lifespan: pterostilbene and (-)-epicatechin. Pterostilbene is a dimethylated resveratrol analog with many reported healthspan benefits (ESTRELA *et al.* 2013). (-)-Epicatechin is a monomeric flavanol molecule that makes up procyanidins, oligomeric flavonoid compounds found in cocoa (MARTIN AND RAMOS 2017). (-)-Epicatechin is reported to improve cardiovascular health

and prevent diabetes (MCCULLOUGH *et al.* 2012). To test if these compounds are sufficient to extend lifespan, we tested dose responses of both compounds. Pterostilbene concentrations ranging from 1-25 μM (similar to that reported in PME) had no effect on yeast lifespan (n = 160-180 for each treatment, p = 0.22-0.38, Wilcoxon rank sum test) (**Figure 2a**). For (-)-epicatechin, we tested a broader dose response, from 1-100 μg/mL. As with pterostilbene alone, (-)-epicatechin did not extend lifespan at the concentrations we tested (n = 119-120 for each treatment, p = 0.59-1, Wilcoxon rank sum test) (**Figure 2b**). So, we conclude that neither pterostilbene nor (-)-epicatechin alone are sufficient to extend lifespan like that of PME.

4.6 Discussion

PME is a new lifespan extending extract that extends yeast replicative lifespan. While PME is less well-known in western medicine, it has been used for centuries to treat diabetes in Aryuvedic medicine (N AND CHOPRA 1933). PME is typically consumed as an aqueous solution produced by steeping water in a tumbler made from *Pterocarpus marsupium* heartwood. Beyond these accounts, lab studies show that PME holds promise in treating age-associated diseases. Sheep tested with intravenous aqueous PME showed elevated glucose clearance and increased plasma insulin (MOHANKUMAR *et al.* 2012). Diabetic rats treated with PME had lowered blood glucose and reduced rates of cataracts (VATS *et al.* 2002; VATS *et al.* 2004). The blood glucose lowering effects are rapid in this model, with even a single dose showing a strong effect (KAR *et al.* 2003). Rats showed suppressed cognitive deficits with PME treatment in a streptozotocin-induced Alzheimer's disease model (LESTER-COLL *et al.* 2006; KOSARAJU *et al.* 2014). With

multiple age-associated conditions reported to be mitigated using PME, this lends support for there being broader utility for PME as a healthspan intervention.

It remains unclear what accounts for PME's lifespan extending effect. PME does not behave as an mTOR inhibitor at concentrations that extend lifespan, suggesting a distinct mechanism. Neither pterostilbene or (-)-epicatechin increased lifespan at concentrations similar to that found in PME. Further lifespan analysis of compounds within PME and genetic analysis of PME mode of action are needed. Combinatorial doses of pterostilbene and (-)-epicatechin may extend lifespan together, even though they failed to do so individually. A broader strategy may first be needed where PME is fractionated and lifespan analysis is performed using fractions to identify those that retain lifespan extending properties. This approach will allow many more compounds within this heterogeneous extract to be screened for effect. Other approaches, like genetic epistasis analyses using mutants in identified longevity pathways and combined dietary restriction and PME treatment in yeast, will allow for a better understanding of PME mode of action. Finally, testing PME in other invertebrate models, like worms and flies, will establish whether PME effect on lifespan translates across evolutionary distance. Understanding PME in both wildtype and disease models will further allow us to understand the broader utility of this extract as a healthspan intervention.

4.7 Acknowledgements

This work was supported by the University of Washington Nathan Shock Center of Excellence in the Basic Biology of Aging Invertebrate Longevity and Healthspan Core (P30AG013280) and a grant to MK from USANA Health Sciences. MBL was supported by the Howard Hughes Medical

Institute (HHMI) Gilliam Fellowship for Advanced Study, the National Institutes of Health (NIH) Cellular and Molecular Biology training grant (T32GM7270-39), and the University of Washington Graduate Opportunities and Minority Achievement Program (UW GO-MAP) Bank of America Fellowship

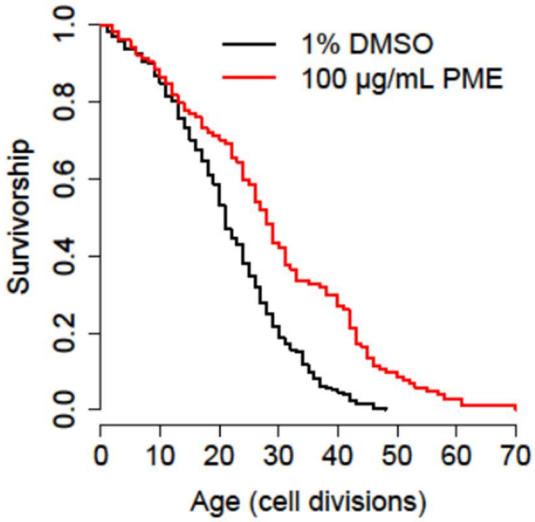

Figure 4.1. *Pterocarpus marsupium* extract (PME) extends replicative lifespan. 100 µg/mL PME (n = 104) extends lifespan compared to 1% DMSO vehicle control (n = 198) ($p < 0.001$, Wilcoxon rank sum test).

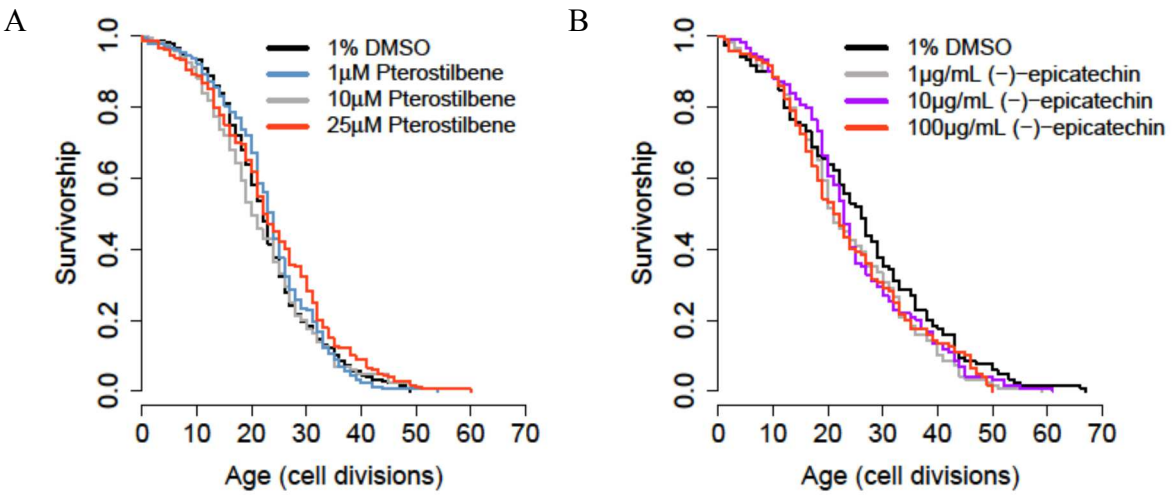

Figure 4.2. Pterostilbene or (-)-epicatechin (Epi) alone does not extend RLS. A) RLS of pterostilbene dose response with similar concentrations (1-25 µM) as found in PME. B) RLS of (-)-epicatechin dose response (1-100 µg/mL).

Table 4.1. Median RLS (95% confidence intervals), number of cells dissected (n), percent change and p-value (Wilcoxon rank sum test) of nutraceuticals compared to vehicle (1% DMSO) control.

Treatment	n	Median RLS (95% CI)	% change	P-value
1% DMSO (vehicle control)	198	21 (20-24)	0.0	-
YPD (standard media)	268	20 (19-22)	-4.8	0.69
100 μg/mL Alpha lipoic acid	40	21 (19-26)	0.0	0.86
1 μg/mL Berberine	155	22 (21-25)	4.8	0.23
10 μg/mL Berberine	160	21 (20-23)	0.0	1
50 μg/mL Berberine	157	10 (9-11)	-52.4	< 0.001
100 μg/mL Broccoli concentrate	80	19.5 (16-24)	-7.1	0.34
100 μg/mL Choline bitartrate	160	21 (19-23)	0.0	0.82
100 μg/mL Glucosamine HCl	116	21 (19-25)	0.0	0.82
100 μg/mL Grape seed extract	118	19.5 (18-24)	-7.1	0.91
100 μg/mL Green tea extract	40	15 (13-19)	-28.6	0.03
100 μg/mL Lutein	39	18 (16-28)	-14.3	0.98
100 μg/mL Lycopene	118	19 (17-22)	-9.5	0.1
100 μg/mL Milk thistle extract	40	19 (15-26)	-9.5	0.54
100 μg/mL N-actetyl L-cysteine	39	20 (17-27)	-4.8	0.66
100 μg/mL Pterocarpus marsupium extract	104	28 (25-31)	33.3	< 0.001
100 μg/mL Quercetin	40	18.5 (16-27)	-11.9	0.84
100 μg/mL Rutin	40	18.5 (15-26)	-11.9	0.31
100 μg/mL Turmeric extract	40	16.5 (14-22)	-21.4	0.12

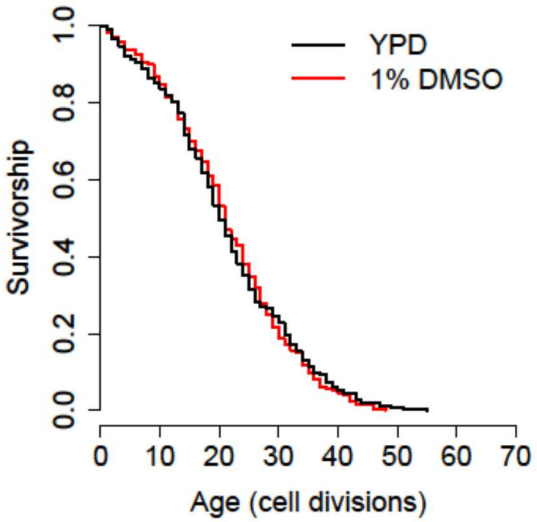

Supplementary Figure 4.1. 1% DMSO (vehicle control) alone does not impact RLS. 1% DMSO n = 198, YPD n = 268.

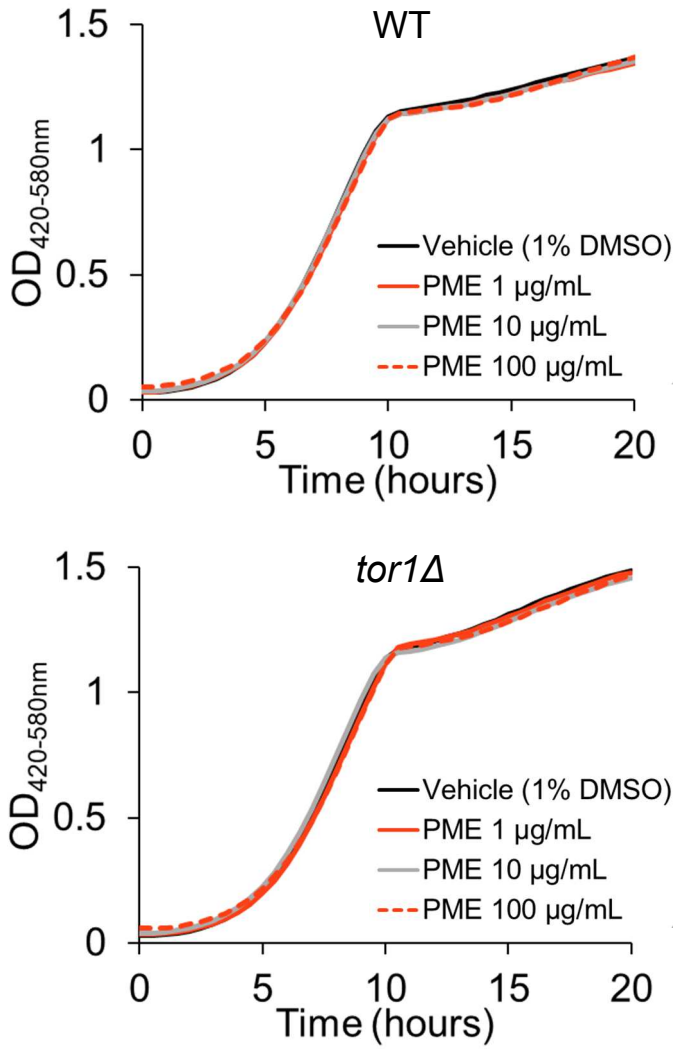

Supplementary figure 4.2. *Pterocarpus marsupium* extract (PME) has no effect on WT or *tor1Δ* outgrowth. Bioscreen-based outgrowth analysis of yeast 1% DMSO vehicle control (black) or 1-100 µg/mL PME.

Bibliography

Adak, T., A. Samadi, A. Z. Unal and S. Sabuncuoglu, 2018 A reappraisal on metformin. Regulatory Toxicology and Pharmacology 92**:** 324-332.

AFAR, A. F. f. A. R., 2016 Biomarkers of Aging: An introduction to aging science brought to you by the American Federation for Aging Research, pp. American Federation for Aging Research, New York, NY.

Alexandrov, L. B., S. Nik-Zainal, D. C. Wedge, S. A. J. R. Aparicio, S. Behjati *et al.*, 2013 Signatures of mutational processes in human cancer. Nature 500**:** 415-421.

Anastasius, N., S. Boston, M. Lacey, N. Storing and S. A. Whitehead, 2009 Evidence that low-dose, long-term genistein treatment inhibits oestradiol-stimulated growth in MCF-7 cells by down-regulation of the PI3-kinase/Akt signalling pathway. J Steroid Biochem Mol Biol 116**:** 50-55.

Anisimov, V. N., L. M. Berstein, P. A. Egormin, T. S. Piskunova, I. G. Popovich *et al.*, 2008 Metformin slows down aging and extends life span of female SHR mice. Cell Cycle 7**:** 2769-2773.

Anisimov, V. N., M. A. Zabezhinski, I. G. Popovich, T. S. Piskunova, A. V. Semenchenko *et al.*, 2011 Rapamycin increases lifespan and inhibits spontaneous tumorigenesis in inbred female mice. Cell Cycle 10**:** 4230-4236.

Arias, E., M. Heron and J. Xu, 2017 United States Life Tables, 2014. Natl Vital Stat Rep 66**:** 1-64.

Austin, C. P., J. F. Battey, A. Bradley, M. Bucan, M. Capecchi *et al.*, 2004 The knockout mouse project. Nature Genetics 36**:** 921-924.

Ayyadevara, S., P. Bharill, A. Dandapat, C. P. Hu, M. Khaidakov *et al.*, 2013 Aspirin Inhibits Oxidant Stress, Reduces Age-Associated Functional Declines, and Extends Lifespan of Caenorhabditis elegans. Antioxidants & Redox Signaling 18**:** 481-490.

Bailey, C. J., and C. Day, 1989 Traditional plant medicines as treatments for diabetes. Diabetes Care 12**:** 553-564.

Bailey , C. J., and R. C. Turner 1996 Metformin. New England Journal of Medicine 334**:** 574-579.

Baker, D. J., B. G. Childs, M. Durik, M. E. Wijers, C. J. Sieben *et al.*, 2016 Naturally occurring p16(Ink4a)-positive cells shorten healthy lifespan. Nature 530**:** 184-189.

Baker, D. J., K. B. Jeganathan, J. D. Cameron, M. Thompson, S. Juneja *et al.*, 2004 BubR1 insufficiency causes early onset of aging-associated phenotypes and infertility in mice. Nat Genet 36**:** 744-749.

Baker, D. J., T. Wijshake, T. Tchkonia, N. K. LeBrasseur, B. G. Childs *et al.*, 2011 Clearance of p16(Ink4a)-positive senescent cells delays ageing-associated disorders. Nature 479**:** 232-236.

Bannister, C. A., S. E. Holden, S. Jenkins-Jones, C. L. Morgan, J. P. Halcox *et al.*, 2014 Can people with type 2 diabetes live longer than those without? A comparison of mortality in people initiated with metformin or sulphonylurea monotherapy and matched, non-diabetic controls. Diabetes Obesity & Metabolism 16**:** 1165-1173.

Barardo, D., D. Thornton, H. Thoppil, M. Walsh, S. Sharifi *et al.*, 2017 The DrugAge database of aging-related drugs. Aging Cell 16**:** 594-597.

Barr, M. M., 2005 Caenorhabditis elegans as a model to study renal development and disease: Sexy cilia. Journal of the American Society of Nephrology 16**:** 305-312.
Barriere, A., and M. A. Felix, 2005 High local genetic diversity and low outcrossing rate in Caenorhabditis elegans natural populations. Curr Biol 15**:** 1176-1184.
Barzilai, N., J. P. Crandall, S. B. Kritchevsky and M. A. Espeland, 2016 Metformin as a Tool to Target Aging. Cell Metabolism 23**:** 1060-1065.
Bassett, D. E., M. S. Boguski and P. Hieter, 1996 Yeast genes and human disease. Nature 379**:** 589-590.
Beaupere, C., B. M. Wasko, J. Lorusso, B. K. Kennedy, M. Kaeberlein *et al.*, 2017 CAN1 Arginine Permease Deficiency Extends Yeast Replicative Lifespan via Translational Activation of Stress Response Genes. Cell Rep 18**:** 1884-1892.
Beevers, C. S., L. Chen, L. Liu, Y. Luo, N. J. Webster *et al.*, 2009 Curcumin disrupts the Mammalian target of rapamycin-raptor complex. Cancer Res 69**:** 1000-1008.
Beevers, C. S., F. Li, L. Liu and S. Huang, 2006 Curcumin inhibits the mammalian target of rapamycin-mediated signaling pathways in cancer cells. Int J Cancer 119**:** 757-764.
Bellantuono, I., and P. K. Potter, 2016 Modelling ageing and age-related disease. Drug Discovery Today: Disease Models 20**:** 27-32.
Benton, B. M., J. H. Zang and J. Thorner, 1994 A novel FK506- and rapamycin-binding protein (FPR3 gene product) in the yeast Saccharomyces cerevisiae is a proline rotamase localized to the nucleolus. J Cell Biol 127**:** 623-639.
Beretta, L., A. C. Gingras, Y. V. Svitkin, M. N. Hall and N. Sonenberg, 1996 Rapamycin blocks the phosphorylation of 4E-BP1 and inhibits cap-dependent initiation of translation. EMBO J 15**:** 658-664.
Bergstrom, A., J. T. Simpson, F. Salinas, B. Barre, L. Parts *et al.*, 2014 A high-definition view of functional genetic variation from natural yeast genomes. Molecular biology and evolution 31**:** 872-888.
Bielas, J., A. Herbst, K. Widjaja, J. Hui, J. M. Aiken *et al.*, 2018 Long term rapamycin treatment improves mitochondrial DNA quality in aging mice. Experimental Gerontology 106**:** 125-131.
Bitto, A., T. K. Ito, V. V. Pineda, N. J. LeTexier, H. Z. Huang *et al.*, 2016 Transient rapamycin treatment can increase lifespan and healthspan in middle-aged mice. Elife 5**:** e16351.
Bitto, A., A. M. Wang, C. F. Bennett and M. Kaeberlein, 2015 Biochemical Genetic Pathways that Modulate Aging in Multiple Species. Cold Spring Harb Perspect Med 5.
Bjedov, I., J. M. Toivonen, F. Kerr, C. Slack, J. Jacobson *et al.*, 2010 Mechanisms of life span extension by rapamycin in the fruit fly Drosophila melanogaster. Cell Metab 11**:** 35-46.
Blagosklonny, M. V., 2010 Increasing healthy lifespan by suppressing aging in our lifetime: preliminary proposal. Cell cycle 9**:** 4788-4794.
Blokzijl, F., J. de Ligt, M. Jager, V. Sasselli, S. Roerink *et al.*, 2016 Tissue-specific mutation accumulation in human adult stem cells during life. Nature 538**:** 260-264.
Bocklandt, S., W. Lin, M. E. Sehl, F. J. Sanchez, J. S. Sinsheimer *et al.*, 2011 Epigenetic Predictor of Age. Plos One 6**:** 6.
Bodmer, M., C. Meier, S. Krahenbuhl, S. S. Jick and C. R. Meier, 2010 Long-Term Metformin Use Is Associated With Decreased Risk of Breast Cancer. Diabetes Care 33**:** 1304-1308.
Boeke, J. D., F. Lacroute and G. R. Fink, 1984 A positive selection for mutants lacking orotidine-5'-phophate decarboxylase activity in yeast: 5-fluoro-orotic acid resistance. Molecular & General Genetics 197**:** 345-346.

Bogue, M. A., L. L. Peters, B. Paigen, R. Korstanje, R. Yuan *et al.*, 2016 Accessing Data Resources in the Mouse Phenome Database for Genetic Analysis of Murine Life Span and Health Span. J Gerontol A Biol Sci Med Sci 71**:** 170-177.

Bonawitz, N. D., M. Chatenay-Lapointe, Y. Pan and G. S. Shadel, 2007 Reduced TOR signaling extends chronological life span via increased respiration and upregulation of mitochondrial gene expression. Cell metabolism 5**:** 265-277.

Bonnett, B. N., A. Egenvall, A. Hedhammar and P. Olson, 2005 Mortality in over 350,000 insured Swedish dogs from 1995-2000: I. Breed-, gender-, age- and cause-specific rates. Acta Veterinaria Scandinavica 46**:** 105-120.

Botta, G., C. S. Turn, N. J. Quintyne and P. A. Kirchman, 2011 Increased iron supplied through Fet3p results in replicative life span extension of Saccharomyces cerevisiae under conditions requiring respiratory metabolism. Experimental gerontology 46**:** 827-832.

Brachmann, C. B., A. Davies, G. J. Cost, E. Caputo, J. Li *et al.*, 1998 Designer deletion strains derived from Saccharomyces cerevisiae S288C: A useful set of strains and plasmids for PCR□mediated gene disruption and other applications. Yeast 14**:** 115-132.

Bratic, I., J. Hench and A. Trifunovic, 2010 Caenorhabditis elegans as a model system for mtDNA replication defects. Methods 51**:** 437-443.

Brauer, M. J., C. Huttenhower, E. M. Airoldi, R. Rosenstein, J. C. Matese *et al.*, 2008 Coordination of growth rate, cell cycle, stress response, and metabolic activity in yeast. Molecular biology of the cell 19**:** 352-367.

Brayton, C. F., P. M. Treuting and J. M. Ward, 2012 Pathobiology of Aging Mice and GEM: Background Strains and Experimental Design. Veterinary Pathology 49**:** 85-105.

Brem, R. B., J. D. Storey, J. Whittle and L. Kruglyak, 2005 Genetic interactions between polymorphisms that affect gene expression in yeast. Nature 436**:** 701-703.

Bridi, J. C., A. G. Barros, L. R. Sampaio, J. C. Ferreira, F. A. Antunes Soares *et al.*, 2015 Lifespan Extension Induced by Caffeine in Caenorhabditis elegans is Partially Dependent on Adenosine Signaling. Front Aging Neurosci 7**:** 220.

Brito, P. M., R. Devillard, A. Negre-Salvayre, L. M. Almeida, T. C. Dinis *et al.*, 2009 Resveratrol inhibits the mTOR mitogenic signaling evoked by oxidized LDL in smooth muscle cells. Atherosclerosis 205**:** 126-134.

Burkle, A., M. Moreno-Villanueva, J. Bernhard, M. Blasco, G. Zondag *et al.*, 2015 MARK-AGE biomarkers of ageing. Mechanisms of Ageing and Development 151**:** 2-12.

Burman, J. L., L. S. Itsara, E. B. Kayser, W. Suthammarak, A. M. Wang *et al.*, 2014 A Drosophila model of mitochondrial disease caused by a complex I mutation that uncouples proton pumping from electron transfer. Disease Models & Mechanisms 7**:** 1165-1174.

Burtner, C. R., C. J. Murakami, B. K. Kennedy and M. Kaeberlein, 2009 A molecular mechanism of chronological aging in yeast. Cell Cycle 8**:** 1256-1270.

Burtner, C. R., C. J. Murakami, B. Olsen, B. K. Kennedy and M. Kaeberlein, 2011 A genomic analysis of chronological longevity factors in budding yeast. Cell Cycle 10**:** 1385-1396.

Bushey, D., K. A. Hughes, G. Tononi and C. Cirelli, 2010 Sleep, aging, and lifespan in Drosophila. Bmc Neuroscience 11**:** 18.

Cabreiro, F., C. Au, K. Y. Leung, N. Vergara-Irigaray, H. M. Cocheme *et al.*, 2013 Metformin Retards Aging in C. elegans by Altering Microbial Folate and Methionine Metabolism. Cell 153**:** 228-239.

Campbell, J. M., S. M. Bellman, M. D. Stephenson and K. Lisy, 2017 Metformin reduces all-cause mortality and diseases of ageing independent of its effect on diabetes control: A systematic review and meta-analysis. Ageing Research Reviews 40**:** 31-44.
Cannon, L., A. C. Zambon, A. Cammarato, Z. Zhang, G. Vogler *et al.*, 2017 Expression patterns of cardiac aging in Drosophila. Aging Cell 16**:** 82-92.
Caruana, E. J., M. Roman, J. Hernández-Sánchez and P. Solli, 2015 Longitudinal studies. Journal of Thoracic Disease 7**:** E537-E540.
Castrillo, J. I., L. A. Zeef, D. C. Hoyle, N. Zhang, A. Hayes *et al.*, 2007 Growth control of the eukaryote cell: a systems biology study in yeast. Journal of biology 6**:** 4.
Chapman, T., and L. Partridge, 1996 Female fitness in Drosophila melanogaster: An interaction between the effect of nutrition and of encounter rate with males. Proceedings of the Royal Society B-Biological Sciences 263**:** 755-759.
Chen, C., Y. Liu and P. Zheng, 2009 mTOR regulation and therapeutic rejuvenation of aging hematopoietic stem cells. Sci Signal 2**:** ra75.
Chen, K. L., M. M. Crane and M. Kaeberlein, 2017 Microfluidic technologies for yeast replicative lifespan studies. Mechanisms of Ageing and Development 161**:** 262-269.
Chen, X., and D. Petranovic, 2015 Amyloid-beta peptide-induced cytotoxicity and mitochondrial dysfunction in yeast. Fems Yeast Research 15**:** 10.
Chesler, E. J., D. R. Miller, L. R. Branstetter, L. D. Galloway, B. L. Jackson *et al.*, 2008 The Collaborative Cross at Oak Ridge National Laboratory: developing a powerful resource for systems genetics. Mammalian Genome 19**:** 382-389.
Chow, C. Y., and L. T. Reiter, 2017 Etiology of Human Genetic Disease on the Fly. Trends in Genetics 33**:** 391-398.
Chresta, C. M., B. R. Davies, I. Hickson, T. Harding, S. Cosulich *et al.*, 2010 AZD8055 is a potent, selective, and orally bioavailable ATP-competitive mammalian target of rapamycin kinase inhibitor with in vitro and in vivo antitumor activity. Cancer Res 70**:** 288-298.
Churchill, G., D. C. Airey, H. Allayee, J. M. Angel, A. D. Attie *et al.*, 2004 The Collaborative Cross, a community resource for the genetic analysis of complex traits. Nature Genetics 36**:** 1133-1137.
Churchill, G. A., D. M. Gatti, S. C. Munger and K. L. Svenson, 2012 The Diversity Outbred mouse population. Mamm Genome 23**:** 713-718.
Clancy, D. J., D. Gems, L. G. Harshman, S. Oldham, H. Stocker *et al.*, 2001 Extension of life-span by loss of CHICO, a Drosophila insulin receptor substrate protein. Science 292**:** 104-106.
Cloughesy, T. F., K. Yoshimoto, P. Nghiemphu, K. Brown, J. Dang *et al.*, 2008 Antitumor activity of rapamycin in a phase I trial for patients with recurrent PTEN-Deficient glioblastoma. Plos Medicine 5**:** 139-151.
Colman, R. J., R. M. Anderson, S. C. Johnson, E. K. Kastman, K. J. Kosmatka *et al.*, 2009 Caloric Restriction Delays Disease Onset and Mortality in Rhesus Monkeys. Science 325**:** 201-204.
Conour, L. A., K. A. Murray and M. J. Brown, 2006 Preparation of animals for research - Issues to consider for rodents and rabbits. Ilar Journal 47**:** 283-293.
Creevy, K. E., S. N. Austad, J. M. Hoffman, D. G. O'Neill and D. E. L. Promislow, 2016 The Companion Dog as a Model for the Longevity Dividend. Cold Spring Harbor Perspectives in Medicine 6**:** 14.

Crespo, J. L., T. Powers, B. Fowler and M. N. Hall, 2002 The TOR-controlled transcription activators GLN3, RTG1, and RTG3 are regulated in response to intracellular levels of glutamine. Proceedings of the National Academy of Sciences of the United States of America 99**:** 6784-6789.

Dai, D. F., P. P. Karunadharma, Y. A. Chiao, N. Basisty, D. Crispin *et al.*, 2014 Altered proteome turnover and remodeling by short-term caloric restriction or rapamycin rejuvenate the aging heart. Aging Cell 13**:** 529-539.

Dandona, P., V. Fonseca, A. Mier and A. G. Beckett, 1983 Diarrhea and metformin in a diabetic clinic. Diabetes Care 6**:** 472-474.

Das, A., G. X. Huang, M. S. Bonkowski, A. Longchamp, C. Li *et al.*, 2018 Impairment of an Endothelial NAD(+)-H2S Signaling Network Is a Reversible Cause of Vascular Aging. Cell 173**:** 74-89.e20.

Dato, S., G. Rose, P. Crocco, D. Monti, P. Garagnani *et al.*, 2017 The genetics of human longevity: an intricacy of genes, environment, culture and microbiome. Mech Ageing Dev 165**:** 147-155.

Dawson, T. M., H. S. Ko and V. L. Dawson, 2010 Genetic Animal Models of Parkinson's Disease. Neuron 66**:** 646-661.

Day, C.-P., G. Merlino and T. Van Dyke, 2015 Preclinical Mouse Cancer Models: A Maze of Opportunities and Challenges. Cell 163**:** 39-53.

Decensi, A., M. Puntoni, P. Goodwin, M. Cazzaniga, A. Gennari *et al.*, 2010 Metformin and cancer risk in diabetic patients: a systematic review and meta-analysis. Cancer Prev Res (Phila) 3**:** 1451-1461.

Deepa, S. S., S. Bhaskaran, S. Espinoza, S. V. Brooks, A. McArdle *et al.*, 2017 A new mouse model of frailty: the Cu/Zn superoxide dismutase knockout mouse. Geroscience 39**:** 187-198.

Defossez, P. A., R. Prusty, M. Kaeberlein, S. J. Lin, P. Ferrigno *et al.*, 1999 Elimination of replication block protein Fob1 extends the life span of yeast mother cells. Molecular Cell 3**:** 447-455.

Delaney, J. R., U. Ahmed, A. Chou, S. Sim, D. Carr *et al.*, 2013 Stress profiling of longevity mutants identifies Afg3 as a mitochondrial determinant of cytoplasmic mRNA translation and aging. Aging Cell 12**:** 156-166.

Delaney, J. R., C. J. Murakami, B. Olsen, B. K. Kennedy and M. Kaeberlein, 2011 Quantitative evidence for early life fitness defects from 32 longevity-associated alleles in yeast. Cell Cycle 10**:** 156-165.

Dellinger, R. W., S. R. Santos, M. Morris, M. Evans, D. Alminana *et al.*, 2017 Repeat dose NRPT (nicotinamide riboside and pterostilbene) increases NAD(+) levels in humans safely and sustainably: a randomized, double-blind, placebo-controlled study. Npj Aging and Mechanisms of Disease 3**:** 9.

Dieleman, J. L., R. Baral, M. Birger, A. L. Bui, A. Bulchis *et al.*, 2016 US Spending on Personal Health Care and Public Health, 1996-2013. Jama-Journal of the American Medical Association 316**:** 2627-2646.

Dillin, A., A. L. Hsu, N. Arantes-Oliveira, J. Lehrer-Graiwer, H. Hsin *et al.*, 2002 Rates of behavior and aging specified by mitochondrial function during development. Science 298**:** 2398-2401.

Dodzian, J., S. Kean, J. Seidel and D. R. Valenzano, 2018 A Protocol for Laboratory Housing of Turquoise Killifish (Nothobranchius furzeri). J Vis Exp.

dos Reis, M., Y. Thawornwattana, K. Angelis, M. J. Telford, P. C. J. Donoghue *et al.*, 2015 Uncertainty in the Timing of Origin of Animals and the Limits of Precision in Molecular Timescales. Current Biology 25**:** 2939-2950.

Dutta, S., and P. Sengupta, 2016 Men and mice: Relating their ages. Life Sciences 152**:** 244-248.

Egenvall, A., B. N. Bonnett, A. Hedhammar and P. Olson, 2005 Mortality in over 350,000 insured Swedish dogs from 1995-2000: II. Breed-specific age and survival patterns and relative risk for causes of death. Acta Veterinaria Scandinavica 46**:** 121-136.

Egilmez, N. K., and S. M. Jazwinski, 1989 Evidence for the involvement of a cytoplasmic factor in the aging of the yeast Saccharomyces cerevisiae. J Bacteriol 171**:** 37-42.

Eisen, H. J., E. M. Tuzcu, R. Dorent, J. Kobashigawa, D. Mancini *et al.*, 2003 Everolimus for the prevention of allograft rejection and vasculopathy in cardiac-transplant recipients. New England Journal of Medicine 349**:** 847-858.

Estrela, J. M., A. Ortega, S. Mena, M. L. Rodriguez and M. Asensi, 2013 Pterostilbene: Biomedical applications. Critical Reviews in Clinical Laboratory Sciences 50**:** 65-78.

Evans, J. M. M., L. A. Donnelly, A. M. Emslie-Smith, D. R. Alessi and A. D. Morris, 2005 Metformin and reduced risk of cancer in diabetic patients. British Medical Journal 330**:** 1304-1305.

Fabris, F., J. P. d. Magalhães and A. A. Freitas, 2017 A review of supervised machine learning applied to ageing research. Biogerontology 18**:** 171-188.

Fabrizio, P., S. Hoon, M. Shamalnasab, A. Galbani, M. Wei *et al.*, 2010 Genome-wide screen in Saccharomyces cerevisiae identifies vacuolar protein sorting, autophagy, biosynthetic, and tRNA methylation genes involved in life span regulation. PLoS Genet 6**:** e1001024.

Fabrizio, P., and V. D. Longo, 2007 The chronological life span of Saccharomyces cerevisiae. Methods Mol Biol 371**:** 89-95.

Fabrizio, P., F. Pozza, S. D. Pletcher, C. M. Gendron and V. D. Longo, 2001 Regulation of longevity and stress resistance by Sch9 in yeast. Science 292**:** 288-290.

Failla, G., 1958 The aging process and cancerogenesis. Annals of the New York Academy of Sciences 71**:** 1124-1140.

Fan, X., J. Wang, J. Hou, C. Lin, A. Bensoussan *et al.*, 2015 Berberine alleviates ox-LDL induced inflammatory factors by up-regulation of autophagy via AMPK/mTOR signaling pathway. J Transl Med 13**:** 92.

Fay, J. C., and J. A. Benavides, 2005 Evidence for domesticated and wild populations of Saccharomyces cerevisiae. PLoS Genet 1**:** 66-71.

Felsenstein, J., 1985 Phylogenies and the Comparative Method. American Naturalist 125**:** 1-15.

Fernandes-Silva, G., M. I. de Paula and E. B. Rangel, 2017 mTOR inhibitors in pancreas transplant: adverse effects and drug-drug interactions. Expert Opinion on Drug Metabolism & Toxicology 13**:** 367-385.

Ferrari, M., I. H. Jain, O. Goldberger, E. Rezoagli, R. Thoonen *et al.*, 2017 Hypoxia treatment reverses neurodegenerative disease in a mouse model of Leigh syndrome. Proc Natl Acad Sci U S A 114**:** 4241-4250.

Finch, C. E., and G. Ruvkun, 2001 The genetics of aging. Annual review of genomics and human genetics 2**:** 435-462.

Fire, A., S. Xu, M. K. Montgomery, S. A. Kostas, S. E. Driver *et al.*, 1998 Potent and specific genetic interference by double-stranded RNA in Caenorhabditis elegans. Nature 391**:** 806-811.

Flynn, J. M., M. N. O'Leary, C. A. Zambataro, E. C. Academia, M. P. Presley *et al.*, 2013 Late-life rapamycin treatment reverses age-related heart dysfunction. Aging Cell 12**:** 851-862.
Folkes, A. J., K. Ahmadi, W. K. Alderton, S. Alix, S. J. Baker *et al.*, 2008 The identification of 2-(1H-indazol-4-yl)-6-(4-methanesulfonyl-piperazin-1-ylmethyl)-4-morpholin-4-yl-t hieno[3,2-d]pyrimidine (GDC-0941) as a potent, selective, orally bioavailable inhibitor of class I PI3 kinase for the treatment of cancer. J Med Chem 51**:** 5522-5532.
Fox, J., 2005 The R commander: A basic-statistics graphical user interface to R. Journal of Statistical Software 14**:** 42.
Fox, J., and M. S. Carvalho, 2012 The RcmdrPlugin.survival Package: Extending the R Commander Interface to Survival Analysis. Journal of Statistical Software 49**:** 1-32.
Freckleton, R. P., P. H. Harvey and M. Pagel, 2002 Phylogenetic analysis and comparative data: a test and review of evidence. American Naturalist 160**:** 712-726.
Freitas, A. A., and J. P. de Magalhaes, 2011 A review and appraisal of the DNA damage theory of ageing. Mutation Research-Reviews in Mutation Research 728**:** 12-22.
Friedman, D. B., and T. E. Johnson, 1988 A mutation in the AGE-1 gene in Caenorhabditis elegans lengthens life and reduces hermaphrodite fertility. Genetics 118**:** 75-86.
Fries, J. F., 1980 Aging, natural death, and the compression of morbidity. The New England journal of medicine 303**:** 130-135.
Funchain, P., A. Yeung, J. L. Stewart, R. Lin, M. M. Slupska *et al.*, 2000 The consequences of growth of a mutator strain of Escherichia coli as measured by loss of function among multiple gene targets and loss of fitness. Genetics 154**:** 959-970.
Gamo, N. J., M. R. Birknow, D. Sullivan, M. A. Kondo, Y. Horiuchi *et al.*, 2017 Valley of death: A proposal to build a “translational bridge” for the next generation. Neuroscience research 115**:** 1-4.
Ganner, A., and E. Neumann-Haefelin, 2017 Genetic kidney diseases: Caenorhabditis elegans as model system. Cell and Tissue Research 369**:** 105-118.
Garcia, A. M., R. B. Calder, M. E. T. Dolle, M. Lundell, P. Kapahi *et al.*, 2010 Age- and Temperature-Dependent Somatic Mutation Accumulation in Drosophila melanogaster. Plos Genetics 6**:** 8.
Gassen, N. C., G. P. Chrousos, E. B. Binder and A. S. Zannas, 2017 Life stress, glucocorticoid signaling, and the aging epigenome: Implications for aging-related diseases. Neurosci Biobehav Rev 74**:** 356-365.
Genade, T., M. Benedetti, E. Terzibasi, P. Roncaglia, D. R. Valenzano *et al.*, 2005 Annual fishes of the genus Nothobranchius as a model system for aging research. Aging Cell 4**:** 223-233.
Genovese, G., A. K. Kahler, R. E. Handsaker, J. Lindberg, S. A. Rose *et al.*, 2014 Clonal hematopoiesis and blood-cancer risk inferred from blood DNA sequence. N Engl J Med 371**:** 2477-2487.
Giaever, G., A. M. Chu, L. Ni, C. Connelly, L. Riles *et al.*, 2002 Functional profiling of the Saccharomyces cerevisiae genome. Nature 418**:** 387-391.
Giaever, G., and C. Nislow, 2014 The Yeast Deletion Collection: A Decade of Functional Genomics. Genetics 197**:** 451-465.
Gitler, A. D., B. J. Bevis, J. Shorter, K. E. Strathearn, S. Hamamichi *et al.*, 2008 The Parkinson's disease protein alpha-synuclein disrupts cellular Rab homeostasis. Proceedings of the National Academy of Sciences of the United States of America 105**:** 145-150.

Gladyshev, V. N., 2012 On the cause of aging and control of lifespan: heterogeneity leads to inevitable damage accumulation, causing aging; control of damage composition and rate of accumulation define lifespan. BioEssays : news and reviews in molecular, cellular and developmental biology 34**:** 925-929.

Grandison, R. C., R. Wong, T. M. Bass, L. Partridge and M. D. W. Piper, 2009 Effect of a Standardised Dietary Restriction Protocol on Multiple Laboratory Strains of Drosophila melanogaster. Plos One 4**:** 8.

Grotewiel, M. S., I. Martin, P. Bhandari and E. Cook-Wiens, 2005 Functional senescence in Drosophila melanogaster. Ageing Research Reviews 4**:** 372-397.

Guan, Y., S. R. Wang, X. Z. Huang, Q. H. Xie, Y. Y. Xu *et al.*, 2017 Nicotinamide Mononucleotide, an NAD(+) Precursor, Rescues Age-Associated Susceptibility to AKI in a Sirtuin 1-Dependent Manner. Journal of the American Society of Nephrology 28**:** 2337-2352.

Guo, F., J. W. Yu, H. J. Jung, K. C. Abruzzi, W. F. Luo *et al.*, 2016 Circadian neuron feedback controls the Drosophila sleep-activity profile. Nature 536**:** 292-297.

Gurkar, A. U., and L. J. Niedernhofer, 2015 Comparison of mice with accelerated aging caused by distinct mechanisms. Experimental Gerontology 68**:** 43-50.

Hallgren, J., M. Pietrzak, G. Rempala, P. T. Nelson and M. Hetman, 2014 Neurodegeneration-associated instability of ribosomal DNA. Biochimica Et Biophysica Acta-Molecular Basis of Disease 1842**:** 860-868.

Halloran, J., S. A. Hussong, R. Burbank, N. Podlutskaya, K. E. Fischer *et al.*, 2012 Chronic inhibition of mammalian target of rapamycin by rapamycin modulates cognitive and non-cognitive components of behavior throughout lifespan in mice. Neuroscience 223**:** 102-113.

Hamilton, B., Y. Dong, M. Shindo, W. Liu, I. Odell *et al.*, 2005 A systematic RNAi screen for longevity genes in C. elegans. Genes Dev 19**:** 1544-1555.

Han, B., P. Sivaramakrishnan, C. J. Lin, I. A. A. Neve, J. He *et al.*, 2017 Microbial Genetic Composition Tunes Host Longevity. Cell 169**:** 1249-1262.e1213.

Hanahan, D., and R. A. Weinberg, 2011 Hallmarks of cancer: the next generation. Cell 144**:** 646-674.

Hannum, G., J. Guinney, L. Zhao, L. Zhang, G. Hughes *et al.*, 2013 Genome-wide Methylation Profiles Reveal Quantitative Views of Human Aging Rates. Molecular Cell 49**:** 359-367.

Hansen, M., A. L. Hsu, A. Dillin and C. Kenyon, 2005 New genes tied to endocrine, metabolic, and dietary regulation of lifespan from a Caenorhabditis elegans genomic RNAi screen. PLoS Genet 1**:** 119-128.

Harel, I., D. R. Valenzano and A. Brunet, 2016 Efficient genome engineering approaches for the short-lived African turquoise killifish. Nat Protoc 11**:** 2010-2028.

Haroon, S., A. Li, J. L. Weinert, C. Fritsch, N. G. Ericson *et al.*, 2018 Multiple Molecular Mechanisms Rescue mtDNA Disease in C-elegans. Cell Reports 22**:** 3115-3125.

Harrison, D. E., R. Strong, D. B. Allison, B. N. Ames, C. M. Astle *et al.*, 2014 Acarbose, 17-alpha-estradiol, and nordihydroguaiaretic acid extend mouse lifespan preferentially in males. Aging Cell 13**:** 273-282.

Harrison, D. E., R. Strong, Z. D. Sharp, J. F. Nelson, C. M. Astle *et al.*, 2009 Rapamycin fed late in life extends lifespan in genetically heterogeneous mice. Nature 460**:** 392-395.

Hartman, M., A. B. Martin, N. Espinosa, A. Catlin and T. The National Health Expenditure Accounts, 2017 National Health Care Spending In 2016: Spending And Enrollment Growth Slow After Initial Coverage Expansions. Health Affairs 37**:** 150-160.
Haun, C., J. Alexander, D. Y. Stainier and P. G. Okkema, 1998 Rescue of Caenorhabditis elegans pharyngeal development by a vertebrate heart specification gene. Proceedings of the National Academy of Sciences of the United States of America 95**:** 5072-5075.
He, C., S. K. Tsuchiyama, Q. T. Nguyen, E. N. Plyusnina, S. R. Terrill *et al.*, 2014 Enhanced Longevity by Ibuprofen, Conserved in Multiple Species, Occurs in Yeast through Inhibition of Tryptophan Import. Plos Genetics 10**:** 16.
He, Y., and H. Jasper, 2014 Studying aging in Drosophila. Methods 68**:** 129-133.
Heitman, J., N. R. Movva and M. N. Hall, 1991 Targets for cell cycle arrest by the immunosuppressant rapamycin in yeast. Science 253**:** 905-909.
Helliwell, S. B., P. Wagner, J. Kunz, M. Deuter-Reinhard, R. Henriquez *et al.*, 1994 TOR1 and TOR2 are structurally and functionally similar but not identical phosphatidylinositol kinase homologues in yeast. Mol Biol Cell 5**:** 105-118.
Heron, M., 2016 Deaths: Leading Causes for 2014. Natl Vital Stat Rep 65**:** 1-96.
Herr, A. J., S. R. Kennedy, G. M. Knowels, E. M. Schultz and B. D. Preston, 2014 DNA replication error-induced extinction of diploid yeast. Genetics 196**:** 677-691.
Herr, A. J., M. Ogawa, N. A. Lawrence, L. N. Williams, J. M. Eggington *et al.*, 2011 Mutator suppression and escape from replication error-induced extinction in yeast. PLoS Genet 7**:** e1002282.
Herskind, A. M., M. McGue, N. V. Holm, T. I. Sorensen, B. Harvald *et al.*, 1996 The heritability of human longevity: a population-based study of 2872 Danish twin pairs born 1870-1900. Hum Genet 97**:** 319-323.
Highfill, C. A., G. A. Reeves and S. J. Macdonald, 2016 Genetic analysis of variation in lifespan using a multiparental advanced intercross Drosophila mapping population. Bmc Genetics 17**:** 13.
Hjelmborg, J., I. Iachine, A. Skytthe, J. W. Vaupel, M. McGue *et al.*, 2006 Genetic influence on human lifespan and longevity. Hum Genet 119**:** 312-321.
Ho, L. S. T., and C. Ane, 2013 A linear-time algorithm for Gaussian and non-Gaussian trait evolution models. Systematic Biology 63**:** 397-408.
Hoffman, J. M., K. E. Creevy, A. Franks, D. G. O'Neill and D. E. L. Promislow, 2018 The companion dog as a model for human aging and mortality. Aging Cell 17**:** 13.
Hollingsworth, M. J., 1969 Temperature and length of life in Drosophila. Exp Gerontol 4**:** 49-55.
Horvath, S., 2013 DNA methylation age of human tissues and cell types. Genome Biology 14**:** 19.
Horvath, S., P. Garagnani, M. G. Bacalini, C. Pirazzini, S. Salvioli *et al.*, 2015 Accelerated epigenetic aging in Down syndrome. Aging Cell 14**:** 491-495.
Horvath, S., and A. J. Levine, 2015 HIV-1 Infection Accelerates Age According to the Epigenetic Clock. Journal of Infectious Diseases 212**:** 1563-1573.
Horvath, S., and K. Raj, 2018 DNA methylation-based biomarkers and the epigenetic clock theory of ageing. Nature Reviews Genetics 19**:** 371-384.
Hou, Y. J., S. Lautrup, S. Cordonnier, Y. Wang, D. L. Croteau *et al.*, 2018 NAD(+) supplementation normalizes key Alzheimer's features and DNA damage responses in a new AD mouse model with introduced DNA repair deficiency. Proceedings of the National Academy of Sciences of the United States of America 115**:** E1876-E1885.

Hu, C. K., and A. Brunet, 2018 The African turquoise killifish: A research organism to study vertebrate aging and diapause. Aging Cell 17**:** 15.
Hu, J., M. Wei, M. G. Mirisola and V. D. Longo, 2013 Assessing chronological Aging in Saccharomyces cerevisiae. Methods in molecular biology (Clifton, N.J.) 965**:** 463-472.
Huang, C., C. J. Xiong and K. Kornfeld, 2004 Measurements of age-related changes of physiological processes that predict lifespan of Caenorhabditis elegans. Proceedings of the National Academy of Sciences of the United States of America 101**:** 8084-8089.
Huang da, W., B. T. Sherman and R. A. Lempicki, 2009 Systematic and integrative analysis of large gene lists using DAVID bioinformatics resources. Nature protocols 4**:** 44-57.
Huang, W., A. Massouras, Y. Inoue, J. Peiffer, M. Ramia *et al.*, 2014 Natural variation in genome architecture among 205 Drosophila melanogaster Genetic Reference Panel lines. Genome Research 24**:** 1193-1208.
Huang, W., S. Richards, M. A. Carbone, D. Zhu, R. R. Anholt *et al.*, 2012 Epistasis dominates the genetic architecture of Drosophila quantitative traits. Proc Natl Acad Sci U S A 109**:** 15553-15559.
Huber, S., C. J. Bruns, G. Schmid, P. C. Hermann, C. Conrad *et al.*, 2007 Inhibition of the mammalian target of rapamycin impedes lymphangiogenesis. Kidney International 71**:** 771-777.
Iliadi, K. G., N. N. Iliadi and G. L. Boulianne, 2009 Regulation of Drosophila life-span: Effect of genetic background, sex, mating and social status. Experimental Gerontology 44**:** 546-553.
Inzucchi, S. E., 2002 Oral antihyperglycemic therapy for type 2 diabetes: scientific review. Jama 287**:** 360-372.
Ivanov, D. K., V. Escott-Price, M. Ziehm, M. M. Magwire, T. F. C. Mackay *et al.*, 2015 Longevity GWAS Using the Drosophila Genetic Reference Panel. Journals of Gerontology Series a-Biological Sciences and Medical Sciences 70**:** 1470-1478.
Jacinto, E., R. Loewith, A. Schmidt, S. Lin, M. A. Ruegg *et al.*, 2004 Mammalian TOR complex 2 controls the actin cytoskeleton and is rapamycin insensitive. Nat Cell Biol 6**:** 1122-1128.
Jackson, A. U., A. Fornes, A. Galecki, R. A. Miller and D. T. Burke, 1999 Multiple-trait quantitative trait loci analysis using a large mouse sibship. Genetics 151**:** 785-795.
Jackson, C., 2016 flexsurv: A Platform for Parametric Survival Modeling in R. 2016 70**:** 33.
Jacobs, K. B., M. Yeager, W. Y. Zhou, S. Wacholder, Z. M. Wang *et al.*, 2012 Detectable clonal mosaicism and its relationship to aging and cancer. Nature Genetics 44**:** 651-658.
Jain, I. H., L. Zazzeron, R. Goli, K. Alexa, S. Schatzman-Bone *et al.*, 2016 Hypoxia as a therapy for mitochondrial disease. Science 352**:** 54-61.
Jaiswal, S., P. Fontanillas, J. Flannick, A. Manning, P. V. Grauman *et al.*, 2014 Age-related clonal hematopoiesis associated with adverse outcomes. N Engl J Med 371**:** 2488-2498.
Janus, C., and H. Welzl, 2010 Mouse models of neurodegenerative diseases: criteria and general methodology. Methods Mol Biol 602**:** 323-345.
Je, Y., and E. Giovannucci, 2014 Coffee consumption and total mortality: a meta-analysis of twenty prospective cohort studies. Br J Nutr 111**:** 1162-1173.
Jensen, L. J., M. Kuhn, M. Stark, S. Chaffron, C. Creevey *et al.*, 2009 STRING 8--a global view on proteins and their functional interactions in 630 organisms. Nucleic acids research 37**:** 412-416.

Jiang, L., Y. Jin, H. Wang, Y. Jiang and J. Dong, 2014 Glucosamine protects nucleus pulposus cells and induces autophagy via the mTOR-dependent pathway. J Orthop Res 32**:** 1532-1542.
Jin, K., J. M. Hoffman, K. E. Creevy, D. G. O'Neill and D. E. L. Promislow, 2016 Multiple morbidities in companion dogs: a novel model for investigating age-related disease. Pathobiology of Aging and Age-related Diseases 6**:** 9.
Johnson, S. C., and M. Kaeberlein, 2016 Rapamycin in aging and disease: maximizing efficacy while minimizing side effects. Oncotarget 7**:** 44876-44878.
Johnson, S. C., G. M. Martin, P. S. Rabinovitch and M. Kaeberlein, 2013a Preserving youth: does rapamycin deliver? Sci Transl Med 5**:** 211fs240.
Johnson, S. C., P. S. Rabinovitch and M. Kaeberlein, 2013b mTOR is a key modulator of ageing and age-related disease. Nature 493**:** 338-345.
Johnson, S. C., M. Sangesland, M. Kaeberlein and P. S. Rabinovitch, 2015 Modulating mTOR in aging and health. Interdiscip Top Gerontol 40**:** 107-127.
Johnson, S. C., M. E. Yanos, E. B. Kayser, A. Quintana, M. Sangesland *et al.*, 2013c mTOR Inhibition Alleviates Mitochondrial Disease in a Mouse Model of Leigh Syndrome. Science 342**:** 1524-1528.
Jones, K. T., and K. Ashrafi, 2009 Caenorhabditis elegans as an emerging model for studying the basic biology of obesity. Disease Models & Mechanisms 2**:** 224-229.
Jones, M. A., and M. Grotewiel, 2011 Drosophila as a model for age-related impairment in locomotor and other behaviors. Experimental Gerontology 46**:** 320-325.
Kaeberlein, M., 2010 Lessons on longevity from budding yeast. Nature 464**:** 513-519.
Kaeberlein, M., 2013a Longevity and aging. F1000Prime Rep 5**:** 5.
Kaeberlein, M., 2013b mTOR Inhibition: From Aging to Autism and Beyond. Scientifica (Cairo) 2013**:** 849186.
Kaeberlein, M., K. E. Creevy and D. E. L. Promislow, 2016 The dog aging project: translational geroscience in companion animals. Mammalian Genome 27**:** 279-288.
Kaeberlein, M., K. T. Kirkland, S. Fields and B. K. Kennedy, 2004 Sir2-independent life span extension by calorie restriction in yeast. Plos Biology 2**:** 1381-1387.
Kaeberlein, M., K. T. Kirkland, S. Fields and B. K. Kennedy, 2005a Genes determining yeast replicative life span in a long-lived genetic background. Mech Ageing Dev 126**:** 491-504.
Kaeberlein, M., T. McDonagh, B. Heltweg, J. Hixon, E. A. Westman *et al.*, 2005b Substrate-specific activation of sirtuins by resveratrol. J Biol Chem 280**:** 17038-17045.
Kaeberlein, M., M. McVey and L. Guarente, 1999 The SIR2/3/4 complex and SIR2 alone promote longevity in Saccharomyces cerevisiae by two different mechanisms. Genes & Development 13**:** 2570-2580.
Kaeberlein, M., R. W. Powers, 3rd, K. K. Steffen, E. A. Westman, D. Hu *et al.*, 2005c Regulation of yeast replicative life span by TOR and Sch9 in response to nutrients. Science 310**:** 1193-1196.
Kaeberlein, M., P. S. Rabinovitch and G. M. Martin, 2015 Healthy Aging: The Ultimate Preventative Medicine. Science 350**:** 1191-1193.
Kamath, R. S., and J. Ahringer, 2003 Genome-wide RNAi screening in Caenorhabditis elegans. Methods 30**:** 313-321.
Kamath, R. S., A. G. Fraser, Y. Dong, G. Poulin, R. Durbin *et al.*, 2003 Systematic functional analysis of the Caenorhabditis elegans genome using RNAi. Nature 421**:** 231-237.

Kamath, R. S., M. Martinez-Campos, P. Zipperlen, A. G. Fraser and J. Ahringer, 2001 Effectiveness of specific RNA-mediated interference through ingested double-stranded RNA in Caenorhabditis elegans. Genome Biol 2**:** Research0002.
Kao, J. Y., S. Lymer, S. H. Hwang, A. Sung and S. V. Nuzhdin, 2015 Postmating reproductive barriers contribute to the incipient sexual isolation of the United States and Caribbean Drosophila melanogaster. Ecol Evol 5**:** 3171-3182.
Kar, A., B. K. Choudhary and N. G. Bandyopadhyay, 2003 Comparative evaluation of hypoglycaemic activity of some Indian medicinal plants in alloxan diabetic rats. Journal of Ethnopharmacology 84**:** 105-108.
Karnewar, S., P. K. Neeli, D. Panuganti, S. Kotagiri, S. Mallappa *et al.*, 2018 Metformin regulates mitochondrial biogenesis and senescence through AMPK mediated H3K79 methylation: Relevance in age-associated vascular dysfunction. Biochimica Et Biophysica Acta-Molecular Basis of Disease 1864**:** 1115-1128.
Kaya, A., A. V. Lobanov and V. N. Gladyshev, 2015a Evidence that mutation accumulation does not cause aging in Saccharomyces cerevisiae. Aging Cell 14**:** 366-371.
Kaya, A., S. Ma, B. Wasko, M. Lee, M. Kaeberlein *et al.*, 2015b Defining Molecular Basis for Longevity Traits in Natural Yeast Isolates. NPJ Aging Mech Dis 1.
Kennedy, B. K., S. L. Berger, A. Brunet, J. Campisi, A. M. Cuervo *et al.*, 2014 Geroscience: linking aging to chronic disease. Cell 159**:** 709-713.
Kennedy, B. K., and D. W. Lamming, 2016 The Mechanistic Target of Rapamycin: The Grand ConducTOR of Metabolism and Aging. Cell Metabolism 23**:** 990-1003.
Kennedy, S. R., E. M. Schultz, T. M. Chappell, B. Kohrn, G. M. Knowels *et al.*, 2015 Volatility of Mutator Phenotypes at Single Cell Resolution. PLOS Genetics 11**:** e1005151.
Kenyon, C., J. Chang, E. Gensch, A. Rudner and R. Tabtiang, 1993 A C. elegans mutant that lives twice as long as wild-type. Nature 366**:** 461-464.
Kenyon, C. J., 2010 The genetics of ageing. Nature 464**:** 504-512.
Keowkase, R., M. Aboukhatwa and Y. A. Luo, 2010 Fluoxetine protects against amyloid-beta toxicity, in part via daf-16 mediated cell signaling pathway, in Caenorhabditis elegans. Neuropharmacology 59**:** 358-365.
Kim, Y., H. G. Nam and D. R. Valenzano, 2016 The short-lived African turquoise killifish: an emerging experimental model for ageing. Disease Models & Mechanisms 9**:** 115-129.
Kimura, K. D., H. A. Tissenbaum, Y. X. Liu and G. Ruvkun, 1997 daf-2, an insulin receptor-like gene that regulates longevity and diapause in Caenorhabditis elegans. Science 277**:** 942-946.
King, E. G., S. J. Macdonald and A. D. Long, 2012a Properties and Power of the Drosophila Synthetic Population Resource for the Routine Dissection of Complex Traits. Genetics 191**:** 935-949.
King, E. G., C. M. Merkes, C. L. McNeil, S. R. Hoofer, S. Sen *et al.*, 2012b Genetic dissection of a model complex trait using the Drosophila Synthetic Population Resource. Genome Research 22**:** 1558-1566.
Kiontke, K. C., M. A. Felix, M. Ailion, M. V. Rockman, C. Braendle *et al.*, 2011 A phylogeny and molecular barcodes for Caenorhabditis, with numerous new species from rotting fruits. Bmc Evolutionary Biology 11**:** 18.
Klass, M. R., 1977 Aging in nematode Caenorhabditis elegans - Major biological and environmental factors influencing life span. Mechanisms of Ageing and Development 6**:** 413-429.

Knight, S. D., N. D. Adams, J. L. Burgess, A. M. Chaudhari, M. G. Darcy *et al.*, 2010 Discovery of GSK2126458, a Highly Potent Inhibitor of PI3K and the Mammalian Target of Rapamycin. ACS Med Chem Lett 1**:** 39-43.

Kol, A., B. Arzi, K. A. Athanasiou, D. L. Farmer, J. A. Nolta *et al.*, 2015 Companion animals: Translational scientist's new best friends. Science translational medicine 7**:** 308ps321-308ps321.

Kosaraju, J., S. V. Madhunapantula, S. Chinni, R. B. Khatwal, A. Dubala *et al.*, 2014 Dipeptidyl peptidase-4 inhibition by Pterocarpus marsupium and Eugenia jambolana ameliorates streptozotocin induced Alzheimer's disease. Behavioural Brain Research 267**:** 55-65.

Kruse, S. E., W. C. Watt, D. J. Marcinek, R. P. Kapur, K. A. Schenkman *et al.*, 2008 Mice with Mitochondrial Complex I Deficiency Develop a Fatal Encephalomyopathy. Cell Metabolism 7**:** 312-320.

Kumar, D. K. V., S. H. Choi, K. J. Washicosky, W. A. Eimer, S. Tucker *et al.*, 2016 Amyloid-beta peptide protects against microbial infection in mouse and worm models of Alzheimer's disease. Science Translational Medicine 8**:** 15.

Kunz, J., R. Henriquez, U. Schneider, M. Deuter-Reinhard, N. R. Movva *et al.*, 1993 Target of rapamycin in yeast, TOR2, is an essential phosphatidylinositol kinase homolog required for G1 progression. Cell 73**:** 585-596.

Ladiges, W., J. M. Snyder, E. Wilkinson, D. M. Imai, T. Snider *et al.*, 2017 A New Preclinical Paradigm for Testing Anti-Aging Therapeutics. Journals of Gerontology Series a-Biological Sciences and Medical Sciences 72**:** 760-762.

Lamming, D. W., L. Ye, P. Katajisto, M. D. Goncalves, M. Saitoh *et al.*, 2012 Rapamycin-Induced Insulin Resistance Is Mediated by mTORC2 Loss and Uncoupled from Longevity. Science 335**:** 1638-1643.

Lara, J., R. Cooper, J. Nissan, A. T. Ginty, K. T. Khaw *et al.*, 2015 A proposed panel of biomarkers of healthy ageing. BMC Med 13**:** 222.

Laschober, G. T., D. Ruli, E. Hofer, C. Muck, D. Carmona-Gutierrez *et al.*, 2010 Identification of evolutionarily conserved genetic regulators of cellular aging. Aging cell 9**:** 1084-1097.

Lassman, D., M. Hartman, B. Washington, K. Andrews and A. Catlin, 2014 US Health Spending Trends By Age And Gender: Selected Years 2002–10. Health Affairs 33**:** 815-822.

Laurie, C. C., C. A. Laurie, K. Rice, K. F. Doheny, L. R. Zelnick *et al.*, 2012 Detectable clonal mosaicism from birth to old age and its relationship to cancer. Nature Genetics 44**:** 642-650.

Lavoy, S., V. G. Chittoor-Vinod, C. Y. Chow and I. Martin, 2018 Genetic Modifiers of Neurodegeneration in a Drosophila Model of Parkinson's Disease. Genetics. [Epub ahead of print]

Leach, M. C., P. D. Thornton and D. C. J. Main, 2008 Identification of appropriate measures for the assessment of laboratory mouse welfare. Animal Welfare 17**:** 161-170.

Lee, E. B., V. M. Y. Lee and J. Q. Trojanowski, 2012a Gains or losses: molecular mechanisms of TDP43-mediated neurodegeneration. Nature Reviews Neuroscience 13**:** 38-50.

Lee, M. B., D. T. Carr, M. G. Kiflezghi, Y. T. Zhao, D. B. Kim *et al.*, 2017 A system to identify inhibitors of mTOR signaling using high-resolution growth analysis in Saccharomyces cerevisiae. Geroscience 39**:** 419-428.

Lee, M. S., C. C. Hsu, M. L. Wahlqvist, H. N. Tsai, Y. H. Chang *et al.*, 2011 Type 2 diabetes increases and metformin reduces total, colorectal, liver and pancreatic cancer incidences

in Taiwanese: a representative population prospective cohort study of 800,000 individuals. Bmc Cancer 11**:** 10.
Lee, S. S., I. Avalos Vizcarra, D. Huberts, L. P. Lee and M. Heinemann, 2012b Whole lifespan microscopic observation of budding yeast aging through a microfluidic dissection platform. Proceedings of the National Academy of Sciences of the United States of America 109**:** 4916-4920.
Lee, S. S., R. Y. Lee, A. G. Fraser, R. S. Kamath, J. Ahringer *et al.*, 2003 A systematic RNAi screen identifies a critical role for mitochondria in C. elegans longevity. Nat Genet 33**:** 40-48.
Leiser, S. F., M. Fletcher, A. Begun and M. Kaeberlein, 2013 Life-span extension from hypoxia in Caenorhabditis elegans requires both HIF-1 and DAF-16 and is antagonized by SKN-1. J Gerontol A Biol Sci Med Sci 68**:** 1135-1144.
Lelegren, M., Y. Liu, C. Ross, S. Tardif and A. B. Salmon, 2016 Pharmaceutical inhibition of mTOR in the common marmoset: effect of rapamycin on regulators of proteostasis in a non-human primate. Pathobiol Aging Age Relat Dis 6**:** 31793.
Lepez-Otin, C., M. A. Blasco, L. Partridge, M. Serrano and G. Kroemer, 2013 The Hallmarks of Aging. Cell 153**:** 1194-1217.
Lester-Coll, N., E. J. Rivera, S. J. Soscia, K. Doiron, J. R. Wands *et al.*, 2006 Intracerebral streptozotocin model of type 3 diabetes: relevance to sporadic Alzheimer's disease. J Alzheimers Dis 9**:** 13-33.
Letunic, I., and P. Bork, 2016 Interactive tree of life (iTOL) v3: an online tool for the display and annotation of phylogenetic and other trees. Nucleic Acids Res 44**:** 242-245.
Li, L. F., X. L. Qi, M. X. Xu, X. F. Ding, X. L. Zhou *et al.*, 2016 The effects of metformin on ovarian cancer: an updated systematic review and meta-analysis. International Journal of Clinical and Experimental Medicine 9**:** 17559-17568.
Li, Y., M. S. Wang, N. O. Otecko, W. Wang, P. Shi *et al.*, 2017 Hypoxia potentially promotes Tibetan longevity. Cell Res 27**:** 302-305.
Li, Z., C. M. Dungan, B. Carrier, T. C. Rideout and D. L. Williamson, 2014 Alpha-lipoic acid supplementation reduces mTORC1 signaling in skeletal muscle from high fat fed, obese Zucker rats. Lipids 49**:** 1193-1201.
Liao, C. Y., B. A. Rikke, T. E. Johnson, V. Diaz and J. F. Nelson, 2010 Genetic variation in the murine lifespan response to dietary restriction: from life extension to life shortening. Aging Cell 9**:** 92-95.
Libby, G., L. A. Donnelly, P. T. Donnan, D. R. Alessi, A. D. Morris *et al.*, 2009 New Users of Metformin Are at Low Risk of Incident Cancer A cohort study among people with type 2 diabetes. Diabetes Care 32**:** 1620-1625.
Lin, S. J., P. A. Defossez and L. Guarente, 2000 Requirement of NAD and SIR2 for life-span extension by calorie restriction in Saccharomyces cerevisiae. Science 289**:** 2126-2128.
Lin, S. J., M. Kaeberlein, A. A. Andalis, L. A. Sturtz, P. A. Defossez *et al.*, 2002 Calorie restriction extends Saccharomyces cerevisiae lifespan by increasing respiration. Nature 418**:** 344-348.
Linford, N. J., C. Bilgir, J. Ro and S. D. Pletcher, 2013 Measurement of Lifespan in Drosophila melanogaster. Jove-Journal of Visualized Experiments**:** 9.
Lithgow, G. J., M. Driscoll and P. Phillips, 2017 A long journey to reproducible results. Nature 548**:** 387-388.

Liti, G., D. M. Carter, A. M. Moses, J. Warringer, L. Parts *et al.*, 2009 Population genomics of domestic and wild yeasts. Nature 458**:** 337-341.
Liti, G., and E. J. Louis, 2012 Advances in quantitative trait analysis in yeast. PLoS genetics 8**:** e1002912.
Liu, M., S. A. Wilk, A. Wang, L. Zhou, R. H. Wang *et al.*, 2010 Resveratrol inhibits mTOR signaling by promoting the interaction between mTOR and DEPTOR. J Biol Chem 285**:** 36387-36394.
Liu, Q., T. Ren, T. Fresques, W. Oppliger, B. J. Niles *et al.*, 2012 Selective ATP-competitive inhibitors of TOR suppress rapamycin-insensitive function of TORC2 in Saccharomyces cerevisiae. ACS Chem Biol 7**:** 982-987.
Livi, C. B., R. L. Hardman, B. A. Christy, S. G. Dodds, D. Jones *et al.*, 2013 Rapamycin extends life span of Rb1(+/-) mice by inhibiting neuroendocrine tumors. Aging-Us 5**:** 100-110.
Lo Muzio, L., C. Arena, G. Troiano and A. Villa, 2018 Oral stomatitis and mTOR inhibitors: A review of current evidence in 20,915 patients. Oral Diseases 24**:** 144-171.
Loewith, R., E. Jacinto, S. Wullschleger, A. Lorberg, J. L. Crespo *et al.*, 2002 Two TOR complexes, only one of which is rapamycin sensitive, have distinct roles in cell growth control. Mol Cell 10**:** 457-468.
Loftfield, E., N. D. Freedman, B. I. Graubard, K. A. Guertin, A. Black *et al.*, 2015 Association of Coffee Consumption With Overall and Cause-Specific Mortality in a Large US Prospective Cohort Study. Am J Epidemiol 182**:** 1010-1022.
Logan, R. W., R. F. Robledo, J. M. Recla, V. M. Philip, J. A. Bubier *et al.*, 2013 High-precision genetic mapping of behavioral traits in the diversity outbred mouse population. Genes Brain Behav 12**:** 424-437.
Longo, V. D., G. S. Shadel, M. Kaeberlein and B. Kennedy, 2012 Replicative and chronological aging in Saccharomyces cerevisiae. Cell Metab 16**:** 18-31.
Lopez-Lluch, G., N. Hunt, B. Jones, M. Zhu, H. Jamieson *et al.*, 2006 Calorie restriction induces mitochondrial biogenesis and bioenergetic efficiency. Proceedings of the National Academy of Sciences of the United States of America 103**:** 1768-1773.
Lopez-Otin, C., M. A. Blasco, L. Partridge, M. Serrano and G. Kroemer, 2013 The hallmarks of aging. Cell 153**:** 1194-1217.
Lorenz, M. C., and J. Heitman, 1995 TOR mutations confer rapamycin resistance by preventing interaction with FKBP12-rapamycin. J Biol Chem 270**:** 27531-27537.
Lu, Q., X. J. Ji, Y. X. Zhou, X. Q. Yao, Y. Q. Liu *et al.*, 2015 Quercetin inhibits the mTORC1/p70S6K signaling-mediated renal tubular epithelial-mesenchymal transition and renal fibrosis in diabetic nephropathy. Pharmacol Res 99**:** 237-247.
Luan, Y. A., X. P. Ren, W. Zheng, Z. H. Zeng, Y. Z. Guo *et al.*, 2018 Chronic Caffeine Treatment Protects Against alpha-Synucleinopathy by Reestablishing Autophagy Activity in the Mouse Striatum. Frontiers in Neuroscience 12**:** 13.
Lucanic, M., W. T. Plummer, E. Chen, J. Harke, A. C. Foulger *et al.*, 2017 Impact of genetic background and experimental reproducibility on identifying chemical compounds with robust longevity effects. Nature Communications 8**:** 14256.
Lundblad, V., and K. Struhl, 2010 *Yeast*. Wiley Interscience.
Lynch, H. T., P. M. Lynch, S. J. Lanspa, C. L. Snyder, J. F. Lynch *et al.*, 2009 Review of the Lynch syndrome: history, molecular genetics, screening, differential diagnosis, and medicolegal ramifications. Clinical genetics 76**:** 1-18.

Mackay, T. F. C., and W. Huang, 2018 Charting the genotype-phenotype map: lessons from the Drosophila melanogaster Genetic Reference Panel. Wiley Interdiscip Rev Dev Biol 7.
Mackay, T. F. C., S. Richards, E. A. Stone, A. Barbadilla, J. F. Ayroles *et al.*, 2012 The Drosophila melanogaster Genetic Reference Panel. Nature 482**:** 173.
MacLean, M., N. Harris and P. W. Piper, 2001 Chronological lifespan of stationary phase yeast cells; a model for investigating the factors that might influence the ageing of postmitotic tissues in higher organisms. Yeast 18**:** 499-509.
Maglioni, S., and N. Ventura, 2016 C. elegans as a model organism for human mitochondrial associated disorders. Mitochondrion 30**:** 117-125.
Maierhofer, A., J. Flunkert, J. Oshima, G. M. Martin, T. Haaf *et al.*, 2017 Accelerated epigenetic aging in Werner syndrome. Aging (Albany NY) 9**:** 1143-1152.
Majumder, S., A. Caccamo, D. X. Medina, A. D. Benavides, M. A. Javors *et al.*, 2012 Lifelong rapamycin administration ameliorates age-dependent cognitive deficits by reducing IL-1beta and enhancing NMDA signaling. Aging cell 11**:** 326-335.
Mannick, J. B., G. Del Giudice, M. Lattanzi, N. M. Valiante, J. Praestgaard *et al.*, 2014 mTOR inhibition improves immune function in the elderly. Science Translational Medicine 6**:** 7.
Mannick, J. B., M. Morris, H.-U. P. Hockey, G. Roma, M. Beibel *et al.*, 2017 TORC1 inhibition as an immunotherapy to reduce infections in the elderly. bioRxiv.
Marek, A., and R. Korona, 2013 Restricted pleiotropy facilitates mutational erosion of major life-history traits. Evolution 67**:** 3077-3086.
Martin-Montalvo, A., E. M. Mercken, S. J. Mitchell, H. H. Palacios, P. L. Mote *et al.*, 2013 Metformin improves healthspan and lifespan in mice. Nature Communications 4**:** 9.
Martin, D. E., and M. N. Hall, 2005 The expanding TOR signaling network. Current opinion in cell biology 17**:** 158-166.
Martin, M. A., and S. Ramos, 2017 Health beneficial effects of cocoa phenolic compounds: a mini-review. Current Opinion in Food Science 14**:** 20-25.
Martincorena, I., and P. J. Campbell, 2015 Somatic mutation in cancer and normal cells. Science 349**:** 1483-1489.
Martins, E. P., and T. Garland, Jr., 1991 Phylogenetic analyses of the correlated evolution of continuous characters: a simulation study. Evolution; international journal of organic evolution 45**:** 534-557.
Matecic, M., D. L. Smith, X. Pan, N. Maqani, S. Bekiranov *et al.*, 2010 A microarray-based genetic screen for yeast chronological aging factors, pp. e1000921 in *PLoS genetics*.
Matsuda, N., S. Sato, K. Shiba, K. Okatsu, K. Saisho *et al.*, 2010 PINK1 stabilized by mitochondrial depolarization recruits Parkin to damaged mitochondria and activates latent Parkin for mitophagy. Journal of Cell Biology 189**:** 211-221.
Mattin, M. J., A. Boswood, D. B. Church, J. Lopez-Alvarez, P. D. McGreevy *et al.*, 2015 Prevalence of and Risk Factors for Degenerative Mitral Valve Disease in Dogs Attending Primary-care Veterinary Practices in England. Journal of Veterinary Internal Medicine 29**:** 847-854.
Mattison, J. A., R. J. Colman, T. M. Beasley, D. B. Allison, J. W. Kemnitz *et al.*, 2017 Caloric restriction improves health and survival of rhesus monkeys. Nature Communications 8**:** 12.
Mattison, J. A., G. S. Roth, T. M. Beasley, E. M. Tilmont, A. M. Handy *et al.*, 2012 Impact of caloric restriction on health and survival in rhesus monkeys from the NIA study. Nature 489**:** 318-321.

McCay, C. M., M. F. Crowell and L. A. Maynard, 1989 The effect of retarded growth upon the length of life span and upon the ultimate body size. 1935. Nutrition 5**:** 155-171; discussion 172.
McColl, G., B. R. Roberts, T. L. Pukala, V. B. Kenche, C. M. Roberts *et al.*, 2012 Utility of an improved model of amyloid-beta (Aβ1-42) toxicity in Caenorhabditis elegansfor drug screening for Alzheimer's disease. Molecular Neurodegeneration 7**:** 57.
McCormick, M. A., J. R. Delaney, M. Tsuchiya, S. Tsuchiyama, A. Shemorry *et al.*, 2015 A Comprehensive Analysis of Replicative Lifespan in 4,698 Single-Gene Deletion Strains Uncovers Conserved Mechanisms of Aging. Cell Metabolism 22**:** 895-906.
McCullough, M. L., J. J. Peterson, R. Patel, P. F. Jacques, R. Shah *et al.*, 2012 Flavonoid intake and cardiovascular disease mortality in a prospective cohort of US adults. Am J Clin Nutr 95**:** 454-464.
McKay, R. M., J. P. McKay, L. Avery and J. M. Graff, 2003 C elegans: a model for exploring the genetics of fat storage. Dev Cell 4**:** 131-142.
Mehta, R., K. A. Steinkraus, G. L. Sutphin, F. J. Ramos, L. S. Shamieh *et al.*, 2009 Proteasomal regulation of the hypoxic response modulates aging in C. elegans. Science 324**:** 1196-1198.
Meng, F. D., Y. Li, X. Tian, P. Ma, C. G. Sui *et al.*, 2015 Synergistic effects of snail and quercetin on renal cell carcinoma Caki-2 by altering AKT/mTOR/ERK1/2 signaling pathways. Int J Clin Exp Pathol 8**:** 6157-6168.
Meric-Bernstam, F., and A. M. Gonzalez-Angulo, 2009 Targeting the mTOR Signaling Network for Cancer Therapy. Journal of Clinical Oncology 27**:** 2278-2287.
Milholland, B., A. Auton, Y. Suh and J. Vijg, 2015 Age-related somatic mutations in the cancer genome. Oncotarget 6**:** 24627-24635.
Miller, H., M. Fletcher, M. Primitivo, A. Leonard, G. L. Sutphin *et al.*, 2017 Genetic interaction with temperature is an important determinant of nematode longevity. Aging Cell 16**:** 1425-1429.
Miller, R. A., S. Austad, D. Burke, C. Chrisp, R. Dysko *et al.*, 1999 Exotic mice as models for aging research: polemic and prospectus. Neurobiology of Aging 20**:** 217-231.
Miller, R. A., D. E. Harrison, C. M. Astle, J. A. Baur, A. R. Boyd *et al.*, 2011 Rapamycin, but not resveratrol or simvastatin, extends life span of genetically heterogeneous mice. J Gerontol A Biol Sci Med Sci 66**:** 191-201.
Miller, R. A., D. E. Harrison, C. M. Astle, E. Fernandez, K. Flurkey *et al.*, 2014 Rapamycin-mediated lifespan increase in mice is dose and sex dependent and metabolically distinct from dietary restriction. Aging Cell 13**:** 468-477.
Miller, R. A., D. E. Harrison, C. M. Astle, R. A. Floyd, K. Flurkey *et al.*, 2007 An Aging Interventions Testing Program: study design and interim report. Aging Cell 6**:** 565-575.
Mirisola, M. G., R. J. Braun and D. Petranovic, 2014 Approaches to study yeast cell aging and death. Fems Yeast Research 14**:** 109-118.
Mohankumar, S. K., T. O'Shea and J. R. McFarlane, 2012 Insulinotrophic and insulin-like effects of a high molecular weight aqueous extract of Pterocarpus marsupium Roxb. hardwood. Journal of Ethnopharmacology 141**:** 72-79.
Morgan, T. H., 1910 Sex limited inheritence in Drosophila. Science 32**:** 120-122.
Mortimer, R. K., and J. R. Johnston, 1959 Life Span of Individual Yeast Cells. Nature 183**:** 1751-1752.

Mortimer, R. K., and J. R. Johnston, 1986 Genealogy of principal strains of the yeast genetic stock center. Genetics 113**:** 35-43.
Mounkes, L. C., S. Kozlov, L. Hernandez, T. Sullivan and C. L. Stewart, 2003 A progeroid syndrome in mice is caused by defects in A-type lamins. Nature 423**:** 298-301.
Mueller, L. D., 1987 Evolution of accelerated senescence in laboratory populations of Drosophila. Proceedings of the National Academy of Sciences of the United States of America 84**:** 1974-1977.
Murakami, C., J. R. Delaney, A. Chou, D. Carr, J. Schleit *et al.*, 2012 pH neutralization protects against reduction in replicative lifespan following chronological aging in yeast. Cell cycle 11**:** 3087-3096.
Murakami, C., and M. Kaeberlein, 2009 Quantifying Yeast Chronological Life Span by Outgrowth of Aged Cells. Journal of Visualized Experiments : JoVE**:** 1156.
Murakami, C. J., C. R. Burtner, B. K. Kennedy and M. Kaeberlein, 2008 A method for high-throughput quantitative analysis of yeast chronological life span. J Gerontol A Biol Sci Med Sci 63**:** 113-121.
Murphy, S. L., J. Q. Xu, K. D. Kochanek, S. C. Curtin and E. Arias, 2017 Deaths: Final data for 2015, pp., edited by N. C. f. H. Statistics. National Vital Statistics Reports, Hyattsville, MD.
N, C. R., and I. C. Chopra, 1933 *Indigenous Drugs Of India*. Academic Publishers.
Nadon, N. L., R. Strong, R. A. Miller and D. E. Harrison, 2017 NIA Interventions Testing Program: Investigating Putative Aging Intervention Agents in a Genetically Heterogeneous Mouse Model. EBioMedicine 21**:** 3-4.
Nadon, N. L., R. Strong, R. A. Miller, J. Nelson, M. Javors *et al.*, 2008 Design of aging intervention studies: the NIA interventions testing program. Age 30**:** 187-199.
Neff, F., D. Flores-Dominguez, D. P. Ryan, M. Horsch, S. Schroder *et al.*, 2013 Rapamycin extends murine lifespan but has limited effects on aging. J Clin Invest 123**:** 3272-3291.
Nie, Z. H., H. L. Zhu and M. J. Gu, 2016 Reduced colorectal cancer incidence in type 2 diabetic patients treated with metformin: a meta-analysis. Pharmaceutical Biology 54**:** 2636-2642.
Nishimura, M., K. Ocorr, R. Bodmer and J. Cartry, 2011 Drosophila as a model to study cardiac aging. Experimental Gerontology 46**:** 326-330.
Noto, H., A. Goto, T. Tsujimoto and M. Noda, 2012 Cancer Risk in Diabetic Patients Treated with Metformin: A Systematic Review and Meta-analysis. Plos One 7**:** 9.
O'Donnell, J. S., D. Massi, M. W. L. Teng and M. Mandala, 2017 PI3K-AKT-mTOR inhibition in cancer immunotherapy, redux. Semin Cancer Biol.
Olsen, B., C. J. Murakami and M. Kaeberlein, 2010 YODA: Software to facilitate high-throughput analysis of chronological life span, growth rate, and survival in budding yeast. Bmc Bioinformatics 11**:** 8.
Olshansky, S. J., 2015 Has the Rate of Human Aging Already Been Modified? Cold Spring Harbor Perspectives in Medicine 5**:** 17.
Olshansky, S. J., 2016 Articulating the Case for the Longevity Dividend. Cold Spring Harbor Perspectives in Medicine 6**:** 6.
Olshansky, S. J., 2018 The Future of Health. Journal of the American Geriatrics Society 66**:** 195-197.
Olshansky, S. J., D. Perry, R. A. Miller and R. N. Butler, 2006 In pursuit of the longevity dividend. Scientist 20**:** 28-36.

Osorio, F. G., A. J. Obaya, C. Lopez-Otin and J. M. P. Freije, 2009 Accelerated ageing: from mechanism to therapy through animal models. Transgenic Research 18**:** 7-15.
Outeiro, T. F., and S. Lindquist, 2003 Yeast cells provide insight into alpha-synuclein biology and pathobiology. Science 302**:** 1772-1775.
Palles, C., J. B. Cazier, K. M. Howarth, E. Domingo, A. M. Jones *et al.*, 2013 Germline mutations affecting the proofreading domains of POLE and POLD1 predispose to colorectal adenomas and carcinomas. Nature Genetics 45**:** 136-144.
Palma-Gudiel, H., A. Cordova-Palomera, E. Eixarch, M. Deuschle and L. Fananas, 2015 Maternal psychosocial stress during pregnancy alters the epigenetic signature of the glucocorticoid receptor gene promoter in their offspring: a meta-analysis. Epigenetics 10**:** 893-902.
Pan, Y., and G. S. Shadel, 2009 Extension of chronological life span by reduced TOR signaling requires down-regulation of Sch9p and involves increased mitochondrial OXPHOS complex density. Aging 1**:** 131-145.
Pandey, U. B., and C. D. Nichols, 2011 Human Disease Models in Drosophila melanogaster and the Role of the Fly in Therapeutic Drug Discovery. Pharmacological Reviews 63**:** 411-436.
Park, D., H. Jeong, M. N. Lee, A. Koh, O. Kwon *et al.*, 2016 Resveratrol induces autophagy by directly inhibiting mTOR through ATP competition. Sci Rep 6**:** 21772.
Partridge, L., and D. Gems, 2002 Mechanisms of aging: public or private? Nature Reviews Genetics 3**:** 165-175.
Passarino, G., F. De Rango and A. Montesanto, 2016 Human longevity: Genetics or Lifestyle? It takes two to tango. Immunity & Ageing : I & A 13**:** 12.
Pettan-Brewer, C., and P. M. Treuting, 2011 Practical pathology of aging mice. Pathobiology of Aging & Age Related Diseases 1**:** 10.3402/pba.v3401i3400.7202.
Phillips, T., and C. Leeuwenburgh, 2004 Lifelong aspirin supplementation as a means to extending life span. Rejuvenation Research 7**:** 243-251.
Pinheiro, J., D. Bates, S. DebRoy, D. Sarkar and R Development Core Team, 2013 nlme: Linear and Nonlinear Mixed Effects Models. R package.
Piper, M. D. W., and L. Partridge, 2016 Protocols to study ageing in Drosophila. Methods in molecular biology (Clifton, N.J.) 1478**:** 291-302.
Pitt, J. N., and M. Kaeberlein, 2015 Why is aging conserved and what can we do about it? PLoS Biol 13**:** e1002131.
Plummer, W. T., J. Harke, M. Lucanic, E. Chen, D. Bhaumik *et al.*, 2017 Standardized Protocols from the Caenorhabditis Intervention Testing Program 2013-2016: Conditions and Assays used for Quantifying the Development, Fertility and Lifespan of Hermaphroditic Caenorhabditis Strains.
Poole, A. C., R. E. Thomas, L. A. Andrews, H. M. McBride, A. J. Whitworth *et al.*, 2008 The PINK1/Parkin pathway regulates mitochondrial morphology. Proceedings of the National Academy of Sciences of the United States of America 105**:** 1638-1643.
Popovich, I. G., V. N. Anisimov, M. A. Zabezhinski, A. V. Semenchenko, M. L. Tyndyk *et al.*, 2014b Lifespan extension and cancer prevention in HER-2/neu transgenic mice treated with low intermittent doses of rapamycin. Cancer Biol Ther 15**:** 586-592.
Powers, R. W., M. Kaeberlein, S. D. Caldwell, B. K. Kennedy and S. Fields, 2006 Extension of chronological life span in yeast by decreased TOR pathway signaling. Genes & Development 20**:** 174-184.

Preston, M. A., A. H. Riis, V. Ehrenstein, R. H. Breau, J. L. Batista *et al.*, 2014 Metformin Use and Prostate Cancer Risk. European Urology 66**:** 1012-1020.
Provinciali, N., M. Lazzeroni, M. Cazzaniga, F. Gorlero, B. K. Dunn *et al.*, 2015 Metformin: risk-benefit profile with a focus on cancer. Expert Opinion on Drug Safety 14**:** 1573-1585.
Quach, A., M. E. Levine, T. Tanaka, A. T. Lu, B. H. Chen *et al.*, 2017 Epigenetic clock analysis of diet, exercise, education, and lifestyle factors. Aging-Us 9**:** 419-446.
R Development Core Team, 2013 *R: A Language and Environment for Statistical Computing*, Vienna, Austria.
Rallis, C., S. Codlin and J. Bahler, 2013 TORC1 signaling inhibition by rapamycin and caffeine affect lifespan, global gene expression, and cell proliferation of fission yeast. Aging Cell 12**:** 563-573.
Ramirez, C. L., J. Cadinanos, I. Varela, J. M. P. Freije and C. Lopez-Otin, 2007 Human progeroid syndromes, aging and cancer: new genetic and epigenetic insights into old questions. Cellular and Molecular Life Sciences 64**:** 155-170.
Ramos, F. J., S. C. Chen, M. G. Garelick, D. F. Dai, C. Y. Liao *et al.*, 2012 Rapamycin reverses elevated mTORC1 signaling in lamin A/C-deficient mice, rescues cardiac and skeletal muscle function, and extends survival. Sci Transl Med 4**:** 144ra103.
Rayner, E., I. C. van Gool, C. Palles, S. E. Kearsey, T. Bosse *et al.*, 2016 A panoply of errors: polymerase proofreading domain mutations in cancer. Nature Reviews Cancer 16**:** 71-81.
Regenberg, B., T. Grotkjaer, O. Winther, A. Fausboll, M. Akesson *et al.*, 2006 Growth-rate regulated genes have profound impact on interpretation of transcriptome profiling in Saccharomyces cerevisiae. Genome biology 7**:** R107.
Reinke, A., J. C. Chen, S. Aronova and T. Powers, 2006 Caffeine targets TOR complex I and provides evidence for a regulatory link between the FRB and kinase domains of Tor1p. J Biol Chem 281**:** 31616-31626.
Reznick, D., G. Buckwalter, J. Groff and D. Elder, 2001 The evolution of senescence in natural populations of guppies (Poecilia reticulata): a comparative approach. Experimental gerontology 36**:** 791-812.
Rikke, B. A., C. Y. Liao, M. B. McQueen, J. F. Nelson and T. E. Johnson, 2010 Genetic dissection of dietary restriction in mice supports the metabolic efficiency model of life extension. Experimental Gerontology 45**:** 691-701.
Risques, R. A., and S. R. Kennedy, 2018 Aging and the rise of somatic cancer-associated mutations in normal tissues. Plos Genetics 14**:** 12.
Robida-Stubbs, S., K. Glover-Cutter, D. W. Lamming, M. Mizunuma, S. D. Narasimhan *et al.*, 2012 TOR signaling and rapamycin influence longevity by regulating SKN-1/Nrf and DAF-16/FoxO. Cell metabolism 15**:** 713-724.
Romano, G. H., Y. Gurvich, O. Lavi, I. Ulitsky, R. Shamir *et al.*, 2010 Different sets of QTLs influence fitness variation in yeast. Molecular systems biology 6**:** 346.
Rose, M. R., 1984 Laboratory evolution of postponed senescence in Drosophila melanogaster. Evolution 38**:** 1004-1010.
Ross, C., A. Salmon, R. Strong, E. Fernandez, M. Javors *et al.*, 2015 Metabolic consequences of long-term rapamycin exposure on common marmoset monkeys (Callithrix jacchus). Aging (Albany NY) 7**:** 964-973.
Ross, C. N., K. Davis, G. Dobek and S. D. Tardif, 2012 Aging Phenotypes of Common Marmosets (Callithrix jacchus). Journal of Aging Research 2012**:** 567143.

Rual, J. F., J. Ceron, J. Koreth, T. Hao, A. S. Nicot *et al.*, 2004 Toward improving Caenorhabditis elegans phenome mapping with an ORFeome-based RNAi library. Genome Res 14**:** 2162-2168.

Ryu, D., H. Zhang, E. R. Ropelle, V. Sorrentino, D. A. Mazala *et al.*, 2016 NAD+ repletion improves muscle function in muscular dystrophy and counters global PARylation. Sci Transl Med 8**:** 361ra139.

Sabatini, D. M., H. Erdjument-Bromage, M. Lui, P. Tempst and S. H. Snyder, 1994 RAFT1: a mammalian protein that binds to FKBP12 in a rapamycin-dependent fashion and is homologous to yeast TORs. Cell 78**:** 35-43.

Sabers, C. J., M. M. Martin, G. J. Brunn, J. M. Williams, F. J. Dumont *et al.*, 1995 Isolation of a protein target of the FKBP12-rapamycin complex in mammalian cells. J Biol Chem 270**:** 815-822.

Saiki, S., Y. Sasazawa, Y. Imamichi, S. Kawajiri, T. Fujimaki *et al.*, 2011 Caffeine induces apoptosis by enhancement of autophagy via PI3K/Akt/mTOR/p70S6K inhibition. Autophagy 7**:** 176-187.

Saitou, N., and M. Nei, 1987 The neighbor-joining method: a new method for reconstructing phylogenetic trees. Molecular biology and evolution 4**:** 406-425.

Salmon, A. B., 2016 Moving toward 'common' use of the marmoset as a non-human primate aging model. Pathobiol Aging Age Relat Dis 6**:** 32758.

Saunders, R. N., M. S. Metcalfe and M. L. Nicholson, 2001 Rapamycin in transplantation: A review of the evidence. Kidney International 59**:** 3-16.

Saxton, R. A., and D. M. Sabatini, 2017 mTOR Signaling in Growth, Metabolism, and Disease. Cell 168**:** 960-976.

Schleit, J., S. C. Johnson, C. F. Bennett, M. Simko, N. Trongtham *et al.*, 2013 Molecular mechanisms underlying genotype-dependent responses to dietary restriction. Aging Cell 12**:** 1050-1061.

Schulenburg, H., and M. A. Felix, 2017 The Natural Biotic Environment of Caenorhabditis elegans. Genetics 206**:** 55-86.

Schulz, T. J., K. Zarse, A. Voigt, N. Urban, M. Birringer *et al.*, 2007 Glucose restriction extends Caenorhabditis elegans life span by inducing mitochondrial respiration and increasing oxidative stress. Cell metabolism 6**:** 280-293.

Seals, D. R., and S. Melov, 2014 Translational Geroscience: Emphasizing function to achieve optimal longevity. Aging-Us 6**:** 718-730.

Seebacher, V., B. Bergmeister, C. Grimm, H. Koelbl, A. Reinthaller *et al.*, 2016 The prognostic role of metformin in patients with endometrial cancer: a retrospective study. European Journal of Obstetrics & Gynecology and Reproductive Biology 203**:** 291-296.

Sgro, C. M., and L. Partridge, 2000 Evolutionary responses of the life history of wild-caught Drosophila melanogaster to two standard methods of laboratory culture. American Naturalist 156**:** 341-353.

Sherman, F., 2002 Getting started with yeast. Guide to Yeast Genetics and Molecular and Cell Biology, Pt B 350**:** 3-41.

Shlien, A., B. B. Campbell, R. de Borja, L. B. Alexandrov, D. Merico *et al.*, 2015 Combined hereditary and somatic mutations of replication error repair genes result in rapid onset of ultra-hypermutated cancers. Nat Genet 47**:** 257-262.

Siegmund, S. E., H. Yang, R. Sharma, M. Javors, O. Skinner *et al.*, 2017 Low-dose rapamycin extends lifespan in a mouse model of mtDNA depletion syndrome. Human Molecular Genetics 26**:** 4588-4605.

Sierra, F., 2016 The Emergence of Geroscience as an Interdisciplinary Approach to the Enhancement of Health Span and Life Span. Cold Spring Harbor Perspectives in Medicine 6**:** a025163.

Sinclair, D. A., and L. Guarente, 1997 Extrachromosomal rDNA circles - A cause of aging in yeast. Cell 91**:** 1033-1042.

Skelly, D. A., G. E. Merrihew, M. Riffle, C. F. Connelly, E. O. Kerr *et al.*, 2013 Integrative phenomics reveals insight into the structure of phenotypic diversity in budding yeast. Genome research 23**:** 1496-1504.

Skytthe, A., N. L. Pedersen, J. Kaprio, M. A. Stazi, J. V. Hjelmborg *et al.*, 2003 Longevity studies in GenomEUtwin. Twin Res 6**:** 448-454.

Smith, E. D., M. Tsuchiya, L. A. Fox, N. Dang, D. Hu *et al.*, 2008 Quantitative evidence for conserved longevity pathways between divergent eukaryotic species. Genome research 18**:** 564-570.

Smith, P., D. Willemsen, M. Popkes, F. Metge, E. Gandiwa *et al.*, 2017 Regulation of life span by the gut microbiota in the short-lived African turquoise killifish. Elife 6.

Snider, T. A., A. Richardson, J. A. Stoner and S. S. Deepa, 2018 The Geropathology Grading Platform demonstrates that mice null for Cu/Zn-superoxide dismutase show accelerated biological aging. Geroscience 40**:** 97-103.

Snyder, J. M., J. M. Ward and P. M. Treuting, 2016 Cause-of-Death Analysis in Rodent Aging Studies. Vet Pathol 53**:** 233-243.

Song, S. J., C. Lauber, E. K. Costello, C. A. Lozupone, G. Humphrey *et al.*, 2013 Cohabiting family members share microbiota with one another and with their dogs. Elife 2**:** 22.

Sonoshita, M., and R. L. Cagan, 2017 Chapter Nine - Modeling Human Cancers in Drosophila, pp. 287-309 in *Current Topics in Developmental Biology*, edited by L. Pick. Academic Press.

Soranna, D., L. Scotti, A. Zambon, C. Bosetti, G. Grassi *et al.*, 2012 Cancer Risk Associated with Use of Metformin and Sulfonylurea in Type 2 Diabetes: A Meta-Analysis. Oncologist 17**:** 813-822.

Speakman, J. R., and S. E. Mitchell, 2011 Caloric restriction. Molecular Aspects of Medicine 32**:** 159-221.

Spor, A., T. Nidelet, J. Simon, A. Bourgais, D. de Vienne *et al.*, 2009 Niche-driven evolution of metabolic and life-history strategies in natural and domesticated populations of Saccharomyces cerevisiae. BMC Evol Biol 9**:** 296.

Stan, R., M. M. McLaughlin, R. Cafferkey, R. K. Johnson, M. Rosenberg *et al.*, 1994 Interaction between FKBP12-rapamycin and TOR involves a conserved serine residue. J Biol Chem 269**:** 32027-32030.

Steffen, K. K., B. K. Kennedy and M. Kaeberlein, 2009 Measuring replicative life span in the budding yeast. J Vis Exp.

Steffen, K. K., V. L. MacKay, E. O. Kerr, M. Tsuchiya, D. Hu *et al.*, 2008 Yeast life span extension by depletion of 60s ribosomal subunits is mediated by Gcn4. Cell 133**:** 292-302.

Sterken, M. G., L. B. Snoek, J. E. Kammenga and E. C. Andersen, 2015 The laboratory domestication of Caenorhabditis elegans. Trends in genetics : TIG 31**:** 224-231.

Strong, R., R. A. Miller, A. Antebi, C. M. Astle, M. Bogue *et al.*, 2016 Longer lifespan in male mice treated with a weakly estrogenic agonist, an antioxidant, an alpha-glucosidase inhibitor or a Nrf2-inducer. Aging Cell 15**:** 872-884.

Strong, R., R. A. Miller, C. M. Astle, J. A. Baur, R. de Cabo *et al.*, 2013a Evaluation of resveratrol, green tea extract, curcumin, oxaloacetic acid, and medium-chain triglyceride oil on life span of genetically heterogeneous mice. J Gerontol A Biol Sci Med Sci 68**:** 6-16.

Strong, R., R. A. Miller, C. M. Astle, R. A. Floyd, K. Flurkey *et al.*, 2008a Nordihydroguaiaretic acid and aspirin increase lifespan of genetically heterogeneous male mice. Aging Cell 7**:** 641-650.

Stroustrup, N., B. E. Ulmschneider, Z. M. Nash, I. F. Lopez-Moyado, J. Apfeld *et al.*, 2013 The Caenorhabditis elegans Lifespan Machine. Nature Methods 10**:** 665-670.

Stubbs, T. M., M. J. Bonder, A. K. Stark, F. Krueger, F. von Meyenn *et al.*, 2017 Multi-tissue DNA methylation age predictor in mouse. Genome Biology 18**:** 14.

Sutphin, G. L., E. Bishop, M. E. Yanos, R. M. Moller and M. Kaeberlein, 2012 Caffeine extends life span, improves healthspan, and delays age-associated pathology in Caenorhabditis elegans. Longev Healthspan 1**:** 9.

Sutphin, G. L., and M. Kaeberlein, 2009 Measuring Caenorhabditis elegans life span on solid media. J Vis Exp.

Svenson, K. L., D. M. Gatti, W. Valdar, C. E. Welsh, R. Y. Cheng *et al.*, 2012 High-Resolution Genetic Mapping Using the Mouse Diversity Outbred Population. Genetics 190**:** 437-447.

Szilard, L., 1959 On the Nature of the Aging Process. Proceedings of the National Academy of Sciences of the United States of America 45**:** 30-45.

Tamura, K., G. Stecher, D. Peterson, A. Filipski and S. Kumar, 2013 MEGA6: Molecular Evolutionary Genetics Analysis version 6.0. Molecular biology and evolution 30**:** 2725-2729.

Tardif, S., C. Ross, P. Bergman, E. Fernandez, M. Javors *et al.*, 2015 Testing efficacy of administration of the antiaging drug rapamycin in a nonhuman primate, the common marmoset. J Gerontol A Biol Sci Med Sci 70**:** 577-587.

Tardif, S. D., K. G. Mansfield, R. Ratnam, C. N. Ross and T. E. Ziegler, 2011 The marmoset as a model of aging and age-related diseases. ILAR J 52**:** 54-65.

Tatar, M., A. Kopelman, D. Epstein, M. P. Tu, C. M. Yin *et al.*, 2001 A Mutant Drosophila Insulin Receptor Homolog That Extends Life-Span and Impairs Neuroendocrine Function. Science 292**:** 107-110.

Tchkonia, T., Y. Zhu, J. van Deursen, J. Campisi and J. L. Kirkland, 2013 Cellular senescence and the senescent secretory phenotype: therapeutic opportunities. Journal of Clinical Investigation 123**:** 966-972.

Team, R. C., 2016 R: A language and environment for statistical computing., pp. R Foundation for Statistical Computing, Vienna, Austria.

Tenreiro, S., and T. F. Outeiro, 2010 Simple is good: yeast models of neurodegeneration. Fems Yeast Research 10**:** 970-979.

Therneau, T., 2015 A Package for Survival Analysis in S, pp.

Therneau, T. G., P., 2000 *Modeling Survival Data: Extending the Cox model*. Springer, New York.

Thomas, I., and B. Gregg, 2017 Metformin; a review of its history and future: from lilac to longevity. Pediatric Diabetes 18**:** 10-16.
Thompson, M. J., B. Vonholdt, S. Horvath and M. Pellegrini, 2017 An epigenetic aging clock for dogs and wolves. Aging-Us 9**:** 1055-1068.
Tillu, D. V., O. K. Melemedjian, M. N. Asiedu, N. Qu, M. De Felice *et al.*, 2012 Resveratrol engages AMPK to attenuate ERK and mTOR signaling in sensory neurons and inhibits incision-induced acute and chronic pain. Mol Pain 8**:** 5.
Tissenbaum, H. A., 2015 Using C. elegans for aging research. Invertebrate Reproduction & Development 59**:** 59-63.
Toivonen, J. M., and L. Partridge, 2009 Endocrine regulation of aging and reproduction in Drosophila. Molecular and Cellular Endocrinology 299**:** 39-50.
Tomasetti, C., L. Li and B. Vogelstein, 2017 Stem cell divisions, somatic mutations, cancer etiology, and cancer prevention. Science 355**:** 1330-1334.
Tomasetti, C., B. Vogelstein and G. Parmigiani, 2013 Half or more of the somatic mutations in cancers of self-renewing tissues originate prior to tumor initiation. Proc Natl Acad Sci U S A 110**:** 1999-2004.
Tu, M. P., D. Epstein and M. Tatar, 2002 The demography of slow aging in male and female Drosophila mutant for the insulin-receptor substrate homologue chico. Aging Cell 1**:** 75-80.
Urfer, S. R., T. L. Kaeberlein, S. Mailheau, P. J. Bergman, K. E. Creevy *et al.*, 2017a Asymptomatic heart valve dysfunction in healthy middle-aged companion dogs and its implications for cardiac aging. Geroscience 39**:** 43-50.
Urfer, S. R., T. L. Kaeberlein, S. Mailheau, P. J. Bergman, K. E. Creevy *et al.*, 2017b A randomized controlled trial to establish effects of short-term rapamycin treatment in 24 middle-aged companion dogs. Geroscience 39**:** 117-127.
Valdesalici, S., and A. Cellerino, 2003 Extremely short lifespan in the annual fish Nothobranchius furzeri. Proc Biol Sci 270 Suppl 2**:** 189-191.
Valenzano, Dario R., Bérénice A. Benayoun, Param P. Singh, E. Zhang, Paul D. Etter *et al.*, 2015 The African Turquoise Killifish Genome Provides Insights into Evolution and Genetic Architecture of Lifespan. Cell 163**:** 1539-1554.
Valenzano, D. R., E. Terzibasi, A. Cattaneo, L. Domenici and A. Cellerino, 2006a Temperature affects longevity and age-related locomotor and cognitive decay in the short-lived fish Nothobranchius furzeri. Aging Cell 5**:** 275-278.
Valenzano, D. R., E. Terzibasi, T. Genade, A. Cattaneo, L. Domenici *et al.*, 2006b Resveratrol prolongs lifespan and retards the onset of age-related markers in a short-lived vertebrate. Curr Biol 16**:** 296-300.
Van Aller, G. S., J. D. Carson, W. Tang, H. Peng, L. Zhao *et al.*, 2011 Epigallocatechin gallate (EGCG), a major component of green tea, is a dual phosphoinositide-3-kinase/mTOR inhibitor. Biochem Biophys Res Commun 406**:** 194-199.
van Alphen, B., and B. van Swinderen, 2013 Drosophila strategies to study psychiatric disorders. Brain Research Bulletin 92**:** 1-11.
Varela, I., J. Cadiñanos, A. M. Pendás, A. Gutiérrez-Fernández, A. R. Folgueras *et al.*, 2005 Accelerated ageing in mice deficient in Zmpste24 protease is linked to p53 signalling activation. Nature 437**:** 564-568.
Vats, V., J. K. Grover and S. S. Rathi, 2002 Evaluation of anti-hyperglycemic and hypoglycemic effect of Trigonella foenum-graecum Linn, Ocimum sanctum Linn and Pterocarpus

marsupium Linn in normal and alloxanized diabetic rats. Journal of Ethnopharmacology 79**:** 95-100.
Vats, V., S. P. Yadav, N. R. Biswas and J. K. Grover, 2004 Anti-cataract activity of Pterocarpus marsupium, bark and Trigonella foenum-graecum seeds extract in alloxan diabetic rats. Journal of Ethnopharmacology 93**:** 289-294.
Verhave, J., A. Boucher, R. Dandavino, S. Collette, L. Senécal *et al.*, 2014 The incidence, management, and evolution of rapamycin□related side effects in kidney transplant recipients. Clinical Transplantation 28**:** 616-622.
Vezina, C., A. Kudelski and S. N. Sehgal, 1975 Rapamycin (AY-22,989), a new antifungal antibiotic. I. Taxonomy of the producing streptomycete and isolation of the active principle. J Antibiot (Tokyo) 28**:** 721-726.
Vijg, J., and M. E. T. Dolle, 2002 Large genome rearrangements as a primary cause of aging. Mechanisms of Ageing and Development 123**:** 907-915.
Vijg, J., and Y. Suh, 2005 Genetics of longevity and aging, in *Annual Review of Medicine*. Annual Reviews, Palo Alto: 193-212.
Wan, Q. L., S. Q. Zheng, G. S. Wu and H. R. Luo, 2013 Aspirin extends the lifespan of Caenorhabditis elegans via AMPK and DAF-16/FOXO in dietary restriction pathway. Experimental Gerontology 48**:** 499-506.
Wang, A., J. Mouser, J. Pitt, D. Promislow and M. Kaeberlein, 2016 Rapamycin enhances survival in a Drosophila model of mitochondrial disease. Oncotarget 7**:** 80131-80139.
Wang, X., K. Salinas, X. Zuo, B. Kucejova and X. J. Chen, 2008 Dominant membrane uncoupling by mutant adenine nucleotide translocase in mitochondrial diseases. Human molecular genetics 17**:** 4036-4044.
Wanke, V., E. Cameroni, A. Uotila, M. Piccolis, J. Urban *et al.*, 2008 Caffeine extends yeast lifespan by targeting TORC1. Mol Microbiol 69**:** 277-285.
Warner, H. R., D. Ingram, R. A. Miller, N. L. Nadon and A. G. Richardson, 2000 Program for testing biological interventions to promote healthy aging. Mech Ageing Dev 115**:** 199-207.
Wasko, B. M., and M. Kaeberlein, 2014 Yeast replicative aging: a paradigm for defining conserved longevity interventions. Fems Yeast Research 14**:** 148-159.
Watanabe, C., 1918 Studies in the metabolic changes induced by administration of guanidine bases. J. biol. Chem 33**:** 253-265.
Weeda, G., I. Donker, J. de Wit, H. Morreau, R. Janssens *et al.*, 1997 Disruption of mouse ERCC1 results in a novel repair syndrome with growth failure, nuclear abnormalities and senescence. Curr Biol 7**:** 427-439.
Welch, J. S., T. J. Ley, D. C. Link, C. A. Miller, D. E. Larson *et al.*, 2012 The origin and evolution of mutations in acute myeloid leukemia. Cell 150**:** 264-278.
WHO, 2018 Global Health Estimates 2016: Deaths by Cause, Age, Sex, by Country and by Region, 2000-2016, pp. World Health Organization, Geneva.
Wiczk, A., D. Hofman, G. Konopa and A. Herman-Antosiewicz, 2012 Sulforaphane, a cruciferous vegetable-derived isothiocyanate, inhibits protein synthesis in human prostate cancer cells. Biochim Biophys Acta 1823**:** 1295-1305.
Wilkinson, J. E., L. Burmeister, S. V. Brooks, C. C. Chan, S. Friedline *et al.*, 2012 Rapamycin slows aging in mice. Aging Cell 11**:** 675-682.

Williams, R. W., B. Bennett, L. Lu, J. Gu, J. C. DeFries *et al.*, 2004 Genetic structure of the LXS panel of recombinant inbred mouse strains: a powerful resource for complex trait analysis. Mammalian Genome 15**:** 637-647.

Wilson, K. A., C. S. Nelson, J. N. Beck, R. B. Brem and P. Kapahi, 2018 Genome-wide analysis reveals distinct genetic mechanisms of diet-dependent lifespan and healthspan in D. melanogaster. bioRxiv.

Winzeler, E. A., D. D. Shoemaker, A. Astromoff, H. Liang, K. Anderson *et al.*, 1999 Functional characterization of the S. cerevisiae genome by gene deletion and parallel analysis. Science 285**:** 901-906.

Wu, T. J., X. Wang, Y. Zhang, L. Meng, J. E. Kerrigan *et al.*, 2015 Identification of a Non-Gatekeeper Hot Spot for Drug-Resistant Mutations in mTOR Kinase. Cell Rep 11**:** 446-459.

Wullschleger, S., R. Loewith and M. N. Hall, 2006 TOR signaling in growth and metabolism. Cell 124**:** 471-484.

Xian, B., J. Shen, W. Chen, N. Sun, N. Qiao *et al.*, 2013 WormFarm: a quantitative control and measurement device toward automated Caenorhabditis elegans aging analysis. Aging Cell 12**:** 398-409.

Xie, M., C. Lu, J. Wang, M. D. McLellan, K. J. Johnson *et al.*, 2014 Age-related mutations associated with clonal hematopoietic expansion and malignancies. Nat Med 20**:** 1472-1478.

Xie, R., X. Li, Y. Ling, C. Shen, X. Wu *et al.*, 2012 Alpha-lipoic acid pre- and post-treatments provide protection against in vitro ischemia-reperfusion injury in cerebral endothelial cells via Akt/mTOR signaling. Brain Res 1482**:** 81-90.

Xu, Z. H., M. Poidevin, X. K. Li, Y. J. Li, L. Q. Shu *et al.*, 2013 Expanded GGGGCC repeat RNA associated with amyotrophic lateral sclerosis and frontotemporal dementia causes neurodegeneration. Proceedings of the National Academy of Sciences of the United States of America 110**:** 7778-7783.

Yanos, M. E., C. F. Bennett and M. Kaeberlein, 2012 Genome-Wide RNAi Longevity Screens in Caenorhabditis elegans. Current Genomics 13**:** 508-518.

Yoshino, J., K. F. Mills, M. J. Yoon and S. I. Imai, 2011 Nicotinamide Mononucleotide, a Key NAD(+) Intermediate, Treats the Pathophysiology of Diet- and Age-Induced Diabetes in Mice. Cell Metabolism 14**:** 528-536.

Yuan, R., S. W. Tsaih, S. B. Petkova, C. Marin de Evsikova, S. Xing *et al.*, 2009 Aging in inbred strains of mice: study design and interim report on median lifespans and circulating IGF1 levels. Aging Cell 8**:** 277-287.

Yue, J. X., J. Li, L. Aigrain, J. Hallin, K. Persson *et al.*, 2017 Contrasting evolutionary genome dynamics between domesticated and wild yeasts. Nat Genet 49**:** 913-924.

Yukilevich, R., and J. R. True, 2008 Incipient sexual isolation among cosmopolitan Drosophila melanogaster populations. Evolution 62**:** 2112-2121.

Zannas, A. S., J. Arloth, T. Carrillo-Roa, S. Iurato, S. Roh *et al.*, 2015 Lifetime stress accelerates epigenetic aging in an urban, African American cohort: relevance of glucocorticoid signaling. Genome Biol 16**:** 266.

Zerofsky, M., E. Harel, N. Silverman and M. Tatar, 2005 Aging of the innate immune response in Drosophila melanogaster. Aging Cell 4**:** 103-108.

Zhang, H., C. Gao, L. Fang, H. C. Zhao and S. K. Yao, 2013 Metformin and reduced risk of hepatocellular carcinoma in diabetic patients: a meta-analysis. Scandinavian Journal of Gastroenterology 48**:** 78-87.

Zhang, H., D. Ryu, Y. Wu, K. Gariani, X. Wang *et al.*, 2016 NAD(+) repletion improves mitochondrial and stem cell function and enhances life span in mice. Science 352**:** 1436-1443.

Zhang, Q., A. P. Kelly, L. Wang, S. W. French, X. Tang *et al.*, 2006 Green tea extract and (-)-epigallocatechin-3-gallate inhibit mast cell-stimulated type I collagen expression in keloid fibroblasts via blocking PI-3K/AkT signaling pathways. J Invest Dermatol 126**:** 2607-2613.

Zhang, Z. J., Y. Y. Bi, S. Y. Li, Q. J. Zhang, G. M. Zhao *et al.*, 2014 Reduced Risk of Lung Cancer With Metformin Therapy in Diabetic Patients: A Systematic Review and Meta-Analysis. American Journal of Epidemiology 180**:** 11-14.

Zhang, Z. J., Z. J. Zheng, H. Kan, Y. Song, W. Cui *et al.*, 2011 Reduced risk of colorectal cancer with metformin therapy in patients with type 2 diabetes: a meta-analysis. Diabetes Care 34**:** 2323-2328.

Zheng, Q., 2015 A new practical guide to the Luria-Delbruck protocol. Mutation Research-Fundamental and Molecular Mechanisms of Mutagenesis 781**:** 7-13.

Zheng, X., L. Boyer, M. Jin, Y. Kim, W. Fan *et al.*, 2016 Alleviation of neuronal energy deficiency by mTOR inhibition as a treatment for mitochondria-related neurodegeneration. eLife 5**:** e13378.

APPENDIX A

Defining Molecular Basis for Longevity Traits in Natural Yeast Isolates

*Alaattin Kaya[1#], Siming Ma[1#], Brian Wasko[2], Mitchell Lee[2], Matt Kaeberlein[2], and Vadim N. Gladyshev[1]**

[1] Division of Genetics, Department of Medicine, Brigham and Women's Hospital and Harvard Medical School, Boston, MA, 02115, USA

[2] Department of Pathology, University of Washington, Seattle, WA, USA

[#] These authors contributed equally to this work

* Corresponding author: Division of Genetics, Department of Medicine, Brigham & Women's Hospital and Harvard Medical School, New Research Building, Room 435, 77 Avenue Louis Pasteur, Boston, MA 02115 USA. Phone: (617) 525-5122. E-mail: vgladyshev@rics.bwh.harvard.edu

Abstract

The budding yeast has served as a useful model organism in aging studies, leading to the identification of genetic determinants of longevity, many of which are conserved in higher eukaryotes. However, factors that promote longevity in laboratory setting often have severe fitness disadvantage in the wild. Here, to obtain an unbiased view on longevity regulation we analyzed how replicative lifespan is shaped by transcriptional, translational, metabolic, and morphological factors across 22 wild-type *Saccharomyces cerevisiae* isolates. We observed significant differences in lifespan across these strains and found that their longevity is strongly associated with up-regulation of oxidative phosphorylation and respiration and down-regulation of amino acid and nitrogen compound biosynthesis. Since calorie restriction and TOR signaling also extend lifespan by adjusting many of the identified pathways, the data suggest that natural plasticity of yeast lifespan is shaped by processes that not only do not impose cost on fitness, but are amenable to dietary intervention.

Introduction

The idea of slowing aging and extending lifespan of organisms has attracted much attention, leading to the identification of numerous factors that mitigate the effects of the aging process. At the cellular level, the driving force behind aging may be the inevitable accumulation of a myriad different forms of molecular damage(GLADYSHEV 2012). Many genetic and pharmacological interventions have been discovered that increase the lifespan of model organisms, including some with single gene effects(FINCH AND RUVKUN 2001; KENYON 2010). In addition, diverse classes of genes have been reported to be involved in lifespan control, pointing to several key regulatory pathways. However, it remains to be seen whether similar strategies may be applied to combat aging in humans. A major challenge in the field is that many of the findings apply to model organisms in laboratory settings, but these longevity conditions may come at the expense of fitness, making them detrimental when organisms are in their natural environment.

Aging is a process that involves complex gene networks. While broad genome manipulation is not yet practical in higher eukaryotes, fine-tuning these gene networks by environmental or dietary factors may offer a solution. It has been shown that manipulations such as calorie restriction (CR), oxygen availability, pH, and alternative carbon sources can modulate gene expression and the aging process(MCCAY *et al.* 1989; BOTTA *et al.* 2011; MURAKAMI *et al.* 2012). CR is among the most studied and widely used longevity interventions, which can extend lifespan in almost all model organisms(FINCH AND RUVKUN 2001). Although the precise mechanisms of CR-mediated lifespan extension remain debatable, it is known that CR causes a metabolic shift from fermentation to respiration in yeast, and that mitochondrial metabolism tends to increase in multicellular eukaryotes subjected to CR(LIN *et al.* 2002; LOPEZ-LLUCH *et al.* 2006;

SCHULZ *et al.* 2007). These findings also agree with the effects observed by manipulating various lifespan-regulating pathways, such as TOR (target of rapamycin) signaling(JOHNSON *et al.* 2013b). Suppression of TOR signaling mimics the reduction of nutritional input under CR in yeast and extends lifespan while concomitantly increasing mitochondrial respiration(BONAWITZ *et al.* 2007; JOHNSON *et al.* 2013b). Taken together, these studies link elevated mitochondrial function with lifespan, suggesting that a metabolic switch to oxidative metabolism is beneficial with regard to delaying aging.

The fact that metabolic pathways can be modulated by both CR and TOR inhibition suggests that complex processes such as aging may also be amenable to environmental and genetic manipulation. It is conceivable that the interaction between environmental factors and gene networks can explain the diverse phenotypes of species inhabiting different ecological niches. It is known that environmental adaptation and parallel evolution help create the genetic diversity for selection in natural populations(REZNICK *et al.* 2001). By evaluating the lifespan differences among natural populations of closely related strains or species, one may obtain insights into the underlying mechanisms that modulate aging and longevity. Towards this goal, in the current work we employed a powerful aging model, the budding yeast. Analyses of the aging process in *Saccharomyces cerevisiae* have mostly been performed on a small number of laboratory-adapted strains, but whether the identified mechanisms can explain the lifespan variation across natural strains is unknown. We evaluated the lifespans of 22 natural isolates of *S. cerevisiae*(LITI *et al.* 2009) and used transcriptome, proteome, metabolome and morphology data(SKELLY *et al.* 2013) to identify the signatures associated with natural lifespan variation. Our data suggest that increased replicative lifespan (RLS) in natural yeast populations is associated with increased oxidative phosphorylation and reduced amino acid biosynthesis. Our study also represents a new approach

that combines phenotypic variation across yeast populations with high-throughput data to elucidate underlying molecular mechanisms driving this variation.

Methods

Yeast strains. Diploid natural isolates of *Saccharomyces cerevisiae* were obtained from the Sanger Institute and are summarized in Table 1. These strains are well-characterized(LITI *et al.* 2009; BERGSTROM *et al.* 2014). The diploid laboratory strain BY4743 was purchased from ATCC.

Replicative lifespan assay. For each strain, cells were freshly grown on YPD plates prior to dissections. Several colonies were streaked onto new YPD plates using pipette tips. After overnight growth, 40-50 dividing cells were lined up. Newborn daughter cells were chosen for RLS assays after the first division using a micromanipulator. Plates were incubated at 30 °C between dissections and left at 4 °C during night. All RLS assays were performed in standard YPD plates with 2% glucose as previously described(STEFFEN *et al.* 2009). For each natural isolate, at least two independent assays were performed. Each assay contained 20-40 mother cells.

Phenotypic data. Growth rates were determined using a Bioscreen C MBR machine by analysis of optical density in the $OD_{420-580}$ range as previously described in combination with the YODA Software package(OLSEN *et al.* 2010). The data on transcripts, peptides, metabolites and morphology were downloaded from Yeast Resource Center (http://www.yeastrc.org/g2p/download.do). Values corresponding to the 22 strains were extracted; metabolite data were not available for 378604X. Metabolites with missing values in more than one

strain (other than 378604X) were discarded; the remaining missing values (6 out of 107 metabolites) were imputed based on 10 nearest neighbors, using "knnImputation" function of R package "DMwR". For comparison across the phenotypic data, the values were standardized across the strain by setting mean = 0 and standard deviation = 1. In addition, for genes represented by multiple peptides, we calculated the mean standardized values to perform the regression.

Principal component analysis (PCA). PCA was performed on standardized values using R package "stats"(R DEVELOPMENT CORE TEAM 2013). To identify the underlying pathways, the factors in each of the first three principal components (PCs) were ranked by their contributions, and pathway enrichment analysis was performed on the top 10% factors using DAVID after correcting for background.

Phylogenetic regression by generalized least square. Phylogenetic regression was performed by generalized least squares method using R packages "nmle" and "phylolm"(HO AND ANE 2013; PINHEIRO *et al.* 2013). Four models of trait evolution were tested: (i) complete absence of phylogenetic relationship ("Null"); (ii) Brownian Motion model ("BM"); (iii) BM transformed by Pagel's lambda ("Lambda"); and (iv) Ornstein-Uhlenbeck model ("OU"). For Lambda and OU models, the parameters were estimated simultaneously with the coefficients using maximum likelihood. The best-fit model was selected based on maximum likelihood. Strength of correlation was based on the p-value of regression slope. To confirm robustness of the results, regression was performed by leaving out each strain, one at a time, and computing p-values using the remaining strains.

Relative coverage of mitochondrial DNA. Genomic reads of strains examined in our study were downloaded from Yeast Resource Center (http://www.yeastrc.org/g2p/download.do) and mapped to reference genome of *Saccharomyces cerevisiae* strain S228c (http://www.yeastgenome.org/download-data/sequence). The average coverage per base across the chromosomes (excluding positions 45,000 to 50,000 of chromosome XII) was calculated using R package "ShortRead" for each strain. The relative coverage of mitochondrial DNA was expressed as the ratio of per-base coverage of mitochondrial DNA to per-base coverage of chromosomes.

Differential expression between long-lived and short-lived groups. Six closely related strains were grouped into long-lived (YJM981, YJM975, DBVPG1373) and short-lived (YJM978, NCY361, YS2). Differential expressions of the phenotypic data were calculated using R package "limma"(R DEVELOPMENT CORE TEAM 2013).

Mitochondrial protein expression. Logarithmically growing cells (5 ml and OD_{600}=0.6) were harvested and incubated in 150 µl extraction buffer (1.85 mM NaOH and 2% β-mercaptoethanol) on ice for 10 min. Then, 150 µl of 50% TCA (trichloroacetic acid) was added and incubated for 30 min on ice. After incubation, the cells were pelleted and supernatant aspirated. After 30 min of air drying, the pellets were heated at 60^{o}C in SDS loading buffer and 4 µl of each sample was analyzed by SDS-PAGE. To examine the expression of a mitochondrial protein, Western blotting was carried out with antibodies against mitochondrial outer membrane protein Por1 (Abcam). The membranes were stripped and developed with antibodies against phosphoglycerate kinase (Pgk1) (Life technologies) as an internal loading control.

Results

Variation in replicative lifespan across natural yeast isolates. Phylogenetic analysis using complete genome sequence alignment of 22 natural *S. cerevisiae* isolates revealed a complex cladogram that could be divided into two main groups (Figure 1). Assaying these isolates at 30 °C on standard YPD plates, we observed over 10-fold variation in RLS (Pearson correlation coefficient = 0.95 between mean and maximum lifespans; Figure 1B and Table 1). BC187 showed the largest number of cell divisions (mean = 39; maximum = 60); NCYC361 and YS2 had the fewest (mean = 3 for both; maximum = 7 for NCYC361 and 9 for YS2); and many strains produced on average 20-30 daughter cells, similar to BY4743, a standard laboratory diploid strain and the parental strain of the yeast ORF deletion collection (Table 1).

Growth of wild-type isolates in liquid culture. Changes in growth rate have previously been shown to affect mRNA, protein and metabolite levels(REGENBERG *et al.* 2006; CASTRILLO *et al.* 2007; BRAUER *et al.* 2008), and a recent study has reported a positive correlation between time spent in the G1 phase of the cell cycle and RLS in yeast(HE *et al.* 2014). To determine a potential relationship between growth rate and lifespan, we monitored the growth of these strains by automated Bioscreen-C growth analyzer and calculated the doubling time in both glucose and glycerol medium. Of the 22 isolates, 21 grew faster than BY4743 strain, and four strains doubled in less than 50 min (Figure 1C, Table 1) in glucose medium. However, we found only a weak negative correlation between the doubling time and mean lifespan (Pearson correlation coefficient

= -0.42). In addition, we observed that all strains can utilize glycerol as a carbon source, which indicates these strains are capable of mitochondrial respiratory metabolism (Table 1).

Phenotypic variation across strains. Gene expression, proteomic, metabolomic, and morphological data for these 22 strains have been reported previously(SKELLY *et al.* 2013). After our filtering and quality control, the dataset contained RNA-seq reads for 6207 transcripts; proteomic measurement of 6842 peptide fragments corresponding to 1643 unique genes; mass spectrometric quantification of 107 metabolites; and quantitative microscopy of 392 morphological phenotypes (Materials and Methods). In particular, 1641 unique genes were represented by both transcripts and peptides, but the correlation between the transcript and peptide levels was not strong (median Spearman correlation coefficient = 0.31; Supplementary Figure 1A). Similar conclusions were reached when we used the mean peptide values for each gene instead (median Spearman correlation coefficient = 0.28; Supplementary Figure 1B).

To visualize phenotypic variation across these strains, we performed Principal Component Analysis on each type of the phenotypic data as well as on the combined data (Figure 2A, Supplementary Figure 2A-D; the combined data excluded metabolites as values were not available for strain 378604X). The observed patterns resembled the phylogenetic relationship, with the first 3 Principal Components (PCs) explaining 36-53% of total variance (Supplementary Figure 2E). Examination of the genes contributing to the first 3 PCs in the combined data revealed a distinctive set of GO terms and KEGG pathways, including oxidative phosphorylation (PC1), aerobic respiration (PC1), mitochondrion (PC1), response to temperature stimulus (PC1), ribosome (PC2), protein synthesis (PC2), regulation of translation (PC2 and PC3), ribonucleoprotein complex (PC3), and ribosome biogenesis (PC3) (Supplementary Table 1). These results suggest that the

strains predominantly differ in energy metabolism, protein synthesis, and ribosome regulation. Consistent with a previous report(SKELLY *et al.* 2013), along PC1 the strains segregated largely according to their relative preferences for aerobic respiration or fermentation (Figure 2B).

Correlation between phenotype and lifespan. To identify a link between phenotypic variation and lifespan, we performed phylogenetic regression by generalized least squares, uncovering the phenotypes associated with longevity after accounting for the phylogenetic relationship of these strains(FELSENSTEIN 1985; MARTINS AND GARLAND 1991; FRECKLETON *et al.* 2002). Regression was performed between phenotypic values and any one of the following lifespan measurements: mean RLS, maximum RLS (Max RLS), log mean RLS (Log Mean RLS), and log maximum RLS (Log Max RLS). Different models of trait evolution were tested and the best-fit model was then selected based on maximal likelihood (Materials and Methods). To assess robustness of the relationship, we also left out one yeast strain at a time and re-calculated regression slopes using the remaining strains. This ensured the overall relationship did not depend on a particular isolate.

The four different RLS measurements yielded very similar results, with Pearson correlation coefficients ranging between 0.90 and 0.98 for the regression slopes. We defined the top hits as phenotypes with statistically significant regression slopes under at least two different RLS measures, and identified 249 gene transcripts, 347 peptide fragments (representing 216 unique genes), 5 metabolites, and 43 morphology features (Supplementary Table 2). Among the top gene transcripts and peptide fragments, only 10 unique genes were supported by both measures (Supplementary Figure 3), consistent with the weak correlation between transcript and peptide levels noted above (Supplementary Figure 1). When the mean peptide values were used for

calculation, 88 genes reached statistical significance, 80 of which were also supported based on peptide fragments (Supplementary Figure 3, Supplementary Table 2).

With regard to morphology measures, features such as "maximal intensity of nuclear brightness divided by average", "nucleus roundness in mother cell", and "length from bud tip to mother cell's short axis on nucleus C" showed significant negative correlation with RLS, whereas "fitness in nucleus C" correlated positively with longevity (see Saccharomyces Cerevisiae Morphological Database (http://scmd.gi.k.u-tokyo.ac.jp/datamine/ParameterHelp.do) for detailed descriptions of the parameters). Among the metabolite top hits, asparagine showed negative correlation with Max RLS (p value = 0.014) and Log Max RLS (p value = 0.017) (Figure 3A). A related amino acid, glutamine, also negatively correlated with Max RLS (p value = 0.042) and weakly with Log Max RLS (p value = 0.055) (Figure 3B). This was of note, since the TOR pathway is known to be regulated by the levels of amino acids, especially intracellular glutamine(MARTIN AND HALL 2005). Treating yeast cells with methionine sulfoximine, an inhibitor of glutamine synthetase, has been shown to decrease both intracellular glutamine levels and TOR-dependent signaling(CRESPO *et al.* 2002) while increasing RLS(KAEBERLEIN *et al.* 2005c), whereas removal of either asparagine or glutamate from the medium produced a dose-dependent effect on chronological lifespan (CLS)(POWERS *et al.* 2006) (CLS is the survival time of populations of nondividing cells, while RLS is the number of daughter cells produced by a mother cell prior to senescence; they are related but not identical). We also found 2-octenoic acid to correlate negatively with Max RLS (p value =0.019) and Log Max RLS (p value =0.014) (Figure 3C). This compound is known to be elevated in mitochondria, but its effect on aging is not known. Some of the transcript and peptide top hits have also been implicated in lifespan regulation in yeast. For example, the protein levels of ADH1p (alcohol dehydrogenase, coded by *YOL086C*) correlated

negatively with both Mean RLS and Max RLS, and deletion of *ADH1* was found to extend RLS by 23% in MATα and 15% in MATa(SMITH *et al.* 2008). *DCW1* (also known as *YKL046C*, coding for a putative mannosidase in cell wall biosynthesis), whose transcript levels correlated negatively with all four RLS measurements, was previously identified in a genetic screen to increase yeast CLS when deleted(MATECIC *et al.* 2010). In addition, a number of top hits correlating positively with longevity at the transcript (e.g. *VRP1* (*YLR337C*), *KGD1* (*YIL125W*)) and protein (e.g. PET9p (YBL030Cp), SP160p (YJL080Cp), GSY2p (YLR258Wp)) levels were previously shown to decrease RLS or CLS when deleted or mutated(SMITH *et al.* 2008; WANG *et al.* 2008; FABRIZIO *et al.* 2010; LASCHOBER *et al.* 2010).

Networks and pathways represented by top hits. To further understand the biological pathways underlying natural regulation of lifespan, we performed pathway enrichment analysis using DAVID(HUANG DA *et al.* 2009) (Supplementary Table 3). The enrichment results for the peptide fragments were especially significant. Among the peptide fragments correlating positively with longevity, the enriched terms included “oxidative phosphorylation”, “mitochondrial respiratory chain”, “ion transport”, “hexose metabolic process”, “glucose metabolic process”, and “aerobic respiration”. On the other hand, for those correlating negatively with longevity, “amino acid biosynthesis”, “organic acid biosynthetic process”, “nitrogen compound biosynthetic process”, “nucleotide binding”, “cofactor binding”, and “glycolysis” were enriched. Many of these terms were similarly enriched when we carried out calculations using the mean peptide values (Supplementary Table 3). In comparison, the enrichment statistics were weaker for the transcripts, even though the numbers of top hits were similar. Among those with positive correlation, enrichment was observed for “ion transport”, “mitochondrial membrane part”, “ATP biosynthetic

process", "oxidative phosphorylation", and "actin binding". For the transcripts with negative correlation to lifespan, the enriched terms included "RNA polymerase II transcription factor activity", "transcription regulator activity", "microtubule", "regulation of RNA metabolic process", and "mRNA splicing". Overall, the results suggest that the long-lived strains tend to up-regulate oxidative phosphorylation, aerobic respiration, and ion transport; and down-regulate transcription, splicing, and various biosynthetic processes (especially amino acid metabolism).

We visualised protein-protein interactions among the top hits using STRING(JENSEN *et al.* 2009) and found the network is significantly enriched in interactions. The top hits identified using the mean peptide values were grouped into several prominent clusters, including oxidative phosphorylation and aerobic respiration (positive correlation); organic acid and nitrogen compound biosynthetic process (negative correlation); and protein targeting (negative correlation) (Figure 3D). Similar clusters of the top hits were observed for transcripts and peptide fragments data (Supplementary Figure 4), suggesting that the top hits, rather than being a random collection of genes, represent interconnected nodes in regulatory networks and pathways.

Mitochondrial abundance and composition of the strains. Since the results suggested a relative up-regulation of oxidative phosphorylation and aerobic respiration among the long-lived strains, we examined more closely the nature of such differences. First, the genomic reads of these strains[15] were used to calculate average coverage of the mitochondrial DNA relative to that of the chromosomes (Table 1, Supplementary Figure 5A), as a proxy for mitochondria copy number. While the relative coverage was highest in YJM381 (8.0) and lowest in YPS128 (3.0), the values were relatively constant for most of the strains (4.0—5.0) and there was no overall correlation with longevity (Pearson correlation p-value = 0.31 with Max RLS and 0.53 with Mean RLS). Moreover,

Western blotting confirmed the similar expression of a mitochondrial marker protein Por1 in these strains (Supplementary Figure 5B). In addition, the doubling times in glycerol media were also similar (100-120 min for most of the strains, with exception of >180 min for YS2, DBVPG1373, and Y55 strains; Supplementary Figure 5C, Table 1), suggesting the longevity variation across these strains could not be simply explained by total mitochondrial content or number.

However, when we examined the top hits based on mean peptide values (Supplementary Table S2), a trend emerged. Approximately 1/3 of these peptides were related to mitochondria, with characteristic distribution patterns across the strains depending on their lifespans (Figure 5). For example, the longer-lived strains generally contained higher levels of proteins belonging to pyruvate dehydrogenase complex (PDH complex), Complex III, Complex IV, mitochondrial ATP synthase, inner membrane ADP/ATP carrier, as well as mitochondrial ribosomal proteins. On the other hand, long-lived strains had lower relative levels of outer membrane translocases, mitochondrial chaperonins, and certain metabolic enzymes. The results suggest that the mitochondrial metabolism may vary widely across the strains according to their longevity. The longer-lived strains seem to enhance the electron transport chain and oxidative phosphorylation capacity, whereas the shorter-lived strains place more emphasis on protein folding and outer membrane transport. While the biological implications underlying these observations need to be further explored, the results show that distinct mitochondrial composition is associated with different yeast strains, and such patterns agree well with the observed lifespan variation.

Comparison of related long-lived and short-lived strains. A number of our strains (YJM978, YJM981, YJM975, DBVPG1373, NCYC361, and YS2) are closely related to each other phylogentically (Figure 1A), but differ significantly in replicative lifespan (Figure 1B). In

particular, they may be grouped into long-lived (YJM981, YJM975, and DBVPG1373) and short-lived (YJM978, NCY361, and YS2). If our findings above were valid, then we should observe similar sets of genes and pathways differentially expressed between these two groups. The analysis showed that the genes involved in "hexose metabolic process", "glucose metabolic process", and "glycolysis" were expressed highly in the long-lived strains, whereas those involved in "organic acid biosynthetic process", "amino acid biosynthesis", and "cofactor binding" were expressed at relatively low levels (Supplementary Table 4). Compared with the pathways we identified above, the genes involved in oxidative phosphorylation and aerobic respiration did not emerge as top hits, and there were not as many proteins related to mitochondria among these 6 strains. This is likely because all of these strains prefer fermentation over aerobic respiration (Figure 2B), and they already share similar mitochondrial composition profiles (Figure 4B). Among the strains designated as YJM are clinical isolates and their adaptation to longevity appears to be different from other strains. For example, YJM975 and YJM981 are long-lived, but their mitochondrial patterns are similar to the short-lived strains. Perhaps, their longevity is based on lineage-specific features that are not shared by other long-lived isolates. Nevertheless, among the long-lived strains we observed lower levels of expression of genes and proteins involved in biosynthetic processes (most of which were cytoplasmic, Supplementary Table 4), in agreement with our observations based on the 22 strains. This suggests that long lifespan can also arise without substantially altering the mitochondrial composition, although the reduction in biosynthesis seems to be a common feature.

Discussion

Availability of high quality genome sequence of *Saccharomyces cerevisiae* has made yeast an attractive model for dissecting complex traits associated with various phenotypes. Comparative genomics across multiple natural yeast isolates enabled the identification of extensive natural genetic variation at the nucleotide polymorphism (SNP) level and the elucidation of genotype to phenotype relation in several traits(LITI AND LOUIS 2012). Here, we ask: can similar strategies be applied to understand the common determinants of aging and longevity?

Using high throughput omics data, we examined 22 yeast natural isolates, which were found to vary over 10 fold in RLS. These isolates occupy diverse ecological niches and face different evolutionary pressures, so their natural lifespan variation must be encoded in their respective genomes. However, it has been challenging to characterize the cumulative effect of multiple alleles on a phenotype, especially if the underlying process involves a complex gene network. Alternatively, one may look at variation in gene transcripts (transcriptome) and gene products (proteome) and correlate them and the associated pathways with the phenotypic traits, since the genotypic variation should be reflected in the expression variation in order to create the associated phenotypic differences(BREM *et al.* 2005).

To identify a link between transcript variation and lifespan, we performed phylogenetic regression and identified genes correlating with RLS, some of which were previously implicated in longevity regulation. Our pathway analysis showed that the long-lived strains tend to up-regulate oxidative phosphorylation, aerobic respiration, and ion transport; and down-regulate transcription, splicing, glycolysis and various biosynthetic processes, most notably amino acid synthesis. In particular, the variation in mitochondrial respiratory composition of these strains agrees well with their differences in lifespan. Mitochondria are at the heart of cellular metabolism and energy production, and increased mitochondrial respiratory capacity has been linked to

longevity(BONAWITZ *et al.* 2007; PAN AND SHADEL 2009). We hypothesize that many of these natural isolates reside in the environments with low fermentable carbon sources, so that they undergo diauxic shift and metabolize respiratory carbon sources. Shifting from fermentable (glucose) to respiratory carbon sources is known to extend both replicative and chronological lifespan in yeast (DELANEY *et al.* 2011).

Genetic variation responsible for lifespan differences may also affect metabolite levels and morphology. Among the examined metabolites, glutamine and asparagine showed strong negative correlation with RLS, which is consistent with the known inhibition of TOR activity and extension of chronological lifespan by removing glutamine or asparagine from yeast media(POWERS *et al.* 2006) and extension of RLS by treating cells with methionine sulfoximine(KAEBERLEIN *et al.* 2005c). In terms of cell morphology, a number of nuclear features such as brightness, roundness and distance to bud tip showed significant negative correlation with RLS, whereas "fitness in nucleus C" correlated positively with longevity. Interestingly, longer-lived strains tend to possess smaller mother cell volume (Supplementary Figure 6), indicative of a potential compromise between mother cell size and lifespan, as has been previously observed for long-lived cells treated with ibuprofen(HE *et al.* 2014). In agreement, inverse correlation between cell size and lifespan has been observed in yeast previously[44]. Thus, here too, natural changes in a phenotype can be linked with longevity interventions and maybe used as aging biomarkers.

It should be noted that our method is limited to identifying the genetic and metabolic processes that show concerted changes in relation to longevity across these 22 strains, which are more likely to be generalizable and do not depend on single or a few strains. On the other hand, an exceptionally long-lived or short-lived strain can also have arisen due to certain strain-specific changes that are not shared by other isolates, and such changes may be missed by our method.

Comparison among the 6 related long-lived and short-lived strains suggests there may be more than one way to achieve long lifespan, and it will be useful to examine strains across different evolutionary distances to identify the common features.

To our knowledge, this is the first report that analyzes inter-strain natural diversity of RLS at the population level using high throughput data. Natural isolates occupying diverse ecological niches may face different selection pressures and have evolved to adjust their gene expression, metabolism, longevity, and reproduction to ensure survival and propagation(SPOR *et al.* 2009). While evolution can sometimes provide different solutions to the same challenge(ROMANO *et al.* 2010), our data suggest a consistent set of genes and pathways are responsible for modulating the lifespan trait across a broad diversity of wild yeast isolates.

Finally, it has been unclear whether the previous findings of various longevity regulator genes identified in the laboratory setting could be translated to the natural environment. A possibility is that these lifespan-extending interventions come at the expense of fitness. For example, many longest-lived *C. elegans* laboratory mutants tend to develop and move slowly and often show reduced fecundity, so they will probably be eliminated quickly for lack of competitive advantage in the wild. Consistent with this, 65% of long lived single gene deletion mutants in yeast demonstrated significantly reduced fitness compared to isogenic wild type cells.(DELANEY *et al.* 2011) Our results show that natural changes in lifespan need not compromise fitness, as longer-lived yeast isolates are presumably well adapted to their respective ecological niches. In addition, our analysis is unbiased with regard to the genes and pathways involved in lifespan control and supports a possibility that multiple correlates cumulatively contribute to the longevity phenotypes. Specifically, we found that the ability of yeast cells to rely more heavily on respiration and repress their anabolic programs, even under conditions of glucose excess, are among the key adaptations

that lead to increased lifespan. Importantly, since CR and TOR signaling are also known to extend lifespan by activating respiration and inhibiting biosynthetic processes, these data show that natural plasticity of yeast lifespan is shaped by pathways that both impose little cost on fitness and are amenable to dietary intervention. Thus, environment may be a trigger for changes associated with increased lifespan that are then fixed in the genomes.

Author contributions

A.K., and V.N.G. designed the experiments. A.K., B.W., and M.L performed the experiments. A.K., S.M., M.L., M.K., and V.N.G analyzed the data. A.K., S.M., M.K and V.N.G wrote the paper. All authors reviewed the paper.

Acknowledgements

The authors thank Margarete Moore, Maryann Li, Daniel Carr, and the Kaeberlein lab yeast replicative lifespan team for technical assistance. This work was supported by NIH grants AG021518 (to VNG), AG047745 (to VNG), AG039390 (to MK) and AG013280. MBL and BW were supported by NIH training grants GM07270 and ES007032.

Supplementary Information

Supplementary information accompanies this paper consist of 3 supplementary tables (Excel) and supplementary information (PDF).

Competing financial interest: The authors declare no competing financial interests.

References

1. Gladyshev VN. On the cause of aging and control of lifespan: heterogeneity leads to inevitable damage accumulation, causing aging; control of damage composition and rate of accumulation define lifespan. *BioEssays : news and reviews in molecular, cellular and developmental biology* 2012; **34**(11): 925-9.
2. Finch CE, Ruvkun G. The genetics of aging. *Annual review of genomics and human genetics* 2001; **2**: 435-62.
3. Kenyon CJ. The genetics of ageing. *Nature* 2010; **464**(7288): 504-12.
4. McCay CM, Crowell MF, Maynard LA. The effect of retarded growth upon the length of life span and upon the ultimate body size. 1935. *Nutrition* 1989; **5**(3): 155-71.
5. Murakami C, Delaney JR, Chou A, Carr D, Schleit J, Sutphin GL, et al. pH neutralization protects against reduction in replicative lifespan following chronological aging in yeast. *Cell cycle* 2012; **11**(16): 3087-96.
6. Botta G, Turn CS, Quintyne NJ, Kirchman PA. Increased iron supplied through Fet3p results in replicative life span extension of Saccharomyces cerevisiae under conditions requiring respiratory metabolism. *Experimental gerontology* 2011; **46**(10): 827-32.
7. Pitt JN, Leiser SF, Kaeberlein M. In: Sprott R, (editor). *Annual Review of Gerontology and Geriatrics*: Springer Publishing Company; 2014. p. 59-81.
8. Lopez-Lluch G, Hunt N, Jones B, Zhu M, Jamieson H, Hilmer S, et al. Calorie restriction induces mitochondrial biogenesis and bioenergetic efficiency. *Proceedings of the National Academy of Sciences of the United States of America* 2006; **103**(6): 1768-73.
9. Schulz TJ, Zarse K, Voigt A, Urban N, Birringer M, Ristow M. Glucose restriction extends Caenorhabditis elegans life span by inducing mitochondrial respiration and increasing oxidative stress. *Cell metabolism* 2007; **6**(4): 280-93.
10. Lin SJ, Kaeberlein M, Andalis AA, Sturtz LA, Defossez PA, Culotta VC, et al. Calorie restriction extends Saccharomyces cerevisiae lifespan by increasing respiration. *Nature* 2002; **418**(6895): 344-8.
11. Johnson SC, Rabinovitch PS, Kaeberlein M. mTOR is a key modulator of ageing and age-related disease. *Nature* 2013; **493**(7432): 338-45.
12. Bonawitz ND, Chatenay-Lapointe M, Pan Y, Shadel GS. Reduced TOR signaling extends chronological life span via increased respiration and upregulation of mitochondrial gene expression. *Cell metabolism* 2007; **5**(4): 265-77.
13. Reznick D, Buckwalter G, Groff J, Elder D. The evolution of senescence in natural populations of guppies (Poecilia reticulata): a comparative approach. *Experimental gerontology* 2001; **36**(4-6): 791-812.
14. Liti G, Carter DM, Moses AM, Warringer J, Parts L, James SA, et al. Population genomics of domestic and wild yeasts. *Nature* 2009; **458**(7236): 337-41.

15. Skelly DA, Merrihew GE, Riffle M, Connelly CF, Kerr EO, Johansson M, et al. Integrative phenomics reveals insight into the structure of phenotypic diversity in budding yeast. *Genome research* 2013; **23**(9): 1496-504.
16. Bergstrom A, Simpson JT, Salinas F, Barre B, Parts L, Zia A, et al. A high-definition view of functional genetic variation from natural yeast genomes. *Molecular biology and evolution* 2014; **31**(4): 872-88.
17. Steffen KK, Kennedy BK, Kaeberlein M. Measuring replicative life span in the budding yeast. *Journal of visualized experiments : JoVE* 2009; (28).
18. Olsen B, Murakami CJ, Kaeberlein M. YODA: software to facilitate high-throughput analysis of chronological life span, growth rate, and survival in budding yeast. *BMC bioinformatics* 2010; **11**: 141.
19. R Development Core Team. R: A Language and Environment for Statistical Computing. Vienna, Austria 2013.
20. Pinheiro J, Bates D, DebRoy S, Sarkar D, R Development Core Team. nlme: Linear and Nonlinear Mixed Effects Models. *R package* 2013.
21. Ho LST, Ane C. A linear-time algorithm for Gaussian and non-Gaussian trait evolution models. *Systematic Biology* 2013; **63**(3): 397-408.
22. Regenberg B, Grotkjaer T, Winther O, Fausboll A, Akesson M, Bro C, et al. Growth-rate regulated genes have profound impact on interpretation of transcriptome profiling in Saccharomyces cerevisiae. *Genome biology* 2006; **7**(11): R107.
23. Castrillo JI, Zeef LA, Hoyle DC, Zhang N, Hayes A, Gardner DC, et al. Growth control of the eukaryote cell: a systems biology study in yeast. *Journal of biology* 2007; **6**(2): 4.
24. Brauer MJ, Huttenhower C, Airoldi EM, Rosenstein R, Matese JC, Gresham D, et al. Coordination of growth rate, cell cycle, stress response, and metabolic activity in yeast. *Molecular biology of the cell* 2008; **19**(1): 352-67.
25. He C, Tsuchiyama SK, Nguyen QT, Plyusnina EN, Terrill SR, Sahibzada S, et al. Enhanced Longevity by Ibuprofen, Conserved in Multiple Species, Occurs in Yeast through Inhibition of Tryptophan Import. PLoS Genet. 2014; 10(12); doi: 10.1371/journal.pgen.1004860.
26. Felsenstein J. Phylogenies and the Comparative Method. *American Naturalist* 1985; **125**(1): 1-15.
27. Martins EP, Garland T, Jr. Phylogenetic analyses of the correlated evolution of continuous characters: a simulation study. *Evolution; international journal of organic evolution* 1991; **45**: 534-57.
28. Freckleton RP, Harvey PH, Pagel M. Phylogenetic analysis and comparative data: a test and review of evidence. *American Naturalist* 2002; **160**(6): 712-26.
29. Martin DE, Hall MN. The expanding TOR signaling network. *Current opinion in cell biology* 2005; **17**(2): 158-66.
30. Crespo JL, Powers T, Fowler B, Hall MN. The TOR-controlled transcription activators GLN3, RTG1, and RTG3 are regulated in response to intracellular levels of glutamine. *Proceedings of the National Academy of Sciences of the United States of America* 2002; **99**(10): 6784-9.
31. Kaeberlein M, Powers RW, 3rd, Steffen KK, Westman EA, Hu D, Dang N, et al. Regulation of yeast replicative life span by TOR and Sch9 in response to nutrients. *Science* 2005; **310**(5751): 1193-6.

32. Powers RW, 3rd, Kaeberlein M, Caldwell SD, Kennedy BK, Fields S. Extension of chronological life span in yeast by decreased TOR pathway signaling. *Genes & development* 2006; **20**(2): 174-84.
33. Smith ED, Tsuchiya M, Fox LA, Dang N, Hu D, Kerr EO, et al. Quantitative evidence for conserved longevity pathways between divergent eukaryotic species. *Genome research* 2008; **18**(4): 564-70.
34. Matecic M, Smith DL, Pan X, Maqani N, Bekiranov S, Boeke JD, et al. A microarray-based genetic screen for yeast chronological aging factors. PLoS genetics. 2010; 6(4); doi: 10.1371/journal.pgen.1000921.
35. Fabrizio P, Hoon S, Shamalnasab M, Galbani A, Wei M, Giaever G, et al. Genome-wide screen in Saccharomyces cerevisiae identifies vacuolar protein sorting, autophagy, biosynthetic, and tRNA methylation genes involved in life span regulation. PLoS genetics. 2010; 6(7); doi: 10.1371/journal.pgen.1001024.
36. Laschober GT, Ruli D, Hofer E, Muck C, Carmona-Gutierrez D, Ring J, et al. Identification of evolutionarily conserved genetic regulators of cellular aging. *Aging cell* 2010; **9**(6): 1084-97.
37. Wang X, Salinas K, Zuo X, Kucejova B, Chen XJ. Dominant membrane uncoupling by mutant adenine nucleotide translocase in mitochondrial diseases. *Human molecular genetics* 2008; **17**(24): 4036-44.
38. Huang da W, Sherman BT, Lempicki RA. Systematic and integrative analysis of large gene lists using DAVID bioinformatics resources. *Nature protocols* 2009; **4**(1): 44-57.
39. Jensen LJ, Kuhn M, Stark M, Chaffron S, Creevey C, Muller J, et al. STRING 8--a global view on proteins and their functional interactions in 630 organisms. *Nucleic acids research* 2009; **37**: D412-6.
40. Liti G, Louis EJ. Advances in quantitative trait analysis in yeast. *PLoS genetics* 2012; **8**(8): e1002912.
41. Brem RB, Storey JD, Whittle J, Kruglyak L. Genetic interactions between polymorphisms that affect gene expression in yeast. *Nature* 2005; **436**(7051): 701-3.
42. Pan Y, Shadel GS. Extension of chronological life span by reduced TOR signaling requires down-regulation of Sch9p and involves increased mitochondrial OXPHOS complex density. *Aging* 2009; **1**(1): 131-45.
43. Delaney JR, Murakami CJ, Olsen B, Kennedy BK, Kaeberlein M. Quantitative evidence for early life fitness defects from 32 longevity-associated alleles in yeast. *Cell cycle* 2011; **10**(1): 156-65.
44. Yang J, Dungrawala H, Hua H, Manukyan A, Abraham L, Lane W, et al. Cell size and growth rate are major determinants of replicative lifespan. *Cell cycle* 2011; **10**(1): 144-55.
45. Spor A, Nidelet T, Simon J, Bourgais A, de Vienne D, Sicard D. Niche-driven evolution of metabolic and life-history strategies in natural and domesticated populations of Saccharomyces cerevisiae. *BMC Evol Biol* 2009; **9**: 296.
46. Romano GH, Gurvich Y, Lavi O, Ulitsky I, Shamir R, Kupiec M. Different sets of QTLs influence fitness variation in yeast. *Molecular systems biology* 2010; **6**: 346.
47. Tamura K, Stecher G, Peterson D, Filipski A, Kumar S. MEGA6: Molecular Evolutionary Genetics Analysis version 6.0. *Molecular biology and evolution* 2013; **30**(12): 2725-9.
48. Saitou N, Nei M. The neighbor-joining method: a new method for reconstructing phylogenetic trees. *Molecular biology and evolution* 1987; **4**(4): 406-25.

Table 1. Strains used in this study. Natural isolates of yeast strains are shown along with their wild niche, mean and maximum lifespan, maximum doubling time in glucose and glycerol media, relative coverage of mitochondrial DNA, and cell size.

			Replicative Lifespan			Doubling Time in glucose (min)		Doubling Time in glycerol (min)		Relative coverage of mitochondria DNA	Cell Size (µm)
Strain Name	Strain Type	Source	maximum	mean	Std. error	mean	Std. error	mean	Std. error		
Y55	lab	grape	47	27	3.43	63.79	3.56	110.31	1.13	4.46	10
SK1	lab	soil	45	27	3.39	51.62	33.95	189.60	11.74	5.36	13
UWOPS87-2421	wild	plant	35	19	3.72	32.91	5.96	107.01	0.74	4.16	12
UWOPS05-227.2	wild	bee	37	23	3.39	56.03	8.23	116.59	4.93	4.41	11
UWOPS05-217.3	wild	plant	42	24	3.51	62.77	9.14	115.71	5.52	4.41	11
UWOPS83-787.3	wild	fruit	52	30	4.16	42.96	9.47	106.65	1.46	4.49	10
Y12	fermentation	palm wine	55	37	3.92	58.91	1.83	117.73	3.92	4.79	10
YPS606	wild	oak tree	44	38	1.76	35.43	7.22	98.50	1.29	3.85	10
YPS128	wild	oak tree	54	33	4.61	34.78	5.68	97.67	1.83	3.02	10
378604X	clinical	sputum	31	23	2.06	65.04	2.64	204.72	10.88	4.42	12
273614N	clinical	fecal	45	28	3.55	72.75	3.63	109.31	1.24	5.60	13
YS9	baking	unknown	37	21	2.90	63.08	4.15	131.35	0.91	3.29	14
BC187	fermentation	barrel	60	39	5.39	64.03	2.46	117.93	0.35	7.38	10
L-1374	fermentation	must	47	30	3.63	58.68	1.75	104.74	1.34	4.99	12
DBVPG6765	unknown	unknown	16	10	1.76	62.60	2.91	99.16	5.06	4.00	13
DBVPG1106	fermentation	grapes	32	24	2.00	64.70	2.26	109.41	1.52	5.46	12
YJM978	clinical	vaginal	18	9	1.76	64.20	1.89	110.30	4.21	5.75	12
YJM981	clinical	vaginal	50	25	4.78	67.68	1.43	102.18	3.16	7.98	14
YJM975	clinical	vaginal	52	34	5.18	63.07	2.89	106.81	3.28	5.95	11
DBVPG1373	wild	soil	35	23	3.02	66.58	4.93	123.39	2.48	4.87	11
NCYC361	fermentation	wort	7	3	0.53	62.97	2.84	117.85	0.75	5.19	12
YS2	baking	unknown	9	3	0.57	87.55	4.67	216.05	2.31	4.24	11
BY4743	lab	grape	44	28	1.67	76.38	2.89	163.62	7.17	4.46	NA

FIGURE 1

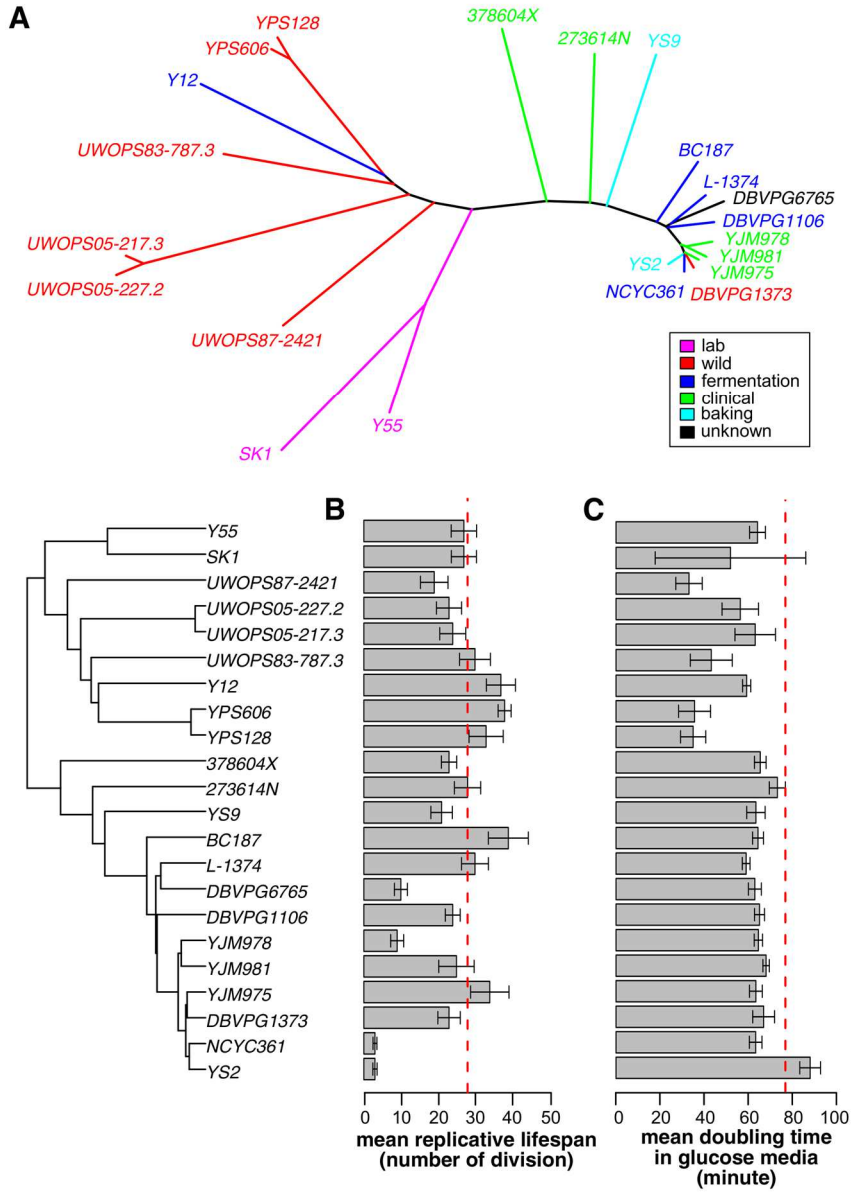

Figure 1. Yeast strains examined in this study.

(A) Phylogenetic relationship. The tree was constructed based on the alignment of complete genome sequences of the strains, using MEGA 6.06 (TAMURA *et al.* 2013) and neighbor joining method(SAITOU AND NEI 1987). The branches are colored according to strain types shown in the legend in the lower right corner.

(B) Mean replicative lifespan and (C) mean growth rate (doubling time) of the strains in glucose media. The strains are ordered by phylogeny. The error bars indicate standard error. Red dotted lines indicate the mean replicative lifespan (B) and doubling time (C) of the reference strain BY4743.

FIGURE 2

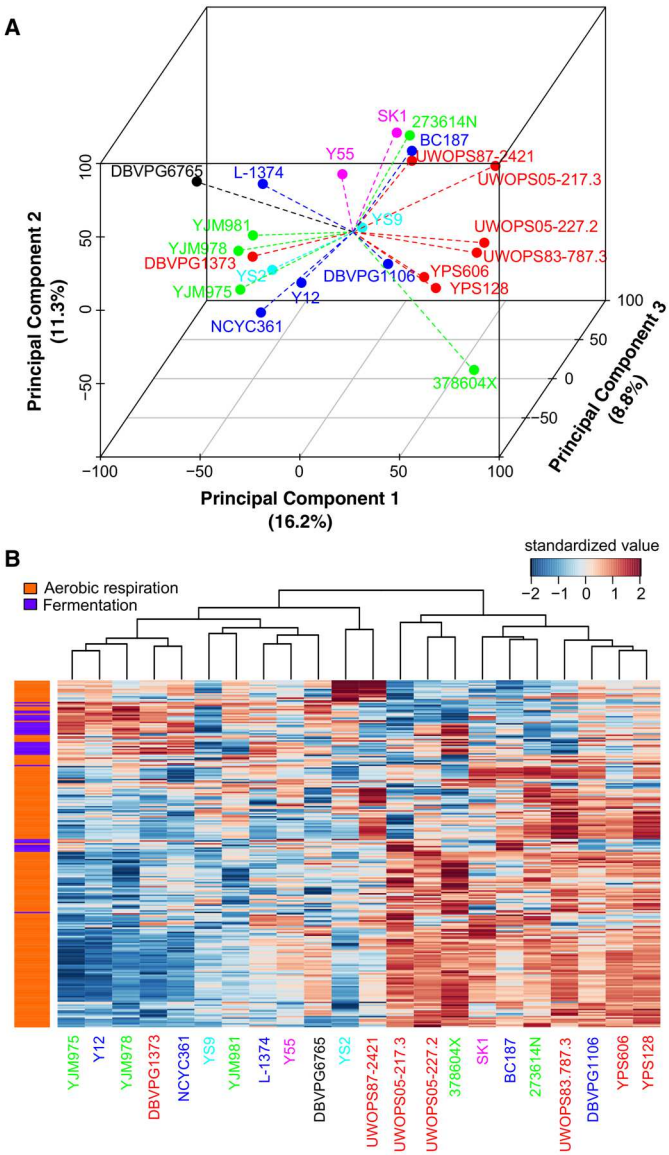

Figure 2. Phenotypic variation across the strains.

(A) Principal Component Analysis (PCA) of combined data. PCA was performed by combining transcripts, peptides, and morphology data (metabolite data were not available for strain 378604X and were omitted). Percentage variance explained by each Principal Component (PC) is shown in the parentheses. The strains are colored using the same scheme as Figure 1A. See Supplementary Figure 2 for separate PCA plots on each class of phenotype data and for cumulative percentage of variance explained by the PCs.

(B) Relative levels of transcripts and peptides involved in aerobic respiration or fermentation. The heat map shows the transcripts and peptides with top contribution to Principal Component 1 and involved in aerobic respiration or fermentation (Supplementary Table 1). Hierarchical clustering was performed using complete linkage.

FIGURE 3

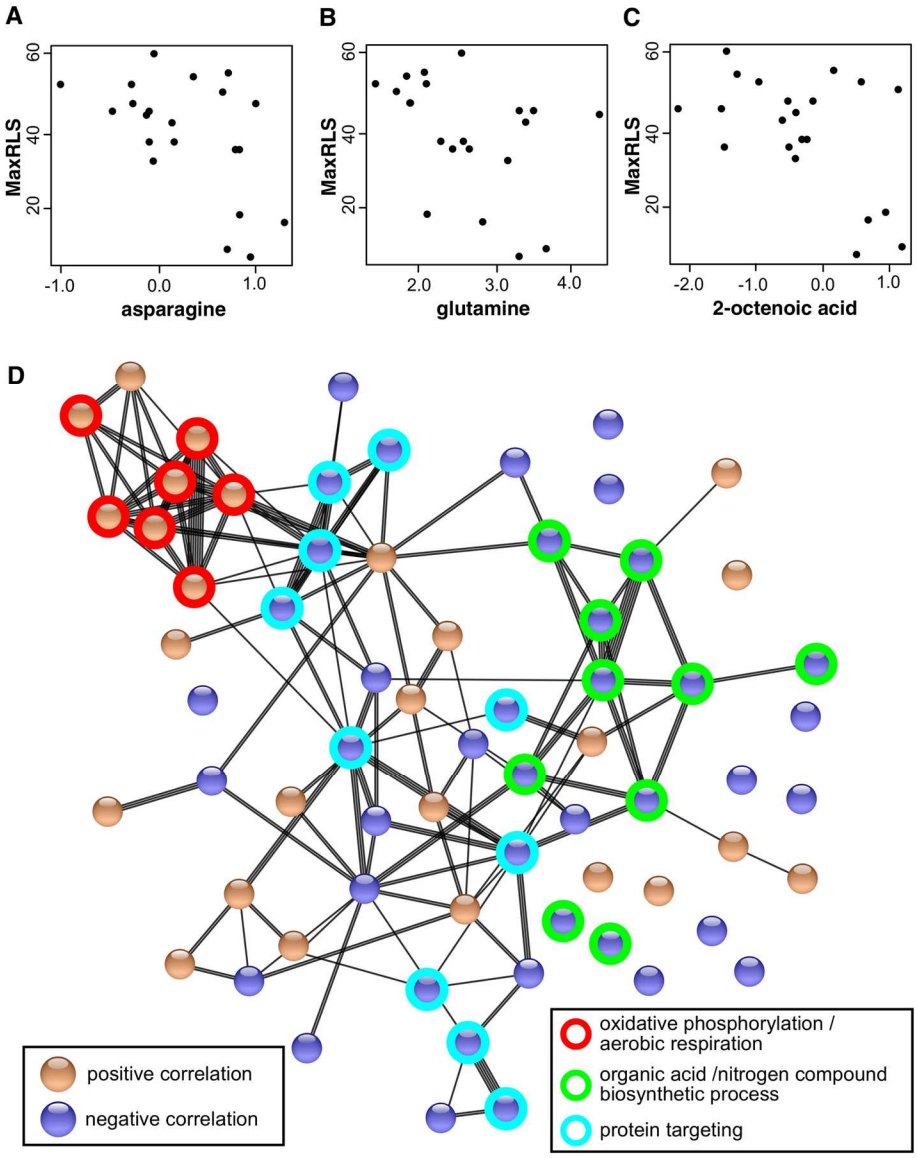

Figure 3. Selected phenotypes correlating with replicative lifespan.

Levels of (A) asparagine, (B) glutamine, and (C) 2-octenoic acid negatively correlate with maximum replicative lifespan (MaxRLS). Regression slope p-values: (A) 0.014; (B) 0.042; (C) 0.019.

(D) Protein-protein interaction network of the top hits identified by the mean peptide values. The interaction network is based on STRING database (evidence view). Genes without interacting partners are omitted. Selected pathways are indicated by colored rings. Most of the peptides here showed significant correlation to all four RLS measures. See Supplementary Table 2 for more detail.

FIGURE 4

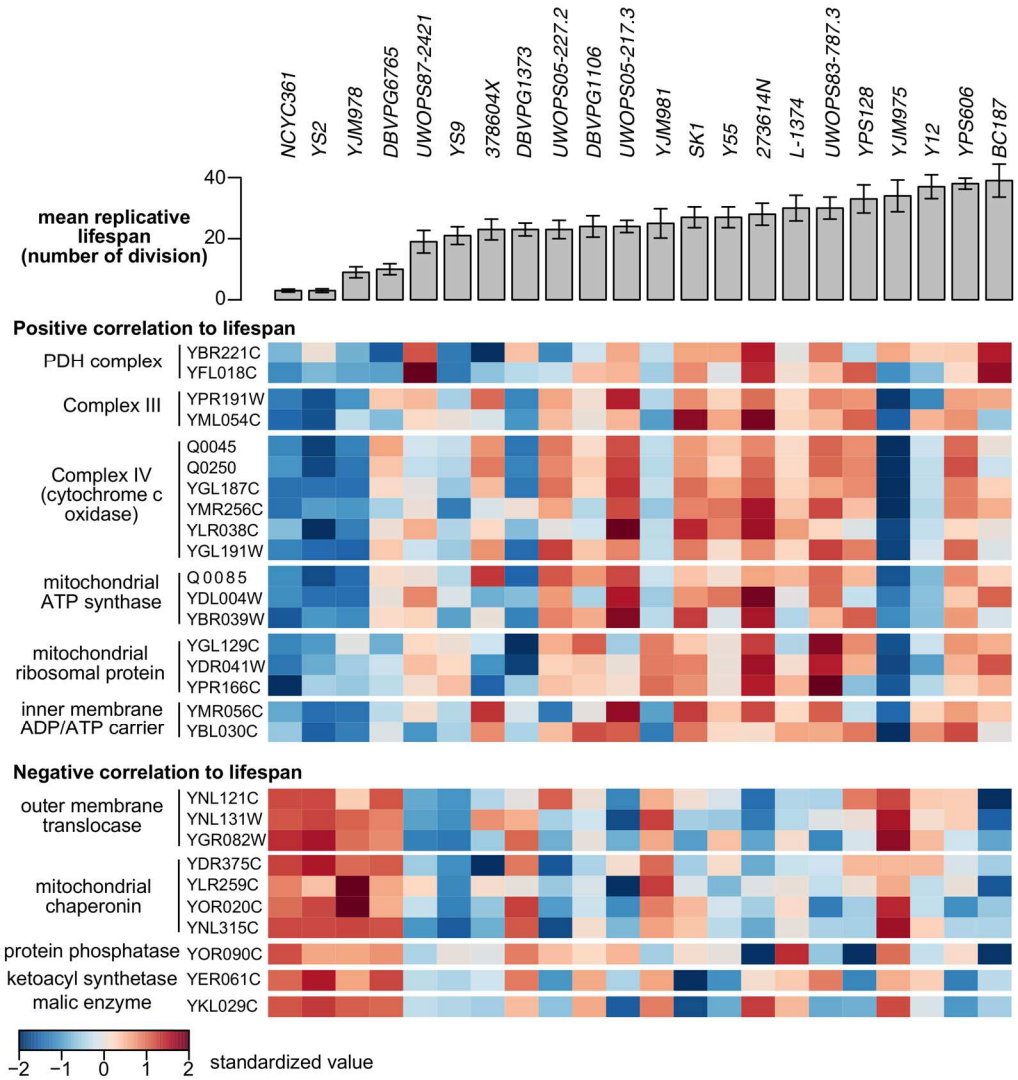

Figure 4. Mitochondrial respiratory composition across the strains according to lifespan. The strains are ordered according to their mean replicative lifespan (see also Figure 1B). The mean values of the selected peptides (related to mitochondria) are shown. For each peptide, the levels were standardized by setting mean = 0 and standard deviation = 1 across the strains. Distinction of mitochondrial pattern of DBPVG1373, YJM981, YJM975 and Y12 out layered among the other strains. See Supplementary Table 2 for more detail.

VITA

Raised in the rural Oklahoma panhandle, Mitchell Lee moved to Washington state shortly after graduating high school. After completing his A.A.S. at Everett Community College with an emphasis in Philosophy, Mitchell completed a B.A. in Philosophy and a B.S. in Biology with an emphasis in Ecology, Evolution, and Organismal Biology at Western Washington University. During undergraduate studies, Mitchell discovered his passion for Molecular Biology and Genetics. He completed a M.Sc. at WWU under the guidance of Lynn Pillitteri where he studied Molecular Neurodevelopment using *C. elegans* (roundworm). Under the combined mentorship of Matt Kaeberlein and Alan Herr, Mitchell currently uses *S. cerevisiae* (budding yeast) to model drivers of cancer and identify novel compounds that can be used to extend the healthy life span of companion pets and ourselves.